Use of Vietnam Steel Slag as Aggregate for Roller-Compacted Concrete Pavement

Lam Ngoc Tra My

Use of Vietnam Steel Slag as Aggregate for Roller-Compacted Concrete Pavement

Lam Ngoc Tra My

A Thesis Submitted in Fulfillment of the Requirements for the
Degree of Doctor of Philosophy in Civil Engineering
Prince of Songkla University
2018

Thesis Title   Use of Vietnam Steel Slag as Aggregate for Roller-Compacted Concrete Pavement

Author   Mrs. Lam Ngoc Tra My

Major Program   Civil Engineering

Major Advisor

…………………………………

(Assoc. Prof. Dr. Saravut Jaritngam)

Co-advisor

…………………………………

(Dr. Duc-Hien Le)

Examining Committee:

……………………….............Chairperson

(Assoc. Prof. Dr. Vatanavongs Ratanavaraha)

……………………………….Committee

(Assoc. Prof. Dr. Saravut Jaritngam)

……………………………….Committee

(Dr. Duc-Hien Le)

……………………………….Committee

(Asst. Prof. Dr. Paramet Luathep)

……………………………….Committee

(Prof. Dr. Pichai Taneerananon)

The Graduate School, Prince of Songkla University, has approved this thesis as fulfillment of the requirements for the Doctor of Philosophy Degree in Civil Engineering.

……………………………………………

(Prof. Dr. Damrongsak Faroongsarng)

Dean of Graduate School

This is to certify that the work here submitted is the result of the candidate's own investigations. Due acknowledgment has been made of any assistance received.

....Signature

(Assoc. Prof. Dr. Saravut Jaritngam)

Major Advisor

....Signature

(Dr. Duc-Hien Le)

Co-advisor

....Signature

(Mrs. Lam Ngoc Tra My)

Candidate

I hereby certify that this work has not been accepted in substance for any degree, and is not being currently submitted in candidature for any degree.

....Signature

(Mrs. Lam Ngoc Tra My)

Candidate

Thesis Title Use of Vietnam Steel Slag as Aggregate for Roller-Compacted Concrete Pavement

Author Mrs. Lam Ngoc Tra My

Major Program Civil Engineering

Academic Year 2017

ABSTRACT

This research was undertaken to investigate the feasibility of using Vietnam electric arc furnace (EAF) slag on roller-compacted concrete pavement (RCCP). In this research, EAF slag with size in range of 4.75 – 19 mm sourced from Southern Vietnam was used to replace natural coarse aggregate at three ratios of replacement (i.e. 0%, 50%, and 100%).

First of all, the feasibility of using Vietnam EAF slag as aggregate in RCCP was evaluated by the expansion testing. Then, RCCP characteristics made of EAF slag were assessed through the mixing proportions, mechanical properties and durability properties. Moreover, the effect of fly ash on RCCP made with EAF slag aggregate (slag-RCCP) also was studied in this work. Fly ash as cement substitution was used at three levels (i.e. 0%, 20%, and 40%) in the RCCP mixtures.

It was observed that the expansion value of EAF slag aggregate caused by hydration reactions is lower than 0.5% that is the limit value given by ASTM D4792. Therefore, Vietnam EAF slag exhibited the volume stability and can be used as coarse aggregate in RCCP after exposing to outdoor condition for several months. Furthermore, it was found that EAF slag used in this study is non-active aggregate by alkali-silica reactions.

The results from this study on RCCP showed that the optimum water content of slag-RCCP is higher than that of traditional RCCP. The natural aggregate replacement by EAF slag aggregate resulted in the compressive strength, splitting tensile strength and elastic modulus of RCCP decreased at all

ages. The higher the replacement ratio of EAF slag aggregate is, the lower the mechanical properties of RCCP is. And, there was a slight reduction of sulfate resistance of slag-RCCP. Nevertheless, slag-RCCP fulfilled the requirements of pavement. Additionally, the higher abrasion resistance of slag-RCCP in comparison with traditional RCCP was found.

On the other hand, fly ash as a partial cement substitution in slag-RCCP resulted in the reduction of mechanical and durability properties at early age. However, the conjunction of EAF slag aggregate and fly ash in the RCCP mixtures improved the mechanical and durability properties in the long-term ages. And, a replacement of 20% fly ash provided slag-RCCP which reached the strength and durability requirements for pavement.

ACKNOWLEDGMENTS

First of all, I would like to give my sincere thanks to my supervisors, Assoc. Prof. Dr. Saravut Jaritngam and Dr. Duc-Hien Le for their guidance and encouragement offered to me throughout my research.

I would like to express my deep appreciation to the examining committee members of this thesis – chaired by Assoc. Prof. Dr. Vatanavongs Ratanavaraha for their comments and recomendations.

I would like to acknowledge the financial support from the Higher Education Research Promotion and the Thailand's Education Hub for Southern Region of ASEAN Countries Project Office of the Higher Education Commission (Contract No. TEH-AC 032/2015) and PSU.GS. Financial Support for Thesis Scholarship.

I give many thanks to Ms. Supit Nontasorn, the staff of Department of Civil Engineering, Faculty of Engineering, Prince of Songkla University who assisted me in the office work. And, I am extremely grateful the kind assistance of Asst. Prof. Dr. Paramet Luathep for my studying.

I would like to convey my deepest gratitude to Mr. Truong Thanh Son – Vice president of Quality Assurance and Testing Center 3 (QUATEST 3) for giving me the testing equipment support in the testing house of QUATEST 3, Road No.1, Bien Hoa Industrial Zone 1, Dong Nai province, Vietnam. Special thanks to Mr. Tran Huynh Chuong and his colleagues at Civil Engineering Testing Lab who helped me make my experiments.

Finally, I would like to give the best wishes to my mother (Nguyen Thi Thuy Tien), my husband (Tran Hung Huan) and my daughter (Tran Ngoc Kim Ngan). Their unconditional love and overall support helped me overcome all difficulties.

CONTENTS

LIST OF TABLES

LIST OF FIGURES

LIST OF ABBREVIATIONS

ACI	American Concrete Institute
ACPA	American Concrete Pavement Association
ASR	Alkali-silica reactivity
ASTM	American Society for Testing and Materials
BOF	Basic Oxygen Furnace
BS EN	British Standard European Norm
CEB-FIP	The International Federation for Structural Concrete
C-S-H	Calcium-Silicate-Hydrate
EAF	Electric Arc Furnace
f-CaO	free lime
f-MgO	free periclase
ITZ	Interfacial transition zone
MAPE	Mean absolute percentage error
OD	Oven-dry
OPC	Ordinary Portland cement
RAP	Recycled asphalt pavement
RCC	Roller-compacted concrete
RCCP	Roller-compacted concrete pavement
SCC	Self-compacting concrete
SSD	Saturated-surface-dry
SSOS	Stainless steel oxidizing slag
SSRS	Stainless steel reducing slag
SEM	Scanning Electron Microscope
UPV	Ultrasonic pulse velocity
XRD	X-ray diffraction
CaO	Calcium oxide
SiO_2	Silica dioxide
FeO	Ferrous oxide

Fe_2O_3	Ferric oxide
Al_2O_3	Alumina
MgO	Magnesium oxide
MnO	Manganese oxide
Na_2O	Sodium oxide
K_2O	Potassium oxide
P_2O_5	Phosphorus pentoxide
$NaOH$	Sodium hydroxide
Na_2SO_4	Sodium sulfate
SO_3	Sulphuric anhydride
$Ca(OH)_2$	Calcium hydroxide
$Mg(OH)_2$	Magnesium hydroxide

LIST OF PUBLICATIONS

1. M.N. Lam, S. Jaritngam, D. Le, Roller-Compacted Concrete Pavement Made of Electric Arc Furnace Slag Aggregate : Mix Design and Mechanical Properties, Constr. Build. Mater. 154 (2017) 482–495. doi:10.1016/j.conbuildmat.2017.07.240.

2. M.N. Lam, S. Jaritngam, D. Le, EAF Slag Aggregate in Roller-Compacted Concrete Pavement: Effects of Delay in Compaction, Sustainability (Switzerland), 10(4), 1122. doi:10.3390/su10041122.

3. M.N. Lam, S. Jaritngam, D. Le, A Study on Mixing Proportion of Roller-Compacted Concrete Pavement Made of EAF Slag Aggregate and Fly Ash by Using Taguchi Method, The oral presentation to be delivered at 2018 2nd International Conference on Civil Engineering, Vietnam (Abstract).

4. M. Lam, S. Jaritngam, K. Wongsopanakul, P. Taneerananon, The possibility of using steel slag for pavement structure application in Vietnam, Proceeding of MAIREPAV8, Singapore 2016. doi:10.3850/978-981-11-0449-7-159-cd (Abstract).

REPRINTS WERE MADE WITH PERMISSION FROM THE PUBLISHERS

Paper 1

Paper 2

CHAPTER 1: INTRODUCTION

1.1. Introduction

Roller-compacted concrete (RCC) is a special type of concrete, that is stiff and no-slump. The first application of RCC for pavement (called roller-compacted concrete pavement) constructed in 1942 in North America. The use of RCCP has been increasing dramatically in recent years because of its strength, durability and its cost efficiency (Figure 1) [1]. RCCP has been used for many applications such as yards and port facilities, industrial access roads, large commercial parking areas, highway shoulders and residential streets.
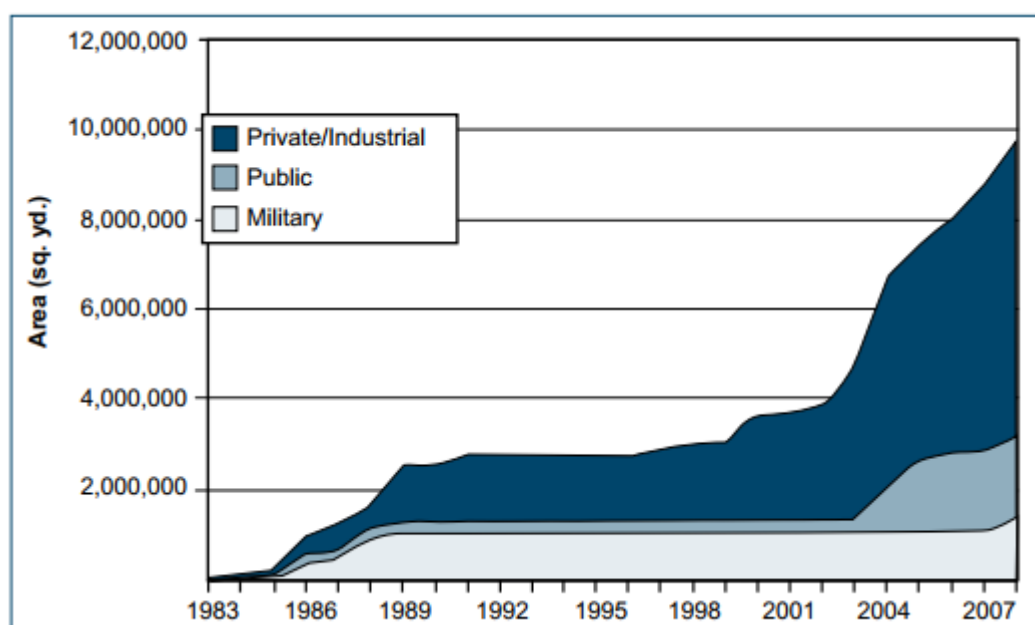
Figure 1. The use of RCCP since 1980s in the United States

Source: Harringtion et al. 2010 [2]

Ketema et al. [3] have proved that rigid pavement has twice longer service life than flexible pavement. And, the routine and periodic maintenance of rigid pavement for 40 years are similar to those of flexible pavement. However, the asphalt concrete pavement (flexible pavement) is the most popular in Vietnam, that was 9,303 km comprising 55% of total road length of Vietnam in 2012, whereas the cement concrete pavement (rigid pavement) was 4% [4]. A lack of construction technology is a main cause to constrain the development of rigid pavement in Vietnam.

Nowadays, a sustainable infrastructure development has become increasingly important to all countries around the world. The using of waste or by-product materials in infrastructure construction is one of solution to achieve the sustainability. World steel production has rapidly increased over the last years (Table 1). For example, the world steel production reached 1,621 million tons in 2015. An increase of 40% as compared to 2005, and an increase of 120% as compared to 1995. On average the production of 1 ton of steel results in 330 kg of by-products. The main by-products are slags. The output of steel slag was estimated in the range of 170 million to 250 million tons in 2015.

Vietnam is the 24 rank of major steel producing countries in 2015) [5]. In Southern Vietnam, the manufacture of steel is electric arc furnace process, and the steel output is 4.1 million tons in 2015 leading to the 1 million tons of electric arc furnace (EAF) slag production. The traditional stockpile method of steel slag in Vietnam has created challenging environmental issues such as a lack of waste storage areas and pollution of soil and underground water. In recent years, the using of EAF slag as aggregate alternative in concrete was attracted many study. The results of these study have demonstrated that EAF slag can be replaced aggregates in many kinds of concrete [6]–[8]. The recycling of EAF slag as aggregate replacement in concrete reduces the environmental impacts. Moreover, a natural aggregate substitution by EAF slag leads to reduce the consumption of natural aggregates.

RCCP mixture contains less binder and higher aggregate which is different with conventional concrete mixture. Typically, the dosage of aggregate is about 75% in RCCP mixture (Figure 2) [2]. On the other hand, the construction of RCCP is similar to that of hot-mix asphalt pavement. RCCP is paved by high-density pavers and compacted by a vibratory/ static rollers combination to attain a target density and homogeneous surface pavement (Figure 3) [2]. Therefore, the replacement of asphalt concrete by RCCP made of EAF slag as aggregate will the new trend with many benefits in Vietnam.

Table 1. World crude steel production from 2000 to 2015 (million tones)

Years	Crude steel production
2000	850
2001	852
2002	905
2003	971
2004	1,063
2005	1,148
2006	1,250
2007	1,348
2008	1,343
2009	1,239
2010	1,433
2011	1,538
2012	1,560
2013	1,650
2014	1,670
2015	1,621

Source: World Steel Association 2016 [5]
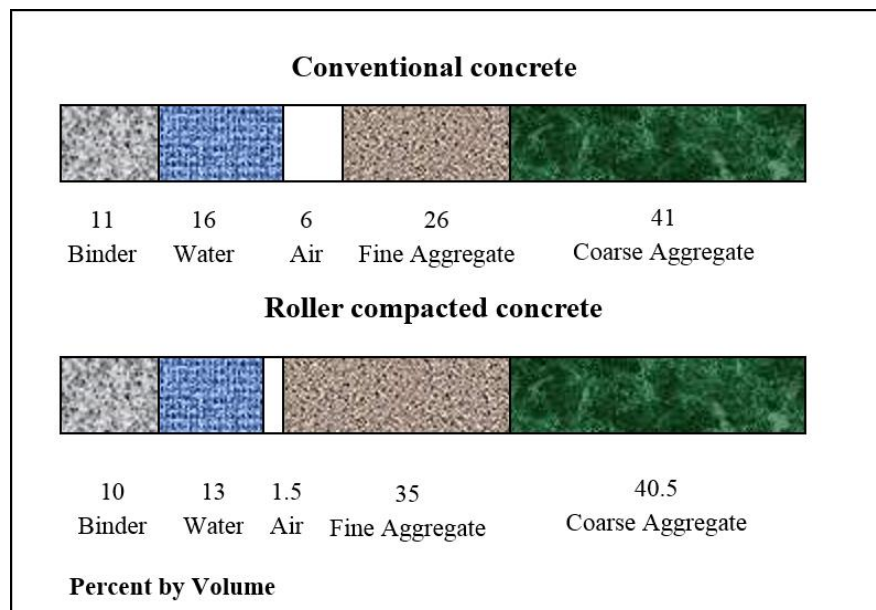
Figure 2. Mixing proportions of conventional and roller-compacted concrete

Source: Harrington et al. 2010 [2]

Figure 3. The placement and compaction of RCCP

Source: Harrington et al. 2010 [2]

Additionally, fly ash is a by-product from burning pulverized coal in electric power plants produced around 16 million tons in Vietnam in 2015. The fly ash output is estimated about 26 million tons in 2020. Nevertheless, the recycling of fly ash in Vietnam was 30% of production over the last years. The storage areas are 700 ha that creates the challenging environmental issues. Furthermore, the use of fly ash as cement substitution in concrete is increasing all the world because it improves some properties of concrete, and often results in lower cost concrete. Fly ash as cement used in concrete enhances workability, ultimate strength and improves durability. American Concrete Institute suggested that the replacement of cement by fly ash is generally in range of 15 – 20% of the total volume of cementitious material [1]. Similar to in Guide of RCCP report of Institute for Transportation, Iowa State University [2]. A maximum of fly ash content in RCCP is 25% following American Concrete Pavement Association [9].

Based on the prior researches, EAF slag aggregate in conjunction with fly ash sourced from Southern Vietnam were employed to develop RCCP in this study as a solution to resolve challenging environmental issues and create the development of sustainable infrastructure.

1.2. Objectives

The aim of this research is to investigate the feasibility of using Vietnam EAF slag as aggregate and fly ash as a partial cement substitution in RCCP.

1.3. Scope of study

This study focuses on the recycling of EAF slag and fly ash in the Southern Vietnam. The following works have been done to meet these objectives of this study.

1.3.1. Study on the physical properties (i.e. specific gravity, density, water absorption, Los Angeles abrasion), the chemical composition and the expansion characteristic from hydration reactions of EAF slag aggregate.

1.3.2. Study on RCCP made of EAF slag aggregate. In this work, EAF slag aggregate with size in range of 4.75 – 19 mm was used to replace natural aggregate in RCCP at three ratios (i.e. 0%, 50%, and 100%).

- The mixing proportions was studied by soil compaction method to determine the optimum moisture content of mixtures.

- The mechanical properties (i.e. compressive strength, splitting tensile strength, modulus of elasticity).

- The durability properties (i.e. water absorption, abrasion resistance, sulfate resistance).

- The effect of delay in compaction on compressive strength, splitting tensile strength and modulus of elasticity.

1.3.3. Study on RCCP made of EAF slag aggregate and fly ash as a partial cement substitution. In this part, the replacement of cement by fly ash was investigated at three levels (i.e. 0%, 20%, and 40%).

- The mixing proportions was studied by soil compaction method to determine the optimum moisture content of mixtures.
- The mechanical properties (i.e. compressive strength, splitting tensile strength, modulus of elasticity).
- The durability properties (i.e. water absorption, abrasion resistance, sulfate resistance).

1.3.4. Expansion of mortar bars made by fine EAF slag aggregate

- Expansion by autoclave testing.
- Expansion by alkali-silica reactions.

CHAPTER 2: LITERATURE REVIEW

2.1. Steel slag

The ferrous slags that are generated from the metal industry can be summarized in two different types: blast furnace slag and steel slag. The melting separation of iron ore produced the pig iron and blast furnace slag (Figure 4). Blast furnace slag can be classified in many types, such as granulated slag, air-cooled slag, and pelletized/expanded slag that depend on the way of formation. After that the pig iron is used to produce steel. Steel slag is a by-product from steelmaking process in which lime or dolomite reacts with the pig iron or steel scrap to produce the quality steel. The output of steel slag is about 150 kg per ton of molten steel [10]. Steel slag can be produced from various processes that include Basic Oxygen Furnace and Electric Arc Furnace.

2.1.1. Basic Oxygen Furnace slag

Basic Oxygen Furnace (BOF) process combines hot molten iron with scrap and fluxing agent (e.g. lime) that produces the quality steel and BOF slag. The oxygen with high pressure is blown into the chamber to remove the impurities (Figure 5a). The constituents of these impurities consist of carbon in the form of gaseous carbon monoxide, silicon, manganese, phosphorous and iron oxides. BOF slag is produced by the combination of the impurities and lime [11].

2.1.2. Electric Arc Furnace slag

Electric Arc Furnace (EAF) process uses steel scrap to produce a new alloy carbon steel. In this process, the scrap-steel is heated by an electric current in the furnace (Figure 5b). During the melting process, other metals with differently chemical elements (e.g. magnesium, aluminum, and silicon) depended on the furnace are added to the mixture to help remove the impurities. The impurities removed from the molten steel is EAF slag [11].

2.1.3. Secondary slags

       Secondary slags are by-product of secondary steelmaking processes in which the molten steel from BOF or EAF process is refined to obtain the high-quality steels. The most common type is Ladle Furnace slag [11].
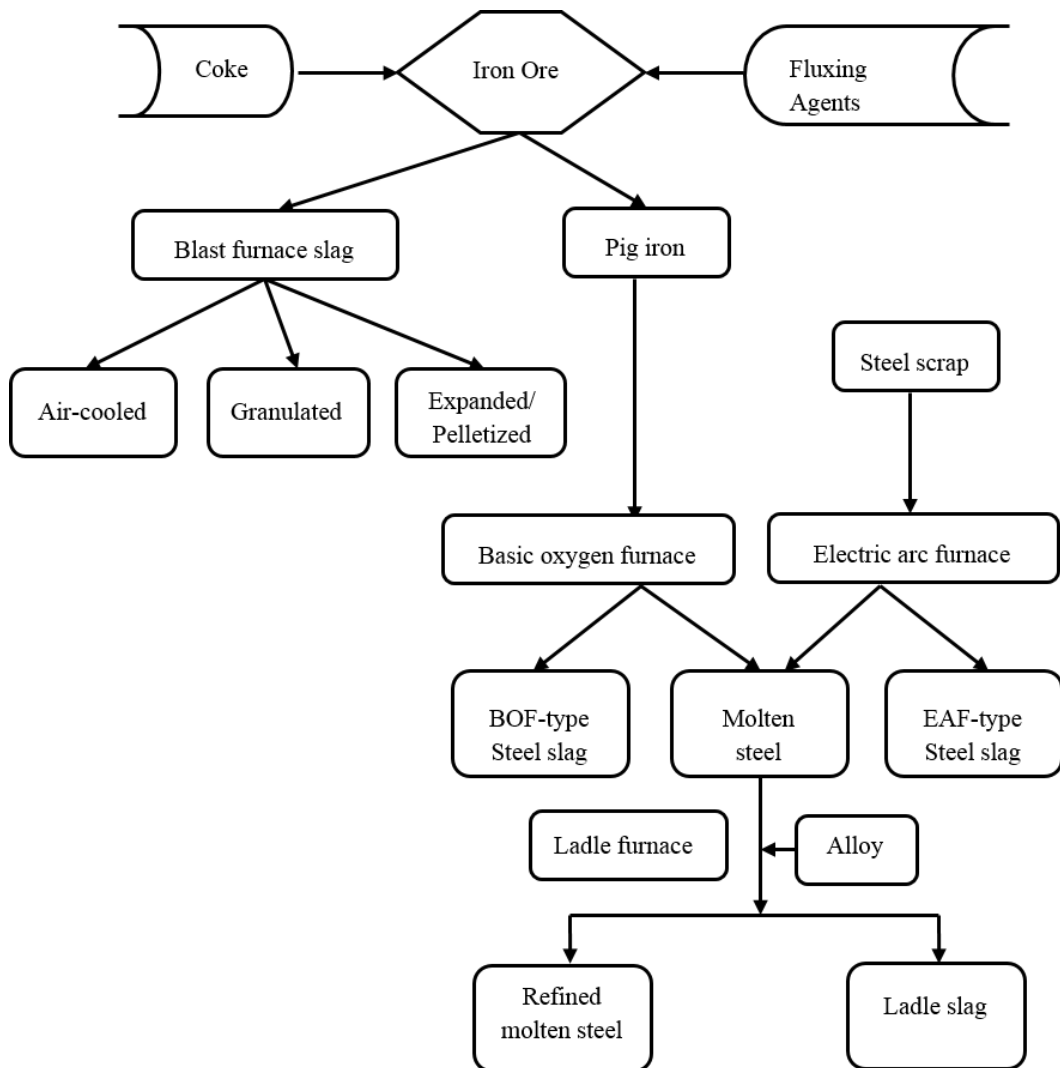
Figure 4. Type of iron making slag (blast furnace slag) and steel making slag

(a) BOF process   (b) EAF process
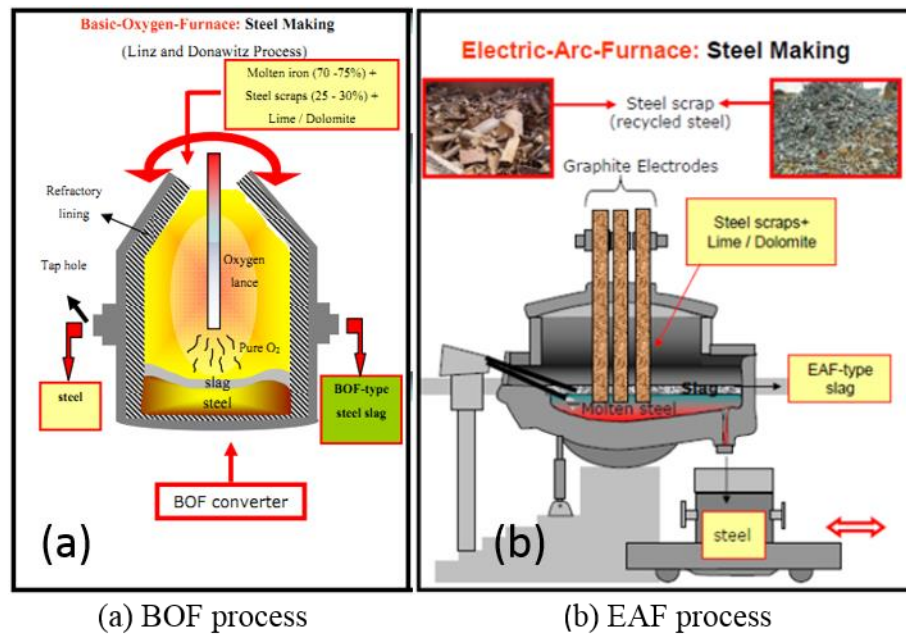
Figure 5. Schematic illustration of BOF and EAF process

Source: Prezzi and Yildirim 2009 [11]

2.2. Utilization of steel slag

2.2.1. An aggregate substitution

2.2.1.1. In asphalt concrete

Ameri et al. [12] used EAF slag as natural coarse aggregate substitution in warm mix asphalt. The results indicated that the marshall stability was improved with the use of EAF slag coarse aggregate in warm mix asphalt. Moreover, the tensile strength, resilient modulus and resistance were also enhanced in warm mixture asphalt containing EAF slag aggregate. Similarly, Pasetto and Baldo [13] have demonstrated that the asphalt concrete with EAF slag exhibited good values of marshall stability and marshall quotient. Furthermore, the high angularity and rough texture of EAF slag improved the durability properties of mixture in comparison to those of control mixture in terms of stiffness, fatigue resistance and the resistance to permanent deformation. Besides, the asphalt concrete pavement using BOF slag as aggregate showed that the marshall stability, indirect tensile strength, and resilient modulus were better than those of the conventional asphalt concrete pavement [14]. After 2 years of service, the quality of BOF slag asphalt concrete decreased at a slower ratio than traditional asphalt concrete [14].

2.2.1.2. In base or subbase layers of road pavement

Rohde et al. [15] stated that the use of EAF slag as pavement material is possible and pavement made by EAF slag had the good quality. For example, the resilient modulus of densely graded steel slag reached 500 MPa that is higher than those of traditional aggregates. The investigation of Mathur et al. [16] presented that both of blast furnace slag and steel slag can be applied in base and subbase layers of a road pavement after left outdoor condition for several months. Additionally, the incorporation of 50 percent blast furnace slag, 20 percent steel slag, 20 percent granulated slag, 6 percent fly ash, and 4 percent lime can be used as a bound material for subbase in road pavement. Pamukcu and Tuncan [17] indicated that the unconfined compressive strength of cement-stabilized steel slag aggregate achieved 158 kPa after 45-day curing, which can be recommended to use in base or subbase layers for both of light and heavy traffic.

2.2.1.3. In concrete

Most of the research focus on the using of steel slag as aggregate in concrete. Manso et al. [18] indicated that concrete made with EAF slag as aggregate showed the good mechanical properties and its durability met the requirements in usage. Similarly, the results of Adegologe et al. [19] presented that the using of EAF slag as aggregate improved slightly the mechanical properties of concrete, whereas there was a reduction of the durability in concrete containing steel slag. However, the characteristic of slag-concrete reached the standards request for using. Besides, steel slag also performed as a good aggregate in high performance concrete. Compressive strength of self-compacting concrete (SCC) containing EAF slag as aggregate increased by 21% over control SCC at 28 days [20], whereas that of SCC containing stainless steel slag is 10-23% better than the control at 91 days [21]. Faleschini et al. [7] showed that the high performance concrete containing 100% EAF slag as coarse aggregate had the mechanical properties better than the reference concrete, including compressive strength, tensile strength and elastic modulus. Additionally, the geopolymer concrete with steel furnace slag coarse aggregate offered higher compressive

strength, surface resistivity and pulse velocity than that of geopolymer concrete with traditional aggregate [22]. The using of steel slag in alkali-activated concrete reduced slightly the durability performance. However, it was found that the durability of alkali-activated slag concrete was better than that of Portland cement concrete [8].

2.2.2. A cement substitution

Qiang et al. [23] used the ground BOF steel slag as a cement substitution in concrete. This research indicated that the cement dosage replaced by 0-15% of steel slag resulted in the mechanical and durability properties of concrete reduction. However, concrete containing steel slag as partial cement replacement fulfilled the requirements of strength and durability to apply in structure. In addition, Sheen et al. [24] presented that stainless steel reducing slag (SSRS) can be replaced partially cement in self-compacting concrete (SCC). SCC made with 30% SSRS or less achieved the required 28-day strength of 35 MPa. SCC containing 0-50% SSRS have the water absorption values in range of 3-5% after 7-day of curing. Moreover, the sulfate resistance of SCC containing 10% SSRS is better than that of reference concrete throughout seven drying-soaking circles in sulfate environment.

2.3. Properties of EAF slag

The properties of EAF slag are very important to its feasibility to replace natural aggregates in RCCP. EAF slag characteristics depends on the grades of scrap-steel, the quantities of additives, and the process of manufacture.

2.3.1. Physical properties

The major difference between the EAF slag and natural aggregate is specific gravity. The specific gravity of EAF slag aggregate is higher than that of natural aggregates because of the higher content of iron oxides in EAF slag (see Table 2). The unit weight of the EAF slag particles is approximately $1500 - 2000$ kg/m^3 [10]. Moreover, EAF slag has the angular shape and rough surface texture. And, it has low crushing value, and high abrasion resistance [25]. Water absorption of EAF slag depends on size of aggregate (see Table 2).

Table 2. Physical properties of EAF slag

Physical property	Adegoloye et al. [19]	Sekaran et al. [26]	Yeih et al. [27]
Specific gravity	2.8	2.9	3.44
Unit weight (kg/m^3)	NA	1540	NA
Water absorption (%)	2.6	2.0	3
Los Angeles abrasion (%)	23	16.4	NA

Note: NA means not available

2.3.2. Chemical composition

The results of many research showed that the main composition of the EAF slag is CaO, SiO$_2$, FeO, Fe$_2$O$_3$ that depends on the smelting and refining process. The rest is Al$_2$O$_3$, MgO, and MnO (see Table 3).

2.3.3. Mineralogical components

EAF slag consists high iron oxide content so wustite is typically obtained in mineralogical component of EAF slag. Additionally, merwinite, olivine, dicalcium silicate, tricalcium silicate, tetra-calcium aluminoferrite, and free lime, and free periclase are the common minerals of EAF slag [25], [31].

2.3.4. Expansion phenomenon

Due to the presence of unstable phases in its mineralogy (e.g. free lime, free periclase), EAF slag may be showed volumetric instability. This phenomenon results from free lime (f-CaO) hydrates to form Ca(OH)$_2$, or free periclase (f-MgO) hydrates to form Mg(OH)$_2$, their volume become about twice their original size. This behavior leads to cracking and deterioration of concrete.

Hydration of free lime Eq. (1)

$$CaO + H_2O \rightarrow Ca(OH)_2 \tag{1}$$

Hydration of free periclase Eq. (2)

$$MgO + H_2O \rightarrow Mg(OH)_2 \tag{2}$$

KuO et al. [32] displayed that the formation of Ca(OH)$_2$ is a primary cause of cracking concrete. Ramachandran et al. [33] have demonstrated that f-CaO immersed in water can hydrate almost completely in a few days. Therefore, one of methods to reduce the f-CaO content of steel slag is the weathering process.

According to this method, steel slag was exposed to outdoor environment and sprayed with water every day. Le et al. observed that f-CaO content of the stainless steel oxidizing slag (SSOS) reduced from 1.2% to 0.61% when SSOS was left in outdoor condition for 8 months [34]. f-CaO content of steel slag used as a granular base or subbase must have less than 4% to limit the effect of volume instability [35]. Nevertheless, some of f-CaO may not hydrate due to embedding in small pockets in steel slag particles, and the hydration of f-MgO occurred slowly for many months or years. Lun et al. [36] have demonstrated that the hydration of f-CaO and f-MgO almost accomplished under autoclave condition. Therefore, the autoclave expansion test of slag-mortar bar can be used to confirm the stabilization of slag [37].

Table 3. Chemical composition of EAF slag (% weight)

Oxide composition (wt. %)	Manso et al. [18]	Arribas et al. [28]	Faleschini et al. [29]	Monosi et al. [30]
CaO	23.9	25.72	30.30	26
$\sum$ Iron oxides	42.5	27.54	33.28	35
SiO_2	15.3	17.88	14.56	14
MgO	5.1	3.82	2.97	5
Al_2O_3	7.4	11.62	10.20	12
MnO	4.5	4.15	4.34	6
Na_2O	NA	0.71	NA	0.41
K_2O	NA	0.1	NA	0.2
P_2O_5	NA	NA	NA	0.1
f-CaO	NA	0.46	NA	NA
	0.45	NA	NA	NA

Note: NA means not available

2.4. Roller-compacted concrete pavement (RCCP)

2.4.1. Mixing proportion of RCCP

Roller-compacted concrete (RCC) is a special type of concrete that is stiff, no-slump. Materials of RCC are similar to those of conventional concrete, including binder, aggregate, water, and admixtures (if any). However, RCC contains less binder than conventional concrete, that is approximately 10% of mix weight. Because of zero-slump feature, pavements that are constructed by RCC do not use forms, dowels, or reinforcing steel. RCC is placed with an asphalt-type paver and compacted by vibratory/ static rollers leading to roller-compacted concrete pavement (RCCP) is strong, dense and durable. In order to attain a target density and homogeneous surface pavement, fine aggregate (0-4.5 mm) in RCCP is higher than conventional concrete, and aggregate must have a good gradation [2]. Moreover, RCCP mixture should be stiff enough to remain the stability of vibratory rollers and wet enough to distribute the paste without segregation. Therefore, the optimum moisture content of mixture is one of primary parameters deciding the quality of RCCP. The soil compaction method to determine the optimum moisture content of RCCP mixtures is the most widely method. According to this method, the RCCP mixture design process consists of following steps:

Step 1: Choose well-graded aggregates

The upper and lower limit gradation with maximum aggregate size of 19mm is listed in Table 4 and Figure 6 [9]. The 0.45-power curve can be used to reach the maximum density of mixture [38]. And, the quality of RCCP depend on the quality of aggregate because aggregate constitutes up to 85% of the volume of RCCP. Thus, aggregate must meet the requirements of ASTM C33 and other RCCP standards.
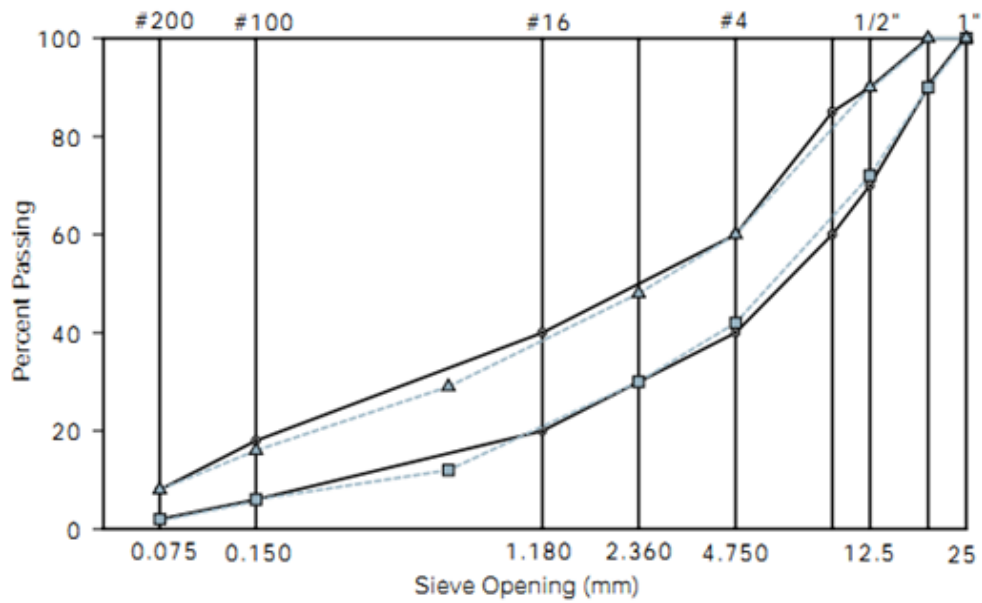
Figure 6. The upper and lower limit gradation of RCCP

Source: ACPA 2014 [9]

Table 4. The upper and lower limit gradation of RCCP

Sieve size	Lower & Upper Specification Limits 3/4 in (19.0 mm)	
1 in. (25 mm)	100	100
3/4 in. (19 mm)	95	100
1/2 in. (12.5 mm)	70	95
3/8 in. (9.5 mm)	60	85
No. 4 (4.75 mm)	40	60
No. 8 (2.36 mm)	30	50
No. 16 (1.18 mm)	20	40
No. 30 (600 μm)	15	30
No. 50 (300 μm)	10	25
No. 100 (150 μm)	2	16
No. 200 (75 μm)	0	8

Source: ACPA 2014 [9]

Step 2: Select a mid-range cementitious content

Literature shows that the weight of binder in RCCP has been typically used in range of 11-13% of the total weight of binder and oven-dried aggregates [2]. Many types of binder can be used in RCCP, such as hydraulic cement, blended cements, or the incorporation of hydraulic cement and pozzolan.

Step 3: Develop moisture-density relationship plots

The relationship between moisture and density of mixture is determined by the modified Proctor test (ASTM D1557). Then, the optimum moisture content of mixture is found from the compaction curve (Figure 7). For most aggregates, the optimum moisture content of RCCP is in range of 5-8% [2].
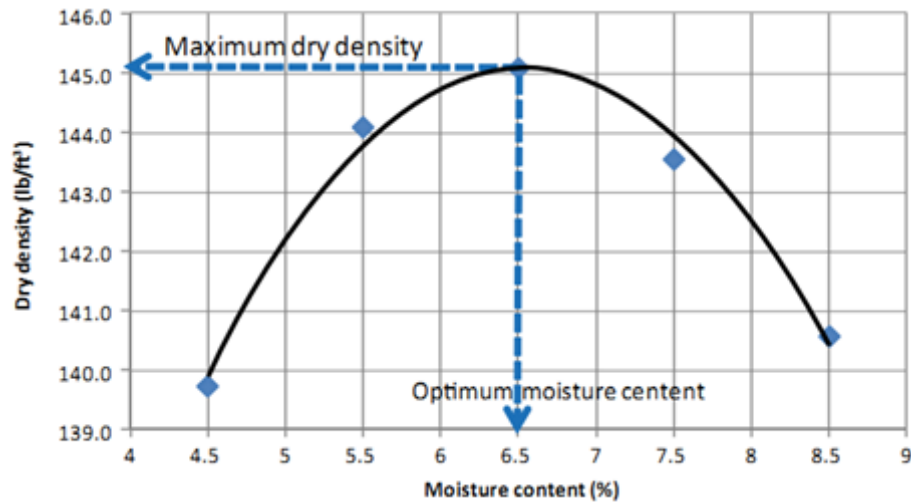
Figure 7. The compaction curve

Source: Harrington et al. 2010 [2]

2.4.2. RCCP made with waste or by-product aggregates

Debieb et al. [39] used virgin and contaminated recycled concrete aggregates created from crushing of natural concrete slabs to produce RCCP. RCCP with 100% of virgin coarse and fine recycled concrete aggregates decreases compressive strength by 30% and splitting tensile strength by 56% as compared to its reference. This study revealed that the contaminated recycled concrete aggregates (e.g. chlorides, sulphates, siliceous gel) do not have an impact on strength. Settari et al. [40] investigated the recycled asphalt pavement (RAP) materials on the performance of RCCP. The test of compressive strength showed a reduction in strength for all replacement ratios of fine, coarse or both fine and

coarse natural aggregates by RAP aggregate. However, when substituting 50% of natural aggregate with RAP aggregate, the mixture can be used as sub-base for road pavements or low traffic pavements. Meddah et al. [41] used shredded rubber tires substituted for crushed gravel at different volumes from 0% to 25% in RCCP. There was a slight decrease in the unit weight, mechanical properties and water absorption of RCCP with increasing rubber content. If the roughness of rubber surface was treated, the compressive strength can be risen from 11% to 28% and the splitting tensile strength can be risen from 15% and 20%. Moreover, recycling shredded rubber improved the ductility and porosity of RCCP.

2.4.3. RCCP made with fly ash as cement substitution

American Concrete Institute suggested that the replacement of cement by fly ash is generally in range of 15 – 20% of the total volume of cementitious material, that is similar to in Guide of RCCP report of Institute for Transportation, Iowa State University. A maximum of fly ash content in RCCP recommened by American Concrete Pavement Association is 25%. However, many scholars try to recycle fly ash as cement substitution in concrete with high-volume. Mardani-Aghabaglou et al. [42] have used 20%, 40%, and 60% of fly ash as cement substitution in RCCP. It was observed that RCCP using fly ash as cement decrease the strength and durability properties at early ages. 60% of fly ash content caused the lowest strength and durability values. However, the pozzolanic of fly ash increased the strength and durability properties of RCCP at long-term age. The strength of RCCP containing 60% fly ash reached the satisfactory requirements for pavement. Besides, cement was replaced by fly ash with high volume ranging from 60% to 70% resulted in the improvement of the permeability, absorption, sorption and chloride diffusivity of RCCP [43]. Additionally, the using of fly ash as cement in RCCP containing the manufactured sand enhanced the Cantabro abrasion resistance and surface abrasion resistance in comparison with its referenced concrete [44].

Table 5 shows the previous study on EAF slag as aggregate replacement in concrete. And, Table 6 shows the previous study on fly ash as a partial cement substitution in RCCP.

Table 5. The previous research on EAF slag as aggregate replacement in concrete

No.	Types of concrete	Research
1	Conventional concrete	Manso et al. [18]
		Sekaran et al. [26]
		Arribas et al. [28]
		Monosi et al. [30]
		Coppola et al. [45]
2	High performance concrete	Sheen et al. [21]
		Faleschini et al. [7]
		Singh et al. [46]
3	Alkali-activated concrete	Khan et al. [22]
		Palankar et al. [8]
4	Roller-compacted concrete	A few research

Table 6. The previous research on fly ash as a partial cement substitution in RCCP

No.	The fly ash content as a partial cement substitution in RCCP	Research
1	15 – 20%	American Concrete Institute [1]
2	15 – 20%	Institute for Transportation, Iowa State University [2]
3	25%	American Concrete Pavement Association [9]
4	40 – 85%	Yerramala and Babu [43]
5	20 – 60%	Mardani – Aghabaglou et al. [42]
6	0 – 60%	Rao et al. [47]

CHAPTER 3: RESEARCH METHOD

This study used lab experiments with four stages as shown in Table 7 to investigate the feasibility of using EAF slag as aggregate in RCCP, and the incorporation of fly ash as a partial cement substitution in RCCP made of EAF slag aggregate.

Table 7. Research framework and method

	Experiments on EAF slag aggregate		
	Content	**Outcome**	**Method**
Stage I	The treatment of EAF slag aggregate	Reduce the expansive potential of EAF slag aggregate	The weathering process at least 3 months
	The study on the physical properties of EAF slag aggregate	Apparent specific gravity	ASTM C127
		Density (OD, SSD)	ASTM C127
		Bulk density	ASTM C127
		Water absorption	ASTM C127
		Los Angeles abrasion	ASTM C131
	The study on the chemical composition of EAF slag aggregate	Chemical composition	ASTM C25
		f-CaO	Test method of Ministry of Transportion of Ontario
	The study on the expansive potential of EAF slag aggregate from hydration reactions	The expansive value	ASTM D4972

Table 7. Research framework and method (cont.)

	Experiments on RCCP made of EAF slag aggregate		
	Content	**Outcome**	**Method**
Stage II	The mixing proportions	The optimum moisture content of mixture	ASTM D1557
	The mechanical properties	The compressive strength	ASTM C39
		The splitting tensile strength	ASTM C496
		The modulus of elasticity	ASTM C469
	The durability properties	The water absorption	BS EN 1338
		The abrasion resistance	BS EN 1338
		The sulfate resistance	-
	The delay in compaction	The compressive strength	ASTM C39
		The splitting tensile strength	ASTM C496
		The modulus of elasticity	ASTM C469
	Experiments on RCCP made of EAF slag aggregate and fly ash		
	Content	**Outcome**	**Methodology**
Stage III	The mixing proportions	The optimum moisture content of mixture	ASTM D1557
	The mechanical properties	The compressive strength	ASTM C39
		The splitting tensile strength	ASTM C496
		The modulus of elasticity	ASTM C469
	The durability properties	The water absorption	BS EN 1338
		The abrasion resistance	BS EN 1338
		The sulfate resistance	-

Table 7. Research framework and method (cont.)

	Experiments on mortar bars		
	Content	**Outcome**	**Method**
Stage IV	Expansion by autoclave testing	The expansion value	ASTM C151
	Expansion by alkali-silica reactions	The expansion value	ASTM C1260

3.1. Experiments on EAF slag aggregate

EAF slag aggregate with size in range of 4.75 – 19 mm sourced from Southern Vietnam (Figure 8) was used to substitute for natural coarse aggregate.

Figure 8. EAF slag aggregate used in this study

First of all, the EAF slag was exposed to outdoor conditions and sprayed with water every day for 90 days in order to reduce the expansive potential.

After the weathering process, the EAF slag aggregate was examined the physical properties, the chemical composition, the f-CaO content and the expansive potential from hydration reactions.

3.1.1. The physical properties of EAF slag aggregate

The physical properties (i.e. specific gravity, unit weight, water absorption, and Los Angeles abrasion) of the EAF slag was examined following ASTM standards [48]–[50].

3.1.2. The chemical composition and f-CaO of EAF slag aggregate

The chemical composition of EAF slag aggregate was examined following the ASTM C25 standard [51].

The f-CaO content of EAF slag aggregate in this study was determined following a test method of Ministry of Transportation of Ontario [52] through ethylene glycol and complexometric titration.

3.1.3. The expansion testing by hydration reactions

The ASTM D4792 [53] standard was used in this study to test the expansive potential of EAF slag aggregate after treatment process.

In order to compare the expansive potential of natural aggregate and EAF slag aggregate, two types of samples were prepared in this test. The first sample is 100% EAF slag aggregate with size in range of $4.75 - 19$ mm. And the second sample is 50% EAF slag aggregate plus 50% crushed stone with size in range of $4.75 - 19$ mm.

Before the expansion testing two samples were determined the optimum moisture content following ASTM D1557 [54]. Then, three specimens of each aggregate sample were prepared in a 6-in cylinder mold following ASTM D1883 [55] with the optimum moisture content determined in the previous step.

After that, the testing specimen molds were stored in water at $70 \pm 3\ ^0$C to accelerate the hydration reaction conforming to ASTM D4792 (Figure 9). After 30 minutes of imersion, the initial dial gage readings of each sample were recorded. The volume expansion was calculated daily for 14 days by dividing the difference between the daily dial gage reading and the base reading and the initial specimen height (116.43mm).
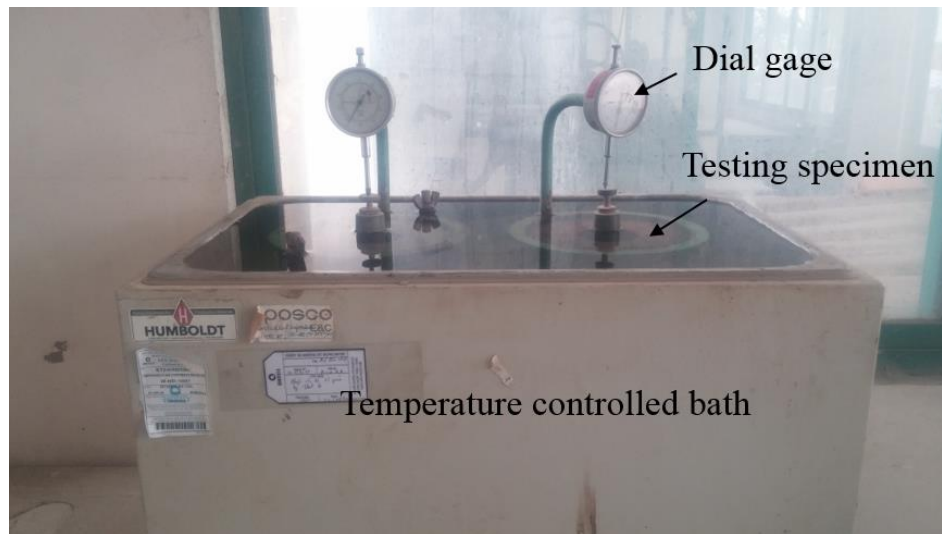
Figure 9. The testing specimens were stored in water at $70 \pm 3\ {}^{0}C$

3.2. Experiments on RCCP made of EAF slag aggregate

3.2.1. Materials

In this work, type I Ordinary Portland Cement (OPC) with the specifications in accordance with ASTM C150 was used in this study [56]. The chemical composition and physical characteristics of OPC are shown in Table 8.

Class F fly ash with chemical composition as listed in Table 4 as cement replacement sourced from Southern Vietnam was used in this study [57].

Natural aggregates (fine and coarse) used in this study are 0-19 mm of crushed stone with the designing gradation as shown in Figure 10. The maximum aggregate size is 19 mm to reduce the potential segregation and improve the smooth pavement surface. Their physical properties were listed in Table 9 fulfilling the quality requirements of ASTM C33 [58].

Table 8. Chemical composition and physical properties of OPC and fly ash

	OPC	Fly ash
Chemical composition (%)		
Silica (SiO_2)	20.7	52.3
Alumina (Al_2O_3)	4.5	24.9
Ferric oxide (Fe_2O_3)	3.3	14.1
Calcium oxide (CaO)	63.0	NA
Magnesium oxide (MgO)	1.8	NA
Sodium oxide (Na_2O)	0.10	0.67
Potassium oxide (K_2O)	0.74	NA
Sulphuric anhydride (SO_3)	2.3	0.47
Loss on ignition (LOI)	2.8	0.15
Physical characteristics		
Fineness (Blaine) (m^2/kg)	347	289
Specific gravity	3.14	2.40
Initial setting time (min)	110	NA
Final setting time (min)	170	NA
Particle composition - Retaining on 45 µm sieve (%)	NA	7.92
Compressive strength (N/mm^2)		
1 day	14.6	NA
3 days	26.2	NA
7 days	33.0	NA
28 days	43.0	NA

Note: NA means not available
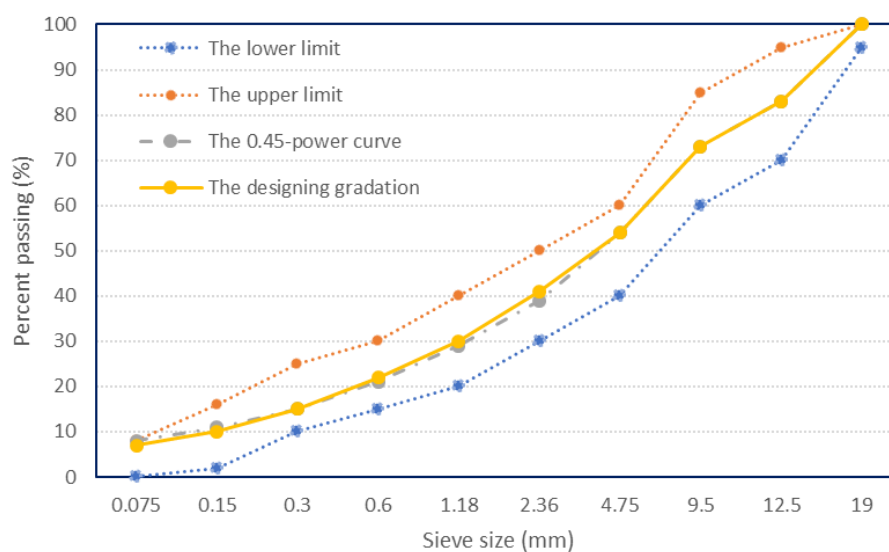
Figure 10. The suggested limits of RCCP aggregate gradation, the 0.45-power curve for 19 mm maximum size and the designing gradation used in this study

Table 9. Physical properties of the crushed stone aggregate

Properties	Crushed stone	
	Fine aggregate (4.75 - 0 mm)	Coarse aggregate (19 - 4.75 mm)
Apparent specific gravity	2.71	2.72
Density (OD) (kg/m^3)	2609	2680
Density (SSD) (kg/m^3)	2644	2691
Bulk density (kg/m^3)	1493	1466
Water absorption (%)	1.36	0.44
Los Angeles abrasion (%)	NA	13.98

Note: NA means not available

3.2.2. Testing program of RCCP

3.2.2.1. Mixing proportion

The weight of binder in RCCP mixtures was fixed at 12% of total weight of binder and oven-dried aggregates in the mixtures. RCCP mixture used three types of coarse aggregate, i.e. group A, group B, and group C.

- Group A was prepared with 100% crushed stone coarse aggregate.

- Group B was prepared with 50% crushed stone coarse aggregate plus 50% EAF slag coarse aggregate.
- Group C was prepared with 100% EAF slag coarse aggregate.

As a result, three mixtures (see Table 10) were conducted the modified Proctor test conforming ASTM D1557 (Figure 11) to determine the optimum moisture content [54]. Then, the results of Proctor test were used to establish the compaction curve that presented the relationship between the dry density and the moisture content of mixtures. The optimum moisture content and maximum dry density of each mixture were determined from the compaction curve.

Table 10. RCCP mixtures were prepared to determine the optimum moisture content

Group	Mixture	Binder	Coarse aggregate			Fine aggregate
		OPC (kg/m^3)	EAF slag (%)	EAF slag (kg/m^3)	Crushed stone (kg/m^3)	Crushed stone (kg/m^3)
A	A00	274	0	0	842	1163
B	B00	275	50	424	424	1172
C	C00	282	100	867	0	1197
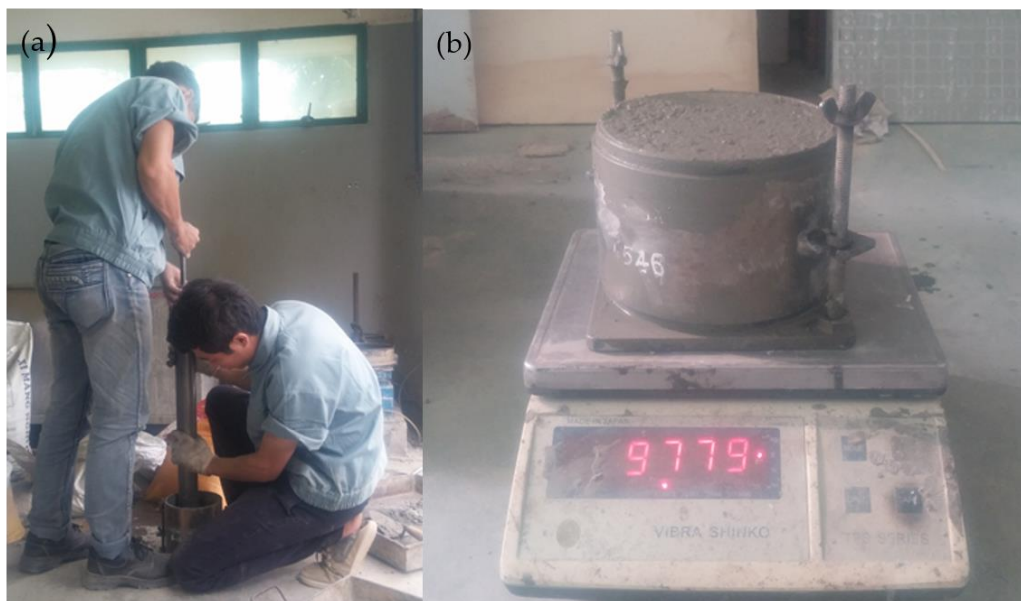
(a) the compaction of mixture, (b) determining the density of mixture

Figure 11. The modified Proctor test

3.2.2.2. Mechanical properties

After identifying the optimum moisture content of RCCP mixtures, the standard cylindrical specimens of 150 mm diameter and 300 mm height were prepared to examine the mechanical properties of RCCP. The cylindrical specimens were casted by vibrating hammer in four layers (Figure 12) and the compaction time is 20 seconds per layer conforming to ASTM C1435 [59].

The fresh unit weight of RCCP was measured after molding. All specimens were molded for 24h at the temperature of 23 ± 2^0C after molding. After 24h, the samples were removed from the mold and their hardened unit weight were measured. Then, all specimens were cured in tap water at the temperature of 23 ± 2^0C until testing ages (Figure 13).

Figure 12. The 150 x 300 mm cylinder specimen and the vibrating hammer

Figure 13. The curing of specimens in tap water

The compressive strength, splitting tensile strength and modulus of elasticity were used to investigate the mechanical properties of RCCP. At least 16h before testing, the cylinder specimens underwent capping procedure in accordance with ASTM C617 [60], in which sulfur mortar was used to give them a plane surface. The compressive strength and splitting tensile strength were tested at 3, 7, 28 and 91-day ages in accordance with ASTM C39 [61] and ASTM C496 [62]. The modulus of elasticity was obtained at the age of 91 days in accordance with ASTM C469 [63].

3.2.2.3. Delay in compaction

In present work, the effect of delay in compaction on the mechanical properties of RCCP (i.e. compressive strength, splitting tensile strength, ultrasonic pulse velocity, and elastic modulus) was assessed. The span time between mixing completion and compaction was 0, 15, 30, 60, and 90 min.

Because the higher water absorption of EAF slag aggregate, the relationship between the water absorption of EAF slag aggregate and the immersion time was investigated. The samples were immersed in water at room temperature for 5 min, 10 min, 15 min, 30 min, 60 min, 90 min, 2 h, 4 h, 8 h, and 24 h. Then, the water absorption of EAF slag aggregate was measured following ASTM C127 [48].

On the other hand, A00 and C00 mixtures were determined the optimum moisture content at various time of compaction (i.e. 0, 15, 30, 60, and 90 min). Secondly, the samples of A00 and C00 mixtures containing the optimum moisture content were compacted after mixing 0, 15, 30, 60, and 90 min to elvaluated the effect of delay in compaction on the mechanical properties of RCCP (i.e. compressive strength, splitting tensile strength, ultrasonic pulse velocity, and elastic modulus) conforming ASTM standards [61]–[64] (Figure 14).
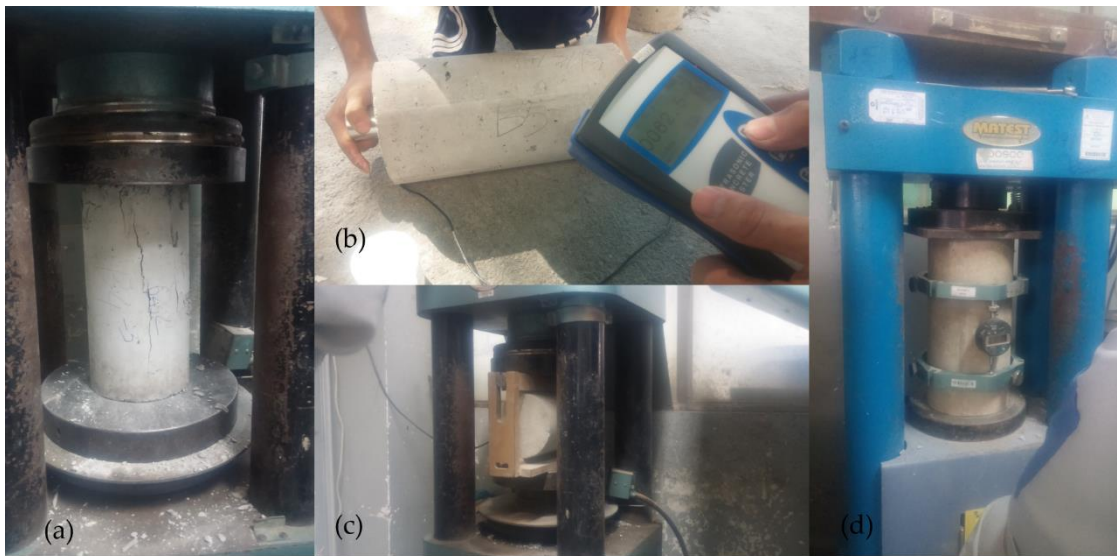
(a) compressive strength test, (b) ultrasonic pulse velocity test, (c) splitting tensile strength test, (d) modulus of elasticity test.

Figure 14. The mechanical test of RCCP

3.2.2.4. Durability properties

3.2.2.4.1. Water absorption

The cylinder specimens (100 mm diameter and 200 mm height) were prepared to measure the total water absorption in accordance with BS EN 1338 standard [65]. The specimens were immersed in water bath for at least 3 days. The initial mass of specimens was recorded when the difference between first and second weight performed at an interval of 24h is less than 1%. Then, the specimens were placed in oven at a temperature of $105 \pm 5\ ^{\circ}C$ until they reached constant mass. The total water absorption of specimen is the ratio of the difference between initial and constant mass of sample and the constant mass of sample.

3.2.2.4.2. Abrasion resistance

Abrasion resistance of RCCP was determined at 91-day age by Wide Wheel Abrasion machine (Figure 15) conforming to BS EN 1338 standard [65]. Eighteen samples with diameter of 100 mm and height of 50 mm were prepared. The samples shall be flat within a tolerance of ± 1 mm, clean and dry. Each result is the average of two readings on two different samples.
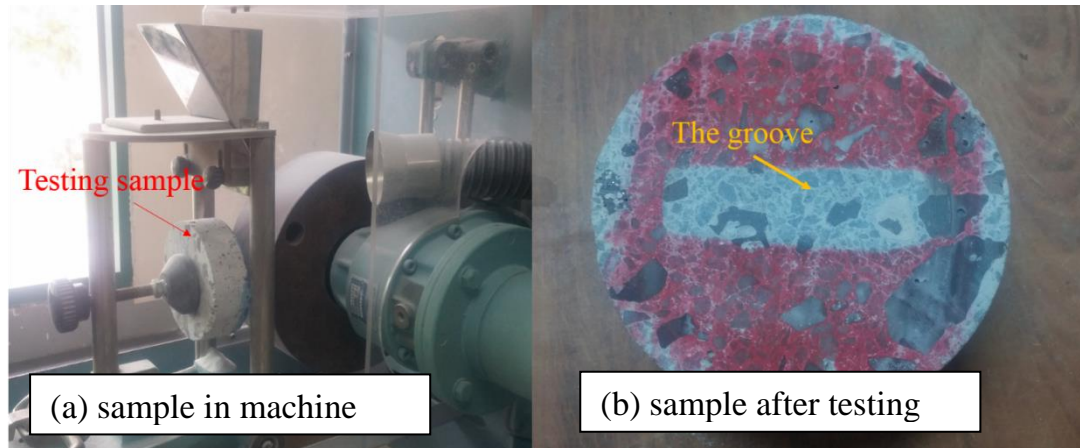
Figure 15. Sample on Wide Wheel Abrasion machine and after testing

3.2.2.4.3. Sulfate resistance

The sulfate resistance of RCCP made of EAF slag aggregate was assessed at 91-day ages. After 91 days of curing, the cubic samples were divided in two groups; one group was immersed in solution of 5% sodium sulfate (Na_2SO_4), whereas the second group was cured continuously in water to study the influence of sulfate attack on the mass and compressive strength. Every two weeks, mass and compressive strength change were determined. The mass change is the difference between the average mass of samples placed in sodium sulfate solution and the average mass of samples placed in water at the same testing time. Consequently, the mass change was calculated by Eq. (3)

$$Mass\ change\ (\%) = \frac{m_S - m_W}{m_W} x100 \tag{3}$$

Where m_W and m_S are the average mass of samples placed in water and in sodium sulfate solution, respectively (g);

In addition, compressive strength change was measured by the change in compressive strength of samples immersed in sodium sulfate solution as compared to that of samples cured in water at the same testing age. The compressive strength change was calculated by Eq. (4)

$$Compressive\ strength\ change\ (\%) = \frac{R_S - R_W}{R_W} x100 \qquad (4)$$

Where R_W and R_S are the average compressive strength of three samples cured in water and immersed in sodium sulfate solution, respectively (MPa);

3.3. Experiments on RCCP made of EAF slag aggregate and fly ash as a partial cement substitution

In this stage, class F fly ash was used to replace cement at two levels (i.e. 20%, and 40%). Six mixtures were prepared to examine in this stage (Table 11).

Table 11. Six mixtures of RCCP made of EAF slag aggregate and fly ash as cement substitution used in this stage

| Group | Mixture | Binder | | | Coarse aggregate | | | Fine aggregate |
		Fly ash (%)	Fly ash (kg/m³)	OPC (kg/m³)	EAF slag (%)	EAF slag (kg/m³)	Crushed stone (kg/m³)	Crushed stone (kg/m³)
A	A20	20	54	217	0	0	835	1154
	A40	40	108	161	0	0	830	1146
B	B20	20	55	220	50	423	423	1171
	B40	40	109	163	50	419	419	1158
C	C20	20	56	225	100	865	0	1195
	C40	40	112	168	100	863	0	1191

The testing programs of RCCP containing EAF slag aggregate and fly ash are similar to that of RCCP containing EAF slag aggregate (section 3.2), including

- The testing programs on mixing proportions
- The testing programs on mechanical properties
- The testing programs on durability properties

3.4. Expansion of mortar bars

In this work, the EAF slag was crushed in a jaw crusher. Fine EAF slag and natural aggregate passed the No.4 (4.75 mm) sieve were collected for making mortar bars. The gradation of fine aggregates conformed ASTM C1260 standard [66] (Table 12). Three aggregate types were prepared to make mortar bars as shown in Table 13.

Table 12. Grading requirement of fine aggregate for making mortar bars

Sieve size		Mass, %
Passing	Retained on	
4.75 mm (No. 4)	2.36 mm (No. 8)	10
2.36 mm (No. 8)	1.18 mm (No. 16)	25
1.18 mm (No. 16)	600 µm (No. 30)	25
600 µm (No. 30)	300 µm (No. 50)	25
300 µm (No. 50)	150 µm (No. 100)	15

Table 13. Mixture proportions of mortars were used in ASR test

Mortar	ID.	Aggregates (g)		Binder (g)	
		Crushed stone	EAF slag	Cement	Fly ash
Mortar made with 100% natural aggregate	MA00	990	0	440	0
	MA20	990	0	352	88
	MA40	990	0	264	176
Mortar made with 50% natural aggregate plus 50% EAF slag aggregate	MB00	495	495	440	0
	MB20	495	495	352	88
	MB40	495	495	264	176
Mortar made with 100% EAF slag aggregate	MC00	0	990	440	0
	MC20	0	990	352	88
	MC40	0	990	264	176

3.4.1. Expansion by autoclave testing

The autoclave method was proposed to observe the expansive potential of EAF slag aggregate after treatment. The autoclave testing was performed according to the procedure described in ASTM C151 standard [67]. Accordingly, mortar bars with dimension of 25 x 25 x 250 mm after molding 24 h $\pm$ 30 min were removed moist room and measured immediately initial length for each bar (Figure 16). Next, the mortar bars underwent autoclave testing with 295 $\pm$ 10 psi of pressure for 3h. Then, the length changes of mortar bars were recorded. Three types of mixture (i.e. MA, MB, MC) were prepared with three types of fine aggregate. For each mixture, the cement dosage was 262 grams to produce two specimens. The cement, aggregate and water mixing ratio was 1:2.75:0.485. As a result, six specimens were observed the length change after autoclave testing. Furthermore, two patterns extracted from MA and MC mortar bars were analyzed XRD to examine the crystalline phases.

Figure 16. Record the comparator reading of the specimen

3.4.2. Expansion by alkali-silica reactivity (ASR)

Aggregates containing certain constituents can react with alkali hydroxides. Products of ASR may be expansion due to the water absorption. If products of ASR are high-swelling, they will result in cracking of concrete. In present work, the potential ASR of EAF slag aggregate was evaluated through the expansion of mortar bars made with EAF slag aggregate following ASTM C1260 standard [66]. In addition, the effects of fly ash as a cement substitution on expansive ASR mitigation were also investigated. The EAF slag was crushed to meet the gradation for making samples (Table 12). Three fine aggregate types and three fly ash ratios replacing cement (i.e. 0%, 20%, and 40%) were prepared to produce mortar mixtures. As a result, a total of nine mortar mixtures were provided, as shown in Table 13. The aggregate-binder (cement + fly ash) ratio was 2.25 and the water-binder ratio was 0.47 by mass in the mixture. In each mortar mixture, three testing specimens (25 x 25 x 250 mm) were produced. After casting, the specimens were remained in the molds for 24 ± 2 h in the moist cabinet. Next, the specimens were removed from the molds and recorded the initial comparator reading. Each sample group was placed in a storage container with sufficient water to totally immerse them. Then, the containers were put in an oven at 80.0 ± 2.0 ℃ for a period of 24 h. After 24 h, the bars were removed the oven and taken the zero reading of each bar immediately. After that, all specimens made with each mortar mixture were placed in a container with 1N NaOH solution and returned the oven at 80.0 ± 2.0 ℃. Make subsequent comparator readings of the specimens periodically. Additionally, XRD analysis of four patterns extracted from four mortar samples (i.e. MA00, MC00, MA40, and MC40) were conducted to detect the crystalline phases.

Table 14 shows the testing approaches and the quantity of samples were used in this study.

Table 14. The testing approaches and the quantity of samples

No.	Testing items	Sample dimension (mm)	Quantity of sample	Standard
1	Expansion of EAF slag aggregate	6-in (152.4 mm) diameter mold	6	ASTM D4792
2	Optimum moisture content	6-in (152.4 mm) diameter mold	45	ASTM D1557
3	Fresh unit weight	-	-	ASTM C138
4	Hardened unit weight	150 x 300, cylinder	-	ASTM C642
5	Compressive strength	150 x 300, cylinder	108	ASTM C39
6	Splitting tensile strength	150 x 300, cylinder	108	ASTM C496
7	Modulus of elasticity	150 x 300, cylinder	27	ASTM C469
8	Delay in compaction			
	Optimum moisture content	6-in (152.4 mm) diameter mold	50	ASTM D1557
	Compressive strength	150 x 300, cylinder	30	ASTM C39
	Splitting tensile strength	150 x 300, cylinder	30	ASTM C496
	Modulus of elasticity	150 x 300, cylinder	30	ASTM C469
	Ultrasonic pulse velocity	150 x 300, cylinder	30	ASTM C597
9	Water absorption	100 x 200, cylinder	18	BS EN 1338
10	Abrasion resistance	100 x 50, cylinder	18	BS EN 1338
11	Sulfate resistance	100 x 100 x 100, cubic	243	NA
12	Expansion of mortar bars by autoclave testing	25 x 25 x 250	9	ASTM C151
13	Expansion of mortar bars by ASR	25 x 25 x 250	27	ASTM C1260
14	X-ray diffraction analysis	-	6	-

CHAPTER 4: RESULTS AND DISCUSSION

4.1. EAF slag aggregate

4.1.1. The physical properties

As can be seen in Table 15, EAF slag aggregate shows the higher apparent specific gravity than natural aggregates. The higher iron oxide content in EAF slag aggregate is a main cause of this result. Furthermore, the higher water absorption of EAF slag aggregate was also observed in this research.

Table 15. Physical properties of EAF slag coarse aggregate

Properties	EAF slag coarse aggregate (19 - 4.75 mm)
Apparent specific gravity	3.40
Density (OD) (kg/m^3)	3085
Density (SSD) (kg/m^3)	3176
Bulk density (kg/m^3)	1686
Water absorption (%)	2.93
Los Angeles abrasion value (%)	19.37

4.1.2. The chemical composition

The chemical composition of EAF slag after weathering treatment process was listed in Table 16. EAF slag used in this study contains 25.94% of CaO. Hence, it can be classified as EAF black basic slag [68]. Several researchers reported the similar common oxide compositions of EAF slag used in this study, as listed in Table 16 [18], [28]–[30].

EAF black basic slag has high density, low water absorption and low porosity. Mombelli et al. [69] demonstrated that EAF slag can be reused if MgO content is in the range of 5% to 7%, Al_2O_3 content is in the range of 7% to 10% by weight, and CaO content is less than 30% by weight. Moreover, it was found that f-CaO content of EAF slag used in this study is less than 0.1%. Therefore, EAF slag in Southern Vietnam has stable and non-leachable characteristics which can be appropriate for recycling.

Table 16. Chemical composition of EAF slag aggregate

Oxide composition (wt. %)	In this study
CaO	25.94
$\sum$ Iron oxides (FeO, Fe_2O_3)	34.73
SiO_2	16.32
MgO	6.86
Al_2O_3	8.31
MnO	5.18
TiO_2	1.98
Na_2O	0.30
K_2O	0.10
P_2O_5	0.25
f-CaO	<0.1%

4.1.3. The expansion of EAF slag aggregate from hydration reactions

The volume expansion of EAF slag aggregate is caused by unstable compound (e.g. f-CaO, f-MgO) that can hydrate and results in the volume increase. Table 17 showed the expansion value of combined aggregate was 0.009% and that of EAF slag aggregate was 0.015% at day 1. After that, the volume expansion rose rapidly within 5 days and reached the peak at day 6. EAF slag aggregate showed a higher volume expansion than the combined aggregate. According to the ASTM D4972 standard, the limit value of expansion is 0.5%. The highest expansion value of EAF slag (0.078%) is lower than the limit value (0.5%) given by the ASTM D4792. As a result, EAF slag aggregate in this study is stable the volume with hydration reactions.

Table 17. Expansion values of EAF slag aggregate and combined aggregate

Day	Expansion values (%)	
	EAF slag aggregate	Combined aggregate (50% crushed stone plus 50% EAF slag)
0	0	0
1	0.015	0.009
2	0.033	0.017
3	0.052	0.026
4	0.064	0.034
5	0.070	0.043
6	0.078	0.047
7	0.078	0.047
8	0.078	0.047
9	0.078	0.047
10	0.078	0.047
11	0.078	0.047
12	0.078	0.047
13	0.078	0.047
14	0.078	0.047

4.2. Roller-compacted concrete pavement

4.2.1. Mixing proportion

In each RCCP mixture, the modified Proctor test was conducted at five points of moisture content with increment by 1% to establish the compaction curve. It began with 5% of moisture content in group A mixtures and 6% of moisture content in group B/C mixtures. From the test results, the compaction curve was plotted in Figure 17. From this figure, the optimum moisture content and maximum dry density of each mixture were determined, as shown in Figure 18.
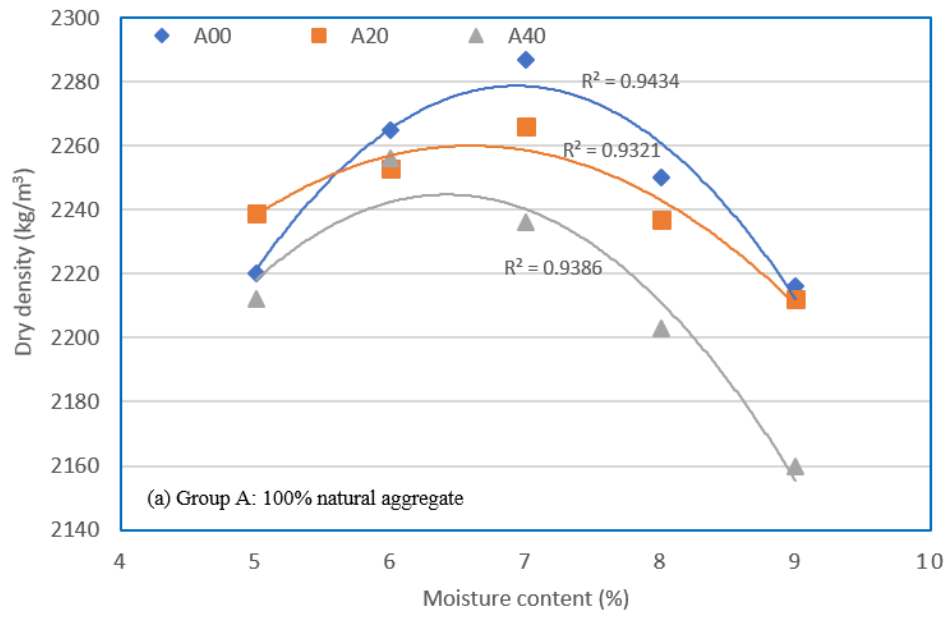
(a) The compaction curve of RCCP mixtures made of natural aggregate
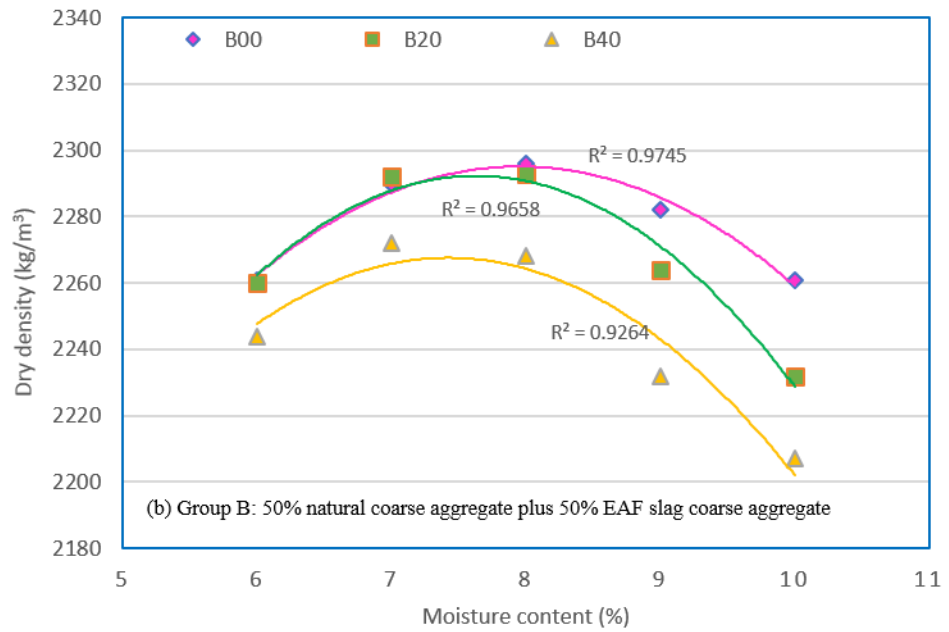
(b) The compaction curve of RCCP mixtures made of 50% natural coarse aggregate

plus 50% EAF slag coarse aggregate
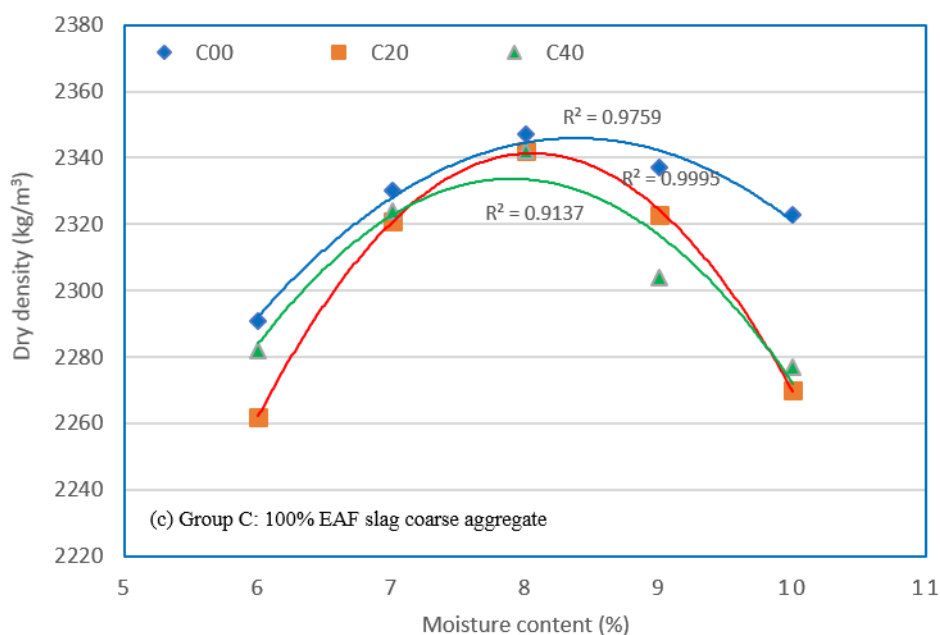
(c) The compaction curve of RCCP mixtures made of 100% EAF slag coarse aggregate

Figure 17. The compaction curve of the RCCP mixtures

It can be observed in Figure 18, the optimum moisture content and maximum dry density increased with a higher amount of EAF slag aggregate. This observation can be explained by higher water absorption and bulk density of EAF slag as compared to crushed stone aggregate. Test results revealed that the optimum moisture content of group B and C grew by 15% and 22% when compared to group A. The maximum dry density in group B and C increased slightly by 1% and 4% when compared to group A. On the other hand, there was a slight decrease in the optimum moisture content and maximum dry density when increasing amount of fly ash used in the mixture. This may be because the spherical-shaped particles of fly ash provide water-reducing characteristics that is similar to a water-reducing admixture and fly ash has lower unit weight as compared to cement. When 20% and 40% of cement was substituted with fly ash, the optimum moisture content of these mixtures decreased by 4% and 7% and the maximum dry density decreased by 0.5% and 1% as compared to the mixtures without fly ash. As a result, nine mixture proportions with optimum water content were prepared to investigate the unit weight and mechanical properties of RCCP.
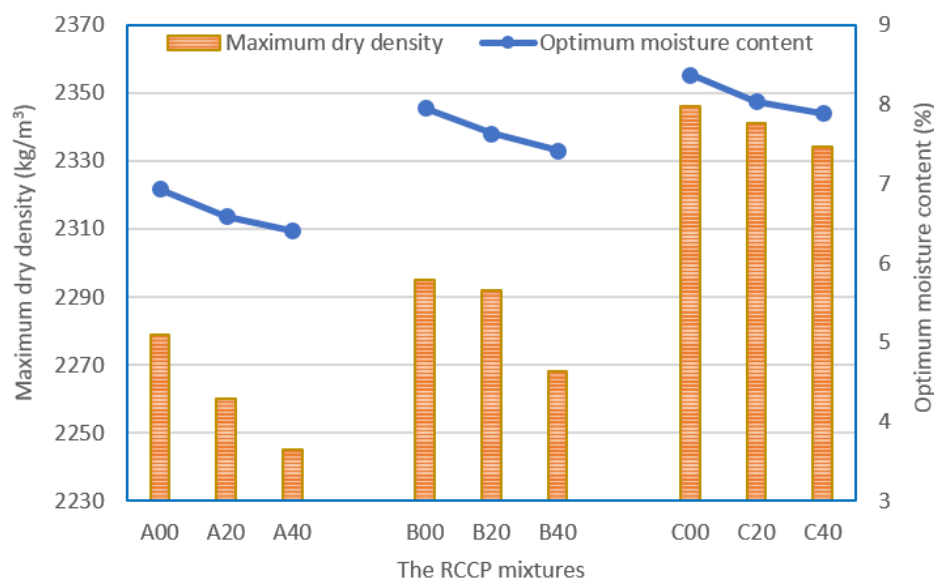
Figure 18. The optimum moisture content and maximum dry density of RCCP mixtures

4.2.2. Mechanical properties

4.2.2.1. Fresh and hardened unit weight

Figure 19 presents the fresh and hardened unit weight of RCCP mixtures. Group A achieved the average fresh unit weight of 2458 kg/m^3, whereas group B and C achieved the average fresh unit weight of 2511 kg/m^3 and 2570 kg/m^3, respectively; an increase of 2% and 4% in comparison with group A. The unit weight increased because EAF slag aggregate has unit weight higher than crushed stone aggregate. Moreover, the hardened unit weight had the same trend of the fresh unit weight. The average hardened unit weight of group C (i.e. 2565 kg/m^3) was highest and group A was lowest (i.e. 2453 kg/m^3). On the other hand, it can be seen that the replacement of cement by fly ash in group C caused a sharp decrease in the fresh and hardened unit weight, leading to an improvement of their unit weight.

Figure 19. Fresh and hardened unit weight of RCCP mixtures

4.2.2.2. *Compressive strength*

The compressive strength, splitting tensile strength of RCCP mixtures were obtained at various ages as presented in Table 18.

Table 18. Compressive strength and splitting tensile strength of RCCP

Group	Mix	Compressive strength (MPa)				Splitting tensile strength (MPa)			
		3-day	7-day	28-day	91-day	3-day	7-day	28-day	91-day
A	A00	25.87	39.63	47.04	56.45	3.68	4.07	4.51	5.28
	A20	22.52	29.39	42.44	58.40	3.01	3.46	4.53	5.54
	A40	17.88	23.77	38.03	50.42	2.07	2.60	4.47	5.14
B	B00	22.08	34.02	41.46	43.01	2.86	3.25	4.12	4.74
	B20	17.45	23.85	37.82	42.84	2.29	2.59	3.99	5.09
	B40	11.89	15.98	26.99	37.69	1.56	2.01	3.76	4.19
C	C00	21.58	27.43	35.56	43.29	2.77	3.09	4.07	4.68
	C20	15.73	21.02	30.07	43.35	2.01	2.43	3.72	4.26
	C40	11.05	15.16	23.20	35.37	1.49	1.97	2.79	4.14
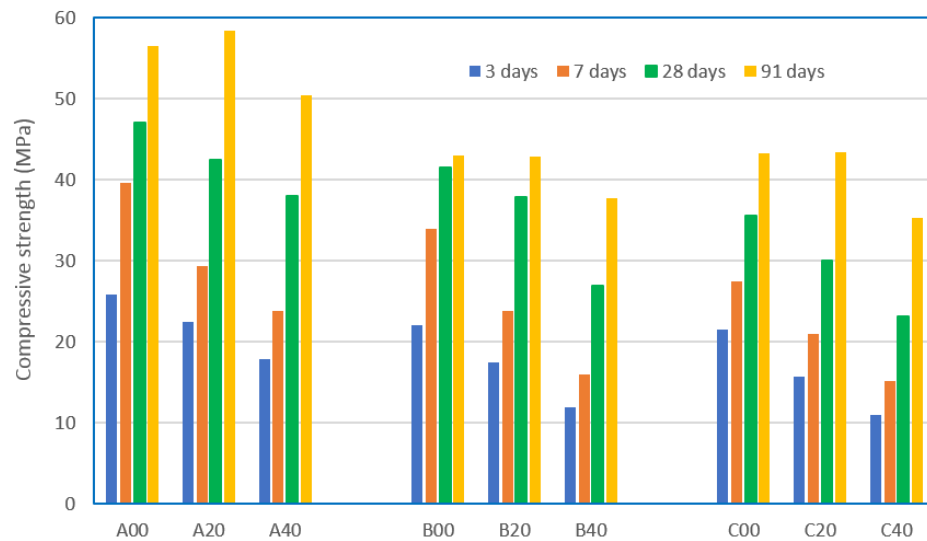
Figure 20. Compressive strength of RCCP mixtures at various ages

Figure 20 presents the compressive strength of the RCCP mixtures at 3, 7, 28 and 91-day ages. From Figure 20, the A00 mixture has the highest values in comparison with B00 and C00 mixtures in all ages. This may be because of the following reasons. Firstly, the A00 mixture has lower water-cement ratio than that in the B00 and C00 mixtures. The water absorption of crushed stone and EAF slag aggregate are 0.44% and 2.93%. Hence, the amount of effective water can be calculated as 154, 168 and 171 L/m^3 from the total water added to the mixtures. As a result, the effective water-cement ratio in the A00, B00, C00 mixtures are 0.56, 0.61 and 0.61, respectively [70]. Secondly, from Figure 21, the width of Interfacial Transition Zone (ITZ) of the RCCP mixture is about 30 µm, which results in the weak bond between EAF slag aggregate and matrix. Moreover, Adegoloye et al. [19] reported that the ITZ in high water-cement ratio concretes are better than in low water-cement ratio concretes. Finally, Palankar et al. [8] showed that the reduction in strength of concrete made with EAF slag aggregate may be the weak bond strength between the cement paste and aggregates. This problem happened due to the formation of calcite coating during the weathering treatment process of EAF slag aggregate. It is all of reasons to explain the strength declined.

At 3-day age, the compressive strength of A00 and B00 mixture reached 25.87 and 22.08 MPa. The strength of these mixtures rose sharply by 54% at 7-day age and 85% at 28-day age when compared to the strength at 3-day age. On the other hand, there was a significant effect on compressive strength in C00 mixture due to the water absorption of EAF slag aggregate. At 7-day and 28-day ages, its strength (i.e. 27.43 MPa, 35.56 MPa) was lower than B00's strength (i.e. 34.02 MPa, 41.46 MPa). However, at 91-day age, its strength (i.e. 43.29 MPa) was similar to B00's strength (i.e. 43.01 MPa). It can be said that EAF slag aggregate retains water and leads to restrain the development of strength at early-age. Nevertheless, the strength was improved in the long run. Figure 22 shows the 28-day compressive strength of A00, B00 and C00 mixtures which have remarkably exceeded the compressive strength requirement for Roller-Compacted concrete pavements [9].
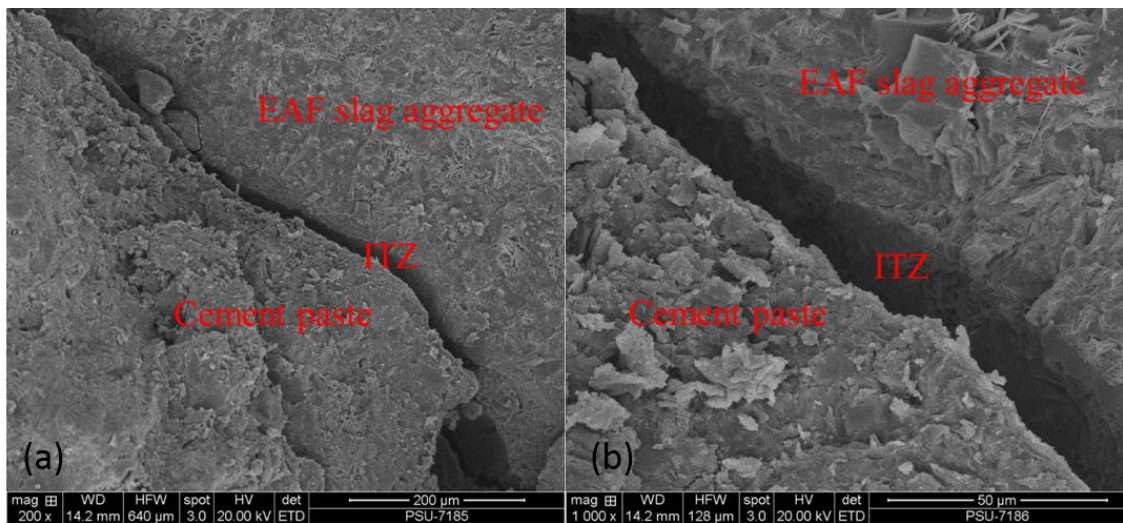
Figure 21. SEM images of ITZ: (a) 200 magnification and (b) 1000 magnification
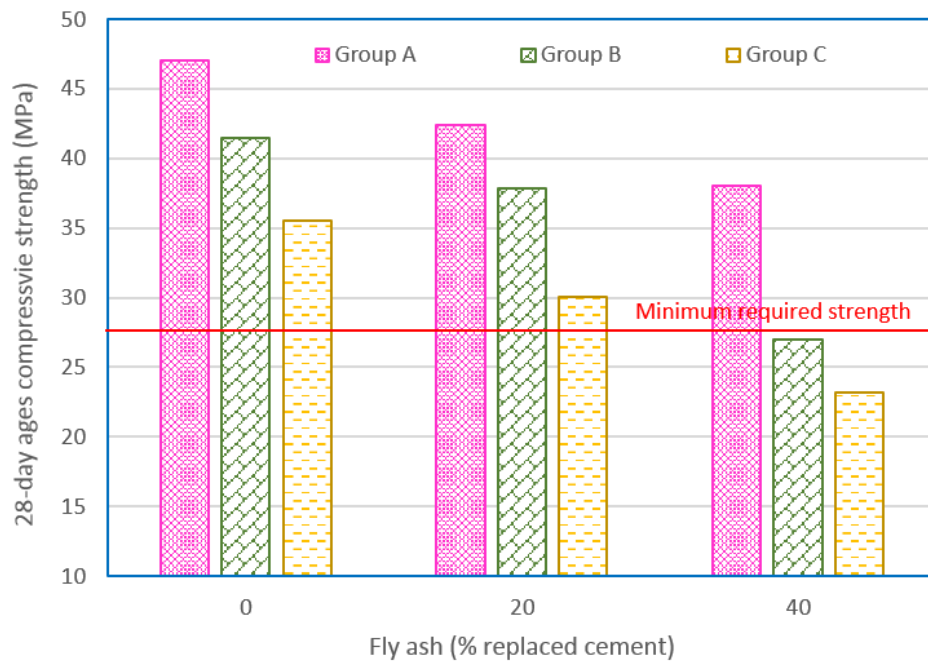
Figure 22. The 28-day compressive strength with various fly ash replacement ratio

From Figure 20, all mixtures with fly ash had low strength at early ages due to the pozzolanic characteristic of fly ash. At 7-day age, the compressive strength of B20 and C20 mixtures (i.e. 23.85, 21.02 MPa) reached approximately 70% of compressive strength of B00 and C00 mixtures (i.e. 34.02, 27.43 MPa). Because of the pozzolanic reactions, their strength increased dramatically and reached 42.84 and 43.35 MPa at 91-day age, which were similar to the strength of B00 and C00 mixtures. In addition, fly ash was also used as a filler that improved strength in the mixture. This result proves that RCCP containing EAF slag aggregate and 20% fly ash produces good concrete, which can be used for pavements [9]. However, if fly ash is used more than the optimum content, this leads the strength will be decreased. This observation was presented in the B40 and C40 mixtures. Their compressive strength was 15.98 and 15.16 MPa at 7-day age and 26.99 and 23.20 MPa at 28-day age. It is because fly ash is not as good as cement in terms of strength contribution. These results are in agreement with some previous studies on Roller-compacted concrete [42], [71], [72]. It was observed that the compressive strength of B40 and C40 mixture are not suitable for Roller-Compacted concrete pavements as an exposed wearing surface [9]. Nevertheless,

the long-term strength was improved by pozzolanic reaction of fly ash. The compressive strength of B40 and C40 mixtures reached 37.69 and 35.37 MPa at 91-day age. These mixtures could be used in application for sub-base construction.

4.2.2.3. Splitting tensile strength

From Figure 23, for the series mixtures without fly ash, the A00 mixture had the highest splitting tensile strength in all ages. When EAF slag was used to replace crushed stone aggregate, there was a dramatic decrease in splitting tensile strength. However, the strength of B00 and C00 mixtures were similar in all ages. That means EAF slag replacement ratio had a minor effect on the splitting tensile strength.
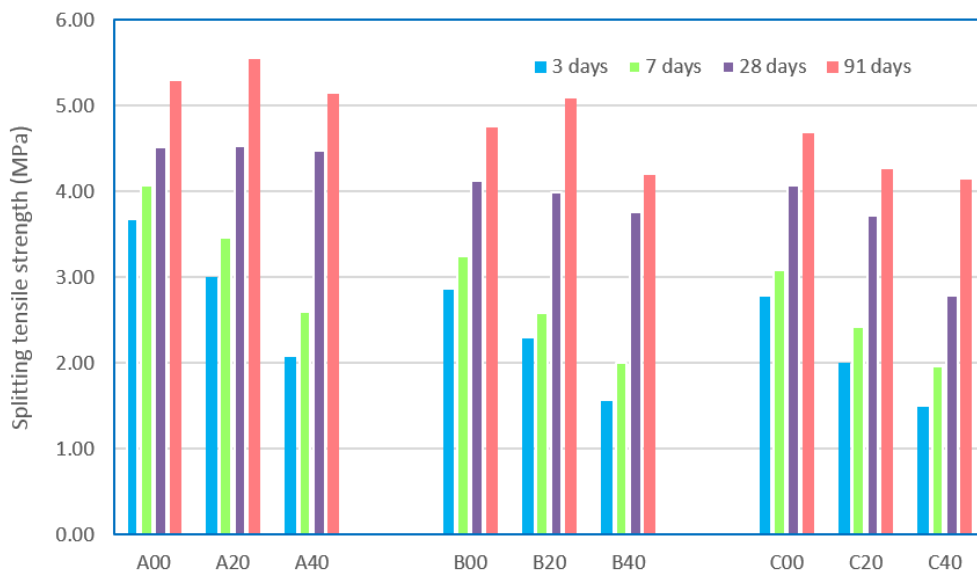
Figure 23. Splitting tensile strength of RCCP mixtures at various ages

For the series mixtures with 20% fly ash used to replace cement, it can be seen that this series mixture had lower strength than the series mixtures without fly ash at early ages. However, there was an improvement on strength at long-term ages. For example, the splitting tensile strength of A20, B20 and C20 mixtures were 5.54, 5.09 and 4.26 MPa at 91-day age (Figure 23). In addition, the effect of fly ash on the splitting tensile strength was different from the compressive

strength. At 91-day age, the splitting tensile strength of C20 mixture was lower than that of B20 mixture, whereas the compressive strength was similar. That means the contribution of 20% fly ash to the splitting tensile strength is lower than the compressive strength.

Similar to the compressive strength trend, the series mixtures with 40% fly ash had the lowest splitting tensile strength at all ages. These were 2.07, 1.56 and 1.49 MPa at 3-day age and 5.14, 4.19 and 4.14 MPa at 91-day age for A40, B40 and C40 mixtures, respectively (Figure 23). These results are in agreement with previous studies conducted on RCCP with fly ash [37]–[39]. These mixtures can be used as sub-base for road pavements.

4.2.2.4. Modulus of elacisity

Figure 24 presents the elastic modulus of RCCP mixtures at 91-day age. In each group, the elastic modulus value was highest in the mixture which replaced 20% cement with fly ash (i.e. A20, B20, C20 mixture). The values were 37.29, 35.71 and 35.56 GPa for A20, B20 and C20, respectively. It was observed that their values were impacted when replaced crushed stone aggregate with EAF slag aggregate. Their values decreased with increasing replaced ratio. Like the strength variation, the lowest elastic modulus values belong to RCCP mixtures that substituted 40% cement with fly ash. There were 34.53, 33.49 and 33.04 GPa for A40, B40 and C00 mixtures, respectively.
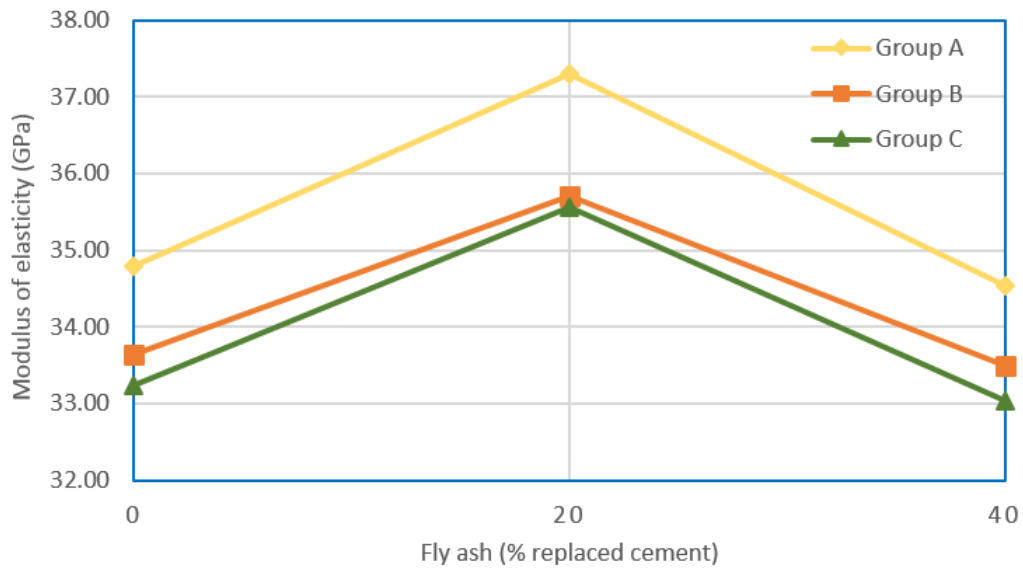
Figure 24. Modulus of elasticity of RCCP mixtures at 91 days

4.2.2.5. Analysis of SEM

The ITZ is a zone surrounding the aggregate particles. The ITZ plays an important role in the strength and porosity of concrete because it is the weakest phase in three phases of concrete (i.e. aggregate, ITZ and matrix). The better the quality of the ITZ, the better the strength. Arribas et al. [28] have demonstrated that EAF oxidizing slag aggregate is very good in terms of strength contribution in conventional concrete because the width of ITZ was 2-4 µm. Based on SEM images (Figure 21), the width of ITZ in the RCCP mixture is about 30 µm, which results in the weak bond between EAF slag aggregate and matrix. Furthermore, SEM images showed that EAF slag aggregate has a rough surface and low porosity.

4.2.2.6. Predicting model for compressive strength

Based on ACI model, a mathematical model was proposed to calculate compressive strength of RCCP. Some previous scholars have used the ACI model for normal concrete to predict compressive strength [21], [24]. According to ACI-Committee 209 [74], compressive strength at $t -$ and 28 days are correlated by the following Eq. (5)

$$f_c(t) = \frac{t}{a + b.t} f_c(28) \tag{5}$$

Where $f_c(t)$ and $f_c(28)$ are the cylindrical compressive strength at t – and 28 days (MPa), respectively; t is testing age (days); a and b are model coefficients and their values are 4 and 0.85 for normal concrete, respectively.

As discussed in section *4.2.2.2.*, the EAF slag aggregate and fly ash replacement level have an impact on compressive strength of RCCP. Moreover, the compressive strength of RCCP with the same fly ash replacement level has the same developing rule. Therefore, this study proposed a predicting model for three groups with three levels of fly ash replacement (i.e. 0%, 20% and 40%).

Based on Eq. (5) and analyzing the compressive strength results, the *a*-coefficient and *b*-coefficient of three groups were shown in Table 19. It can be said that the *a*-coefficient and *b*-coefficient in each group depend on EAF slag coarse aggregate replacement level (i.e. 0%, 50% and 100%).

Table 19. The a-coefficient and b-coefficient values

Group	Mixture	*a*-coefficient	*b*-coefficient	R^2
0% fly ash	A00	2.9124	0.8289	0.9839
	B00	2.8624	0.8909	0.9825
	C00	2.4199	0.9624	0.9624
20% fly ash	A20	3.3662	0.8238	0.9429
	B20	3.9908	0.8873	0.9788
	C20	3.5100	0.8001	0.9446
40% fly ash	A40	4.1052	0.8336	0.9528
	B40	4.6415	0.8120	0.9483
	C40	4.1885	0.7739	0.9475

The *a*-coefficient and *b*-coefficient values were plotted in Figure 25 and 26 From Figure 25, the relationship between *a*-coefficient and EAF slag coarse aggregate replacement level can be described with a hyperbolic function, which is presented by Eq. (6). The *b*-coefficient values were the average of three values in

each group. The *b*-coefficient is constant because the testing values were close (Figure 26).

$$a = a_1 x S^2 + a_2 x S + a_3 \tag{6}$$

Where *S* is the EAF slag coarse aggregate replacement level; a_1, a_2, a_3 are model coefficients.
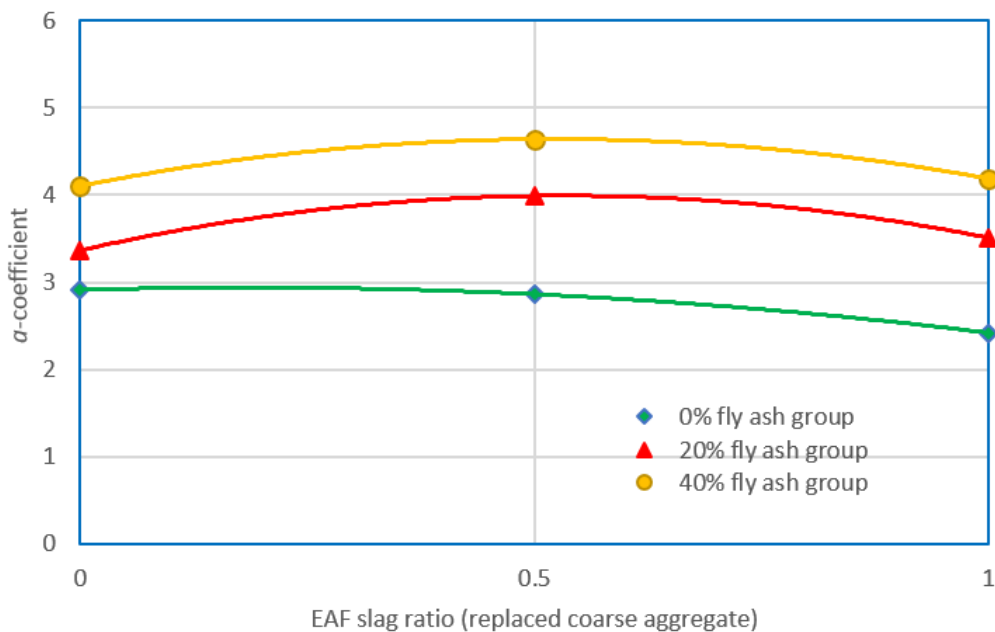
Figure 25. *a* -coefficient versus various EAF slag ratio
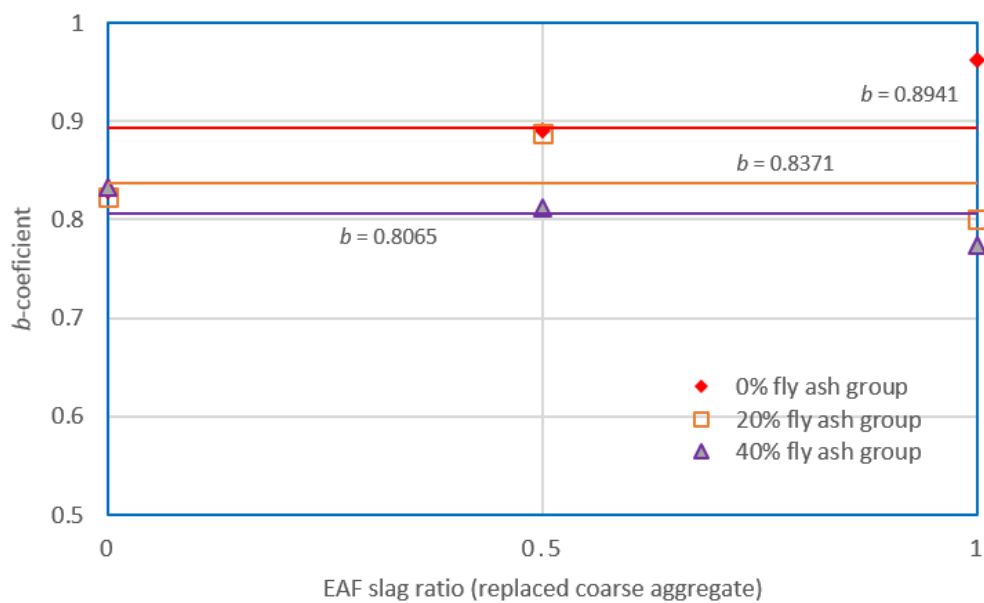
Figure 26. *b* -coefficient versus various EAF replacement ratio

Consequently, the a_1, a_2, a_3, b values are summarized in Table 20. Figure 27 shows the relationship between the measured strength and the calculated strength by ACI equation and the proposed equation with the model coefficients were taken from Table 20. It was observed that most of the calculated values by the proposed model had error in the range within ±10%.

Table 20. The a_1, a_2, a_3, b values

Group	a_1	a_2	a_3	b
0% fly ash	-0.7850	0.2925	2.9124	0.8941
20% fly ash	-2.2108	2.3546	3.3662	0.8371
40% fly ash	-1.9786	2.0619	4.1052	0.8065

The mean absolute percentage error (MAPE) is expressed by Eq. (7), which describes the error between the measured values and the model analysis values.

$$MAPE(\%) = \frac{1}{p}\sum_{j}^{p}\left(\left|\frac{o_j - t_j}{o_j}\right| x100\right) \tag{7}$$

Where t_j and o_j are measured values and model analysis values; p is the number of data points.
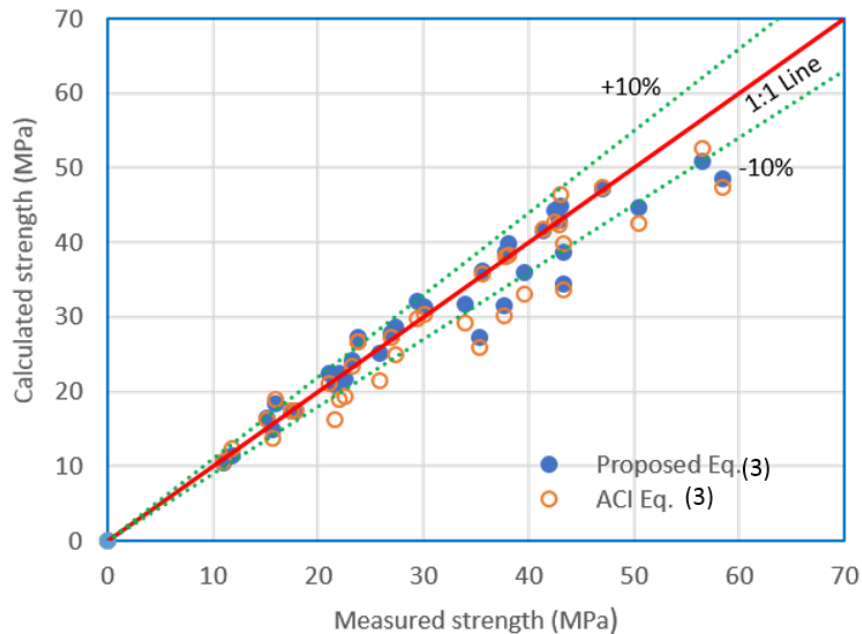
Figure 27. Measured strength and calculated strength values of proposed and ACI model

According to Eq. (7), the MAPE value was 7.51% calculated from measured data and calculated data by the proposed model; and the MAPE value was 10.15% calculated from measured data and calculated data by ACI model. It demonstrated that the proposed model performed good predictive ability because the MAPE value is less than 10%.

4.2.3. Delay in compaction

4.2.3.1. The relationship between the water absorption of EAF slag aggregate and immersion time

It can be seen in Table 21 that the water absorption of EAF slag aggregate after 10 min of immersing comprised over 80% of the total water absorption. Therefore, the new mixing method (Figure 28) was proposed to mix RCCP in this part of research.

Table 21. The water absorption ratio of EAF slag aggregate and immersion time

The immersing time	% of total water absorption
5 min	77.66
10 min	81.16
15 min	83.06
30 min	86.86
60 min	88.94
90 min	91.10
2 h	93.46
4 h	94.25
8 h	96.03
24 h	100.00
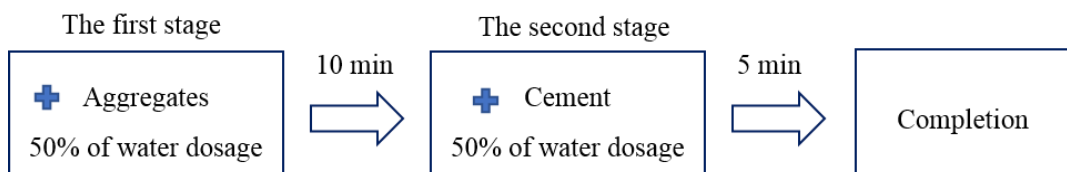
Figure 28. The new mixing method of RCCP in this stage of research

4.2.3.2. The optimum moisture content

     The optimum moisture content of RCCP mixtures was determined from the compaction curve established by the results of Proctor test as listed in Figure 29.
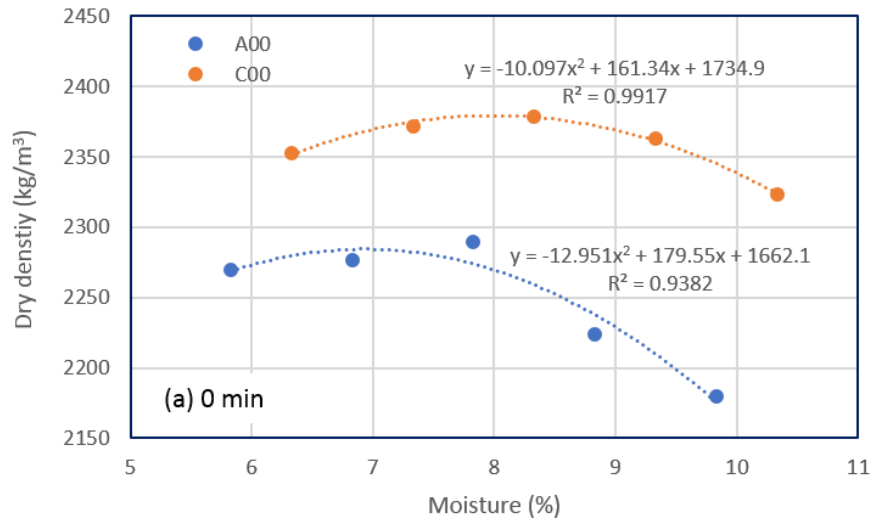
(a) The compaction curve of mixtures compacted immediately after mixing
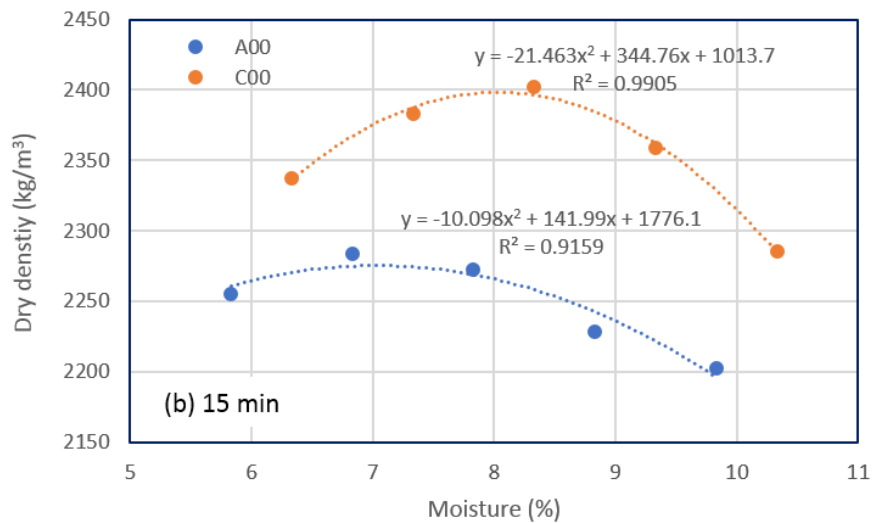
(b) The compaction curve of mixtures compacted after 15 min of mixing
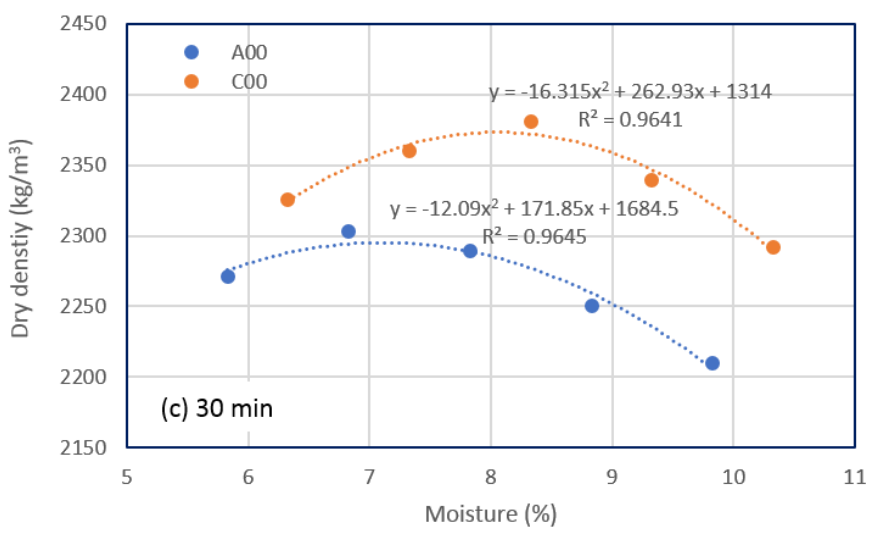
(c) The compaction curve of mixtures compacted after 30 min of mixing
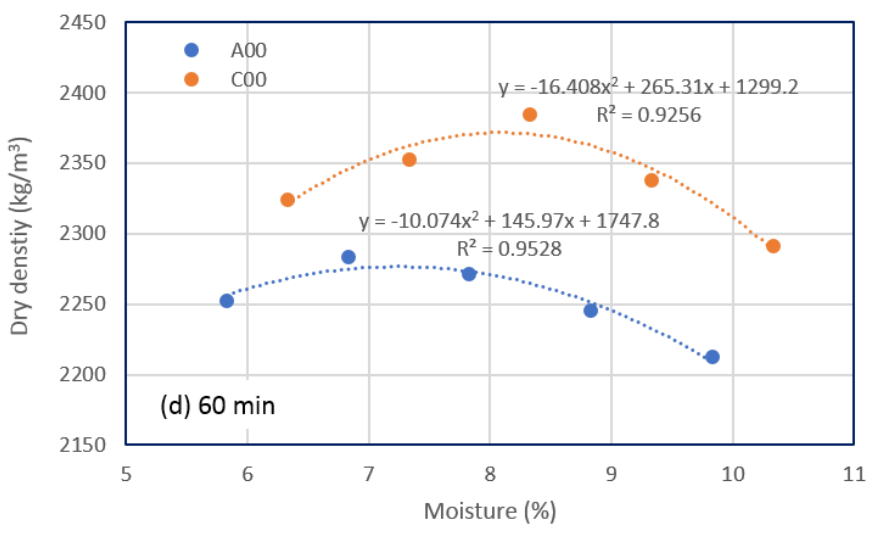
(d) The compaction curve of mixtures compacted after 60 min of mixing
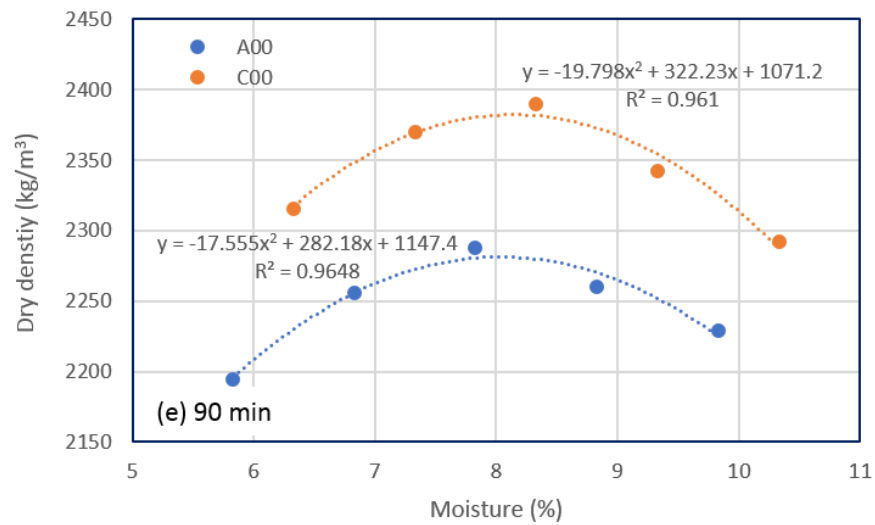
(e) The compaction curve of mixtures compacted after 90 min of mixing

Figure 29. The compaction curve of the RCCP at various time of compaction

4.2.3.3. The compressive strength

The delay affected significantly on the compressive strength of A00 and C00. As shown in Figure 30, the compressive strength of A00 and C00 attained the highest value (i.e. 51.46 and 43.54 MPa, respectively) with compacting immediately after mixing completion. Good workability of mixtures resulted in the effective compacting process. Increasing the delay led to a compressive strength reduction. However, both of A00 and C00 grew slightly the compressive strength after 15 min of delay. This behavior may be resulted from the formation of ettringite of the hydrated cement process. The formation of ettringite filled up the pores in structure concrete. Nevertheless, when mixture was compacted in period of the formation of C-S-H phase resulted in the crystallize product was destroyed. As a result, A00 and C00 mixtures were compacted at 90 min was observed the decrease of compressive strength.
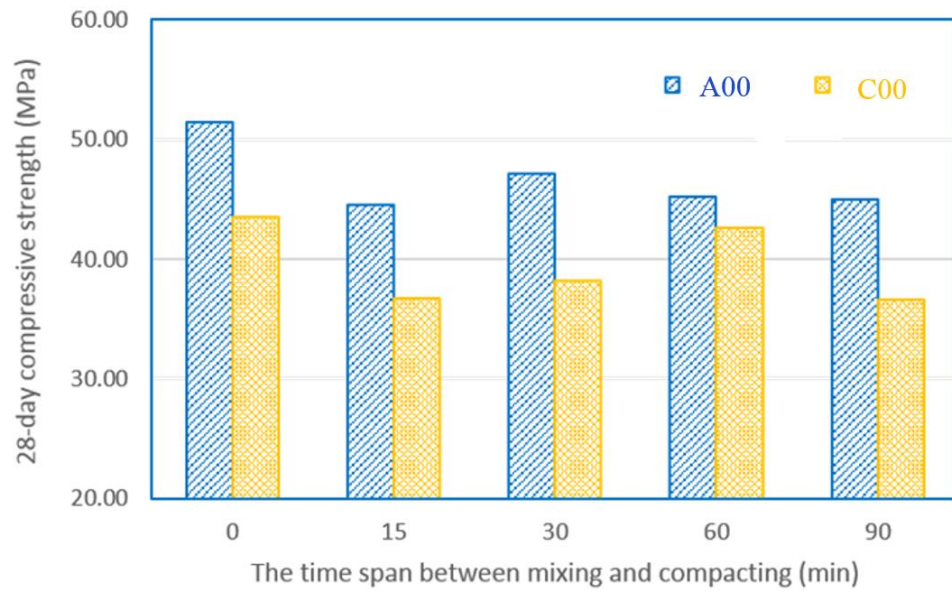
Figure 30. Compressive strength of RCCP at various time of compaction

4.2.3.4. The ultrasonic pulse velocity (UPV) of RCCP
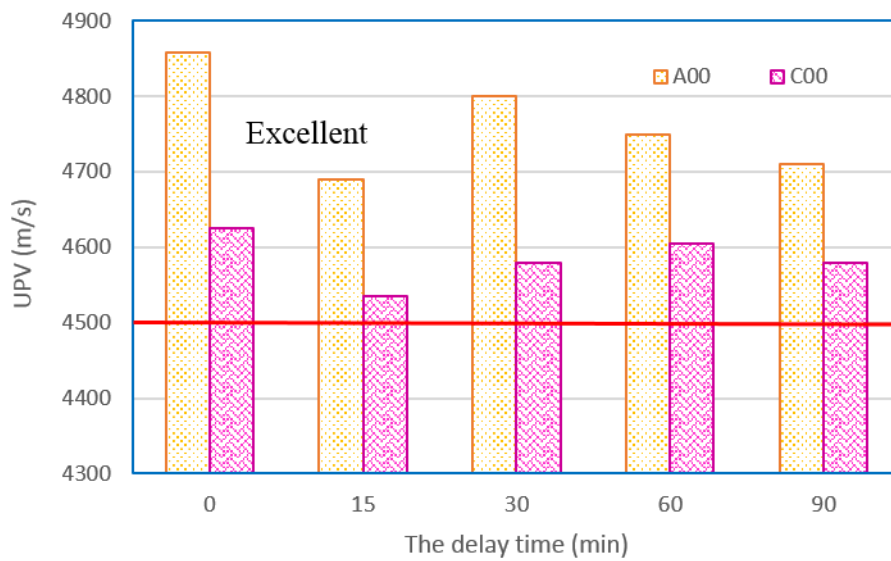
Figure 31. The ultrasonic pulse velocity of RCCP at various time of compaction

Both of A00 and C00 specimens with various time of compaction are classified "excellent" quality (UPV > 4500 m/s) [75]. It was observed that there was a good relationship between UPV and compressive strength values. Increasing UPV values accompanied by the compressive strength increase.

4.2.3.5. The splitting tensile strength of RCCP
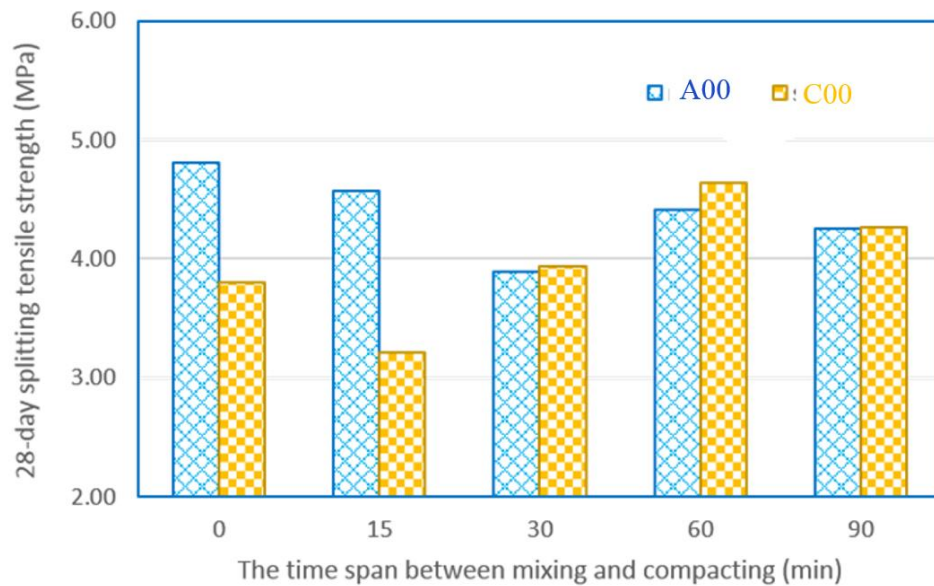
Figure 32. The splitting tensile strength of RCCP at various time of compaction

The samples compacted at various time were shown the splitting tensile strength at 28-day age in Figure 32. A00 mixture attained the highest splitting tensile strength (4.81 MPa) with compaction immediately after mixing completion, whereas C00 mixture obtained the highest splitting tensile strength with compaction at 60 min of delay.

4.2.3.6. The elastic modulus of RCCP

As can be seen from Figure 33, the delay in compacting affected slightly on the elastic modulus of RCCP at 28-day age. Similar to conventional concrete, the elastic modulus at 28-day age of all RCCP mixtures in this study was in range of 30-36 GPa.
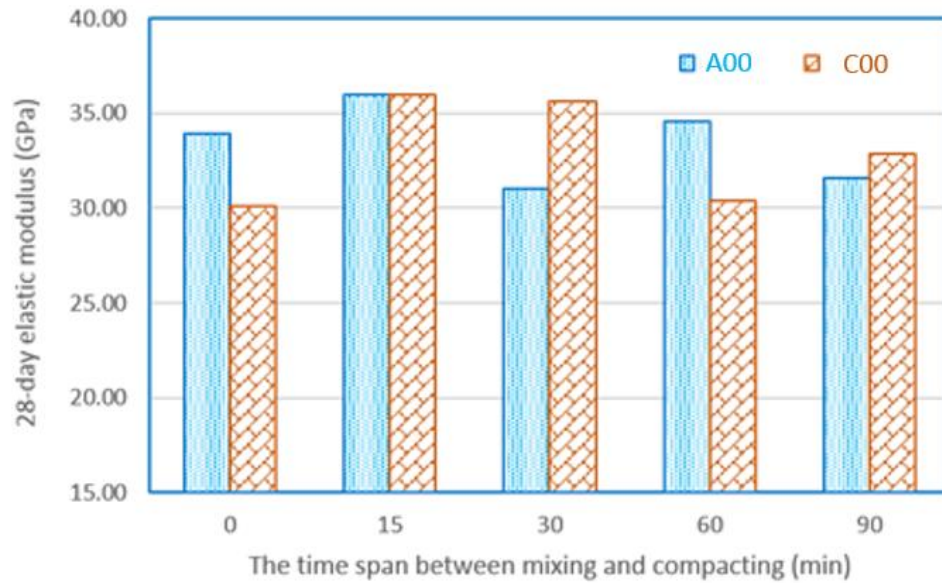
Figure 33. The elastic modulus of RCCP at various time of compaction

4.2.4. Durability properties

4.2.4.1. Water absorption
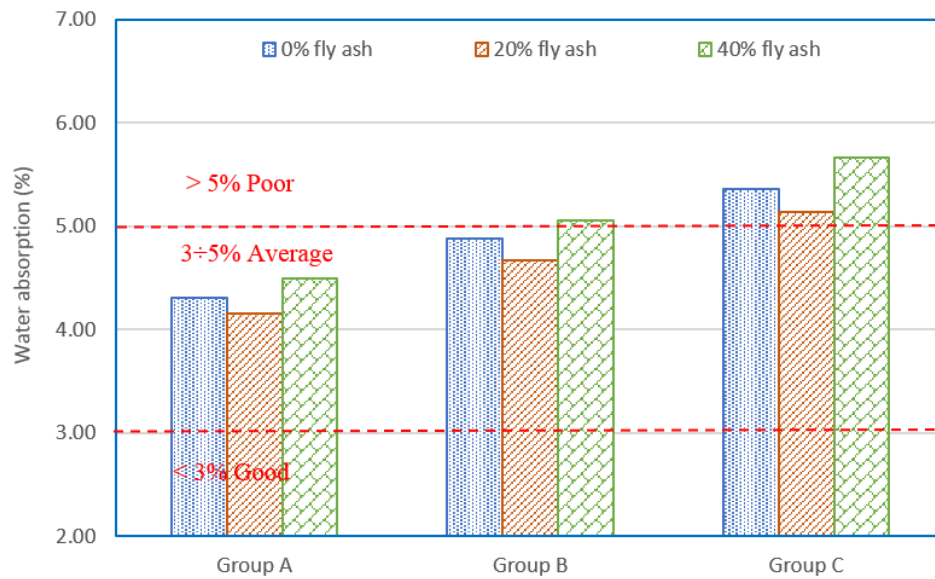
Figure 34. Water absorption values of RCCP at 91-day age

The total water absorption of RCCP was determined at 91 day-age as presented in Figure 34. According to CEB-FIP [76], all mixtures of group C were classified as "poor concrete", whereas group A was classified as "average concrete". This result caused by the higher water absorption of EAF slag aggregate.

4.2.4.2. Abrasion resistance

Abrasion resistance of RCCP at 91-day age was determined by the dimension of groove created by Wide Wheel Abrasion machine. The average dimension of groove obtained from two different specimens as shown in Figure 35. All grooves showed the dimension in range of 21-23 mm leading to all mixtures can be classified as Class 3 [65]. Because of the rough texture of slag, the abrasion resistance of group C was higher than that of group A. Besides, abrasion resistance in each group had a strong relationship with compressive strength [44]. Higher compressive strength resulted in higher resistance. It was observed that A20 was the highest resistance in group A and C20 was the highest resistance in group C. Meanwhile, mixtures containing 40% fly ash (i.e. A40, B40, and C40) performed the lowest resistance in its group.
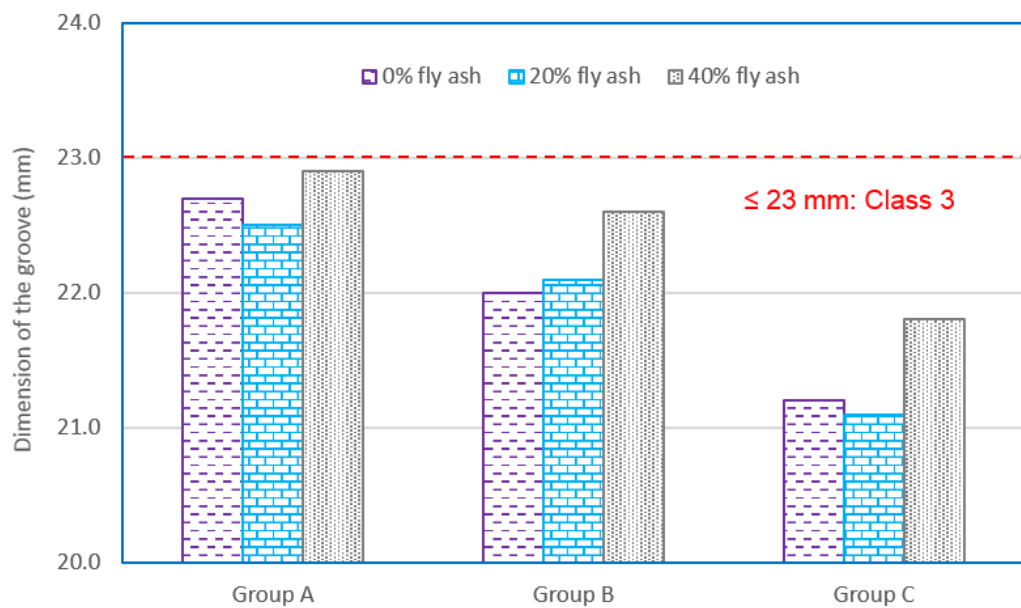
Figure 35. Abrasion resistance of RCCP at 91-day age

4.2.4.3. Sulfate resistance

4.2.4.3.1. Mass change

Mass change of nine RCCP mixtures exposed to sulfate environment is shown in Figure 36. It can be seen that mass of samples without fly ash (i.e. A00, B00, and C00) increased gradually in testing period (8 weeks). A00 increased from 0.33% in 2 weeks to 0.38% in 8 weeks, B00 increased from 0.37% in 2 weeks to 0.39% in 8 weeks, and C00 increased from 0.39% in 2 weeks to 0.46% in 8 weeks. Similarly, there was a dramatical mass increase in mixtures containing 20% fly ash (i.e. A20, B20, and C20) in first two weeks; a mass increase of A20, B20, and C20 was 0.85%, 1.04%, and 1.03%, respectively. In contrast, the low compressive strength mixtures (i.e. B40 and C40) manifested a mass decrease in early period of immersion. The breaking of specimens at the rim is a main cause of this result (Figure 38).
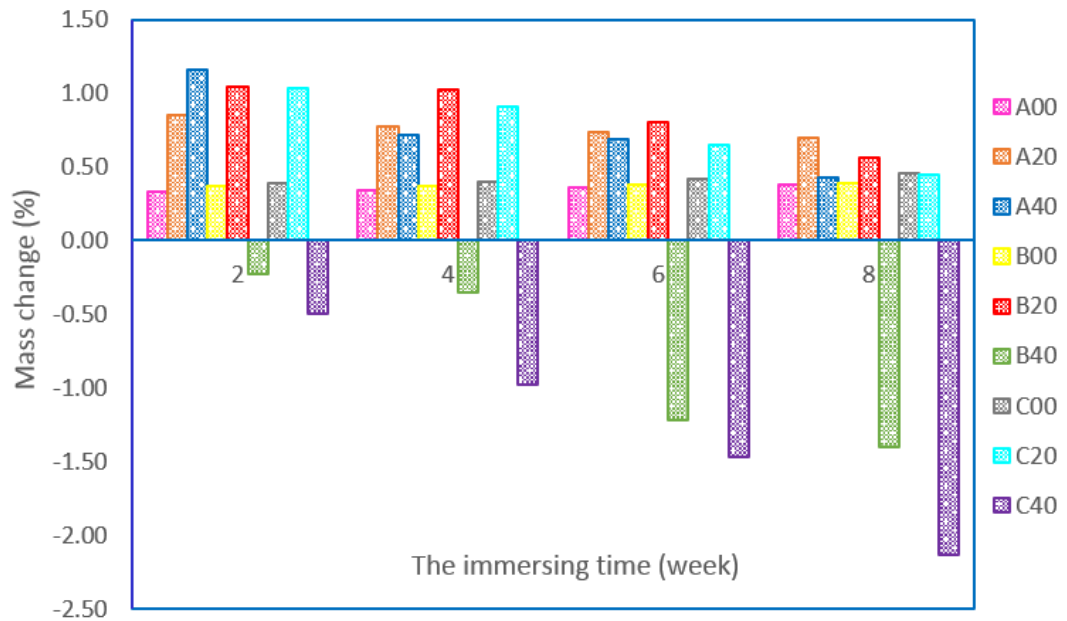
Figure 36. Mass change of RCCP exposed to sulfate environment

4.2.4.3.2. Compressive strength change

Figure 37 shows compressive strength change of RCCP exposed to sulfate solution. For mixtures without fly ash, the strength change trend of mixtures using EAF slag aggregate (i.e. B00 and C00) was similar to that of mixture using natural aggregate (A00). A strength development occurred within first four weeks. After that, the compressive strength reduction was obtained Because EAF slag aggregate absorbs water higher than natural one, C00 mixture displayed the least sulfate resistance.

Similarly, there was a continuous strength development of mixtures containing fly ash in early exposing period. As shown in the Figure 37, A20 mixture exhibited the best resistance to sulfate attack. The effect of fly ash on B20 and C20 mixture displayed similar behavior of A20 mixture. Nevertheless, when 40% fly ash was used to replace cement, compressive strength of RCCP decreased dramatically. The low compressive strength of mixtures containing 40% fly ash is a main cause of the less sulfate resistance.
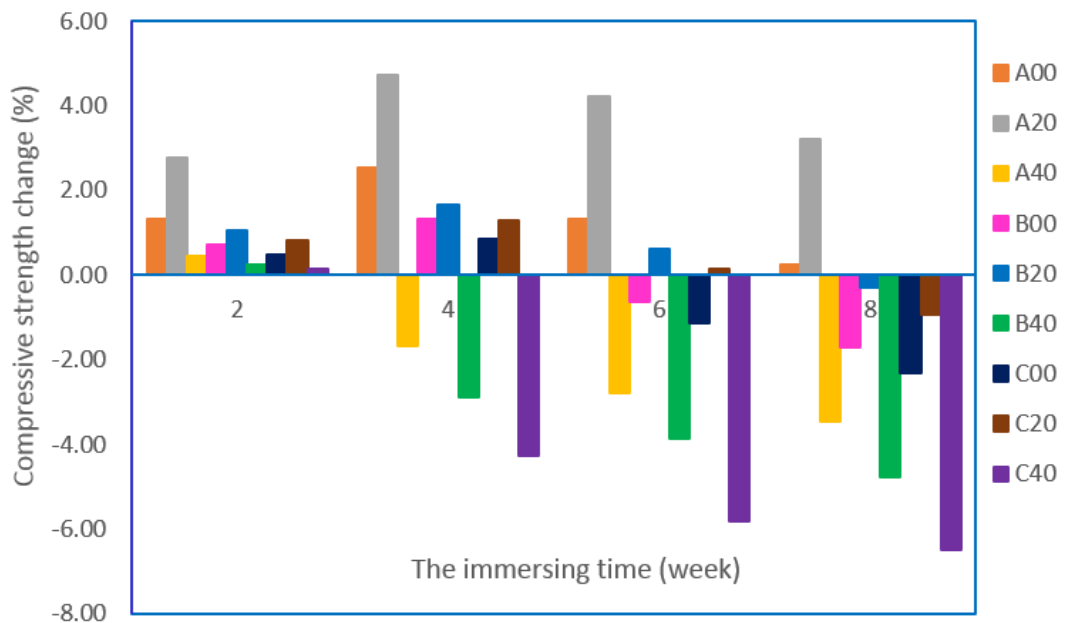
Figure 37. Compressive strength change of RCCP exposed to sulfate environment

Figure 38. Cracking image of C40's sample exposed to sulfate environment 8 weeks

4.3. Expansion of mortar bars

4.3.1. Expansion by autoclave testing

Expansion in terms of length change of mortar bars between before and after autoclave testing is listed in Table 22. The expansion values of MA, MB, and MC mixture were 0.038%, 0.043% and 0.057%, respectively. MC mixture was the highest expansion value, whereas MA mixture was the lowest expansion value. The expansion of MA mixture occurred due to the hydration of CaO which is often present in cement only. Meanwhile, the higher expansion of EAF slag aggregate than that of natural aggregate was observed in the previous research [77].

The XRD analysis (Figure 39) revealed that the crystalline phases of mortar made with natural aggregate after autoclave condition were portlandite, calcite, quartz, albite, microcline and clinochlore. Meanwhile, portlandite, calcite, larnite and wustite were the crystalline phases of mortar made with EAF slag aggregate

Table 22. Autoclave expansion results

Sample	ID.	Test no.	Expansion value (%)	
			Each mortar bar	Average
Mortar bar made with 100% natural aggregate.	MA	MA-1	0.038	0.038
		MA-2	0.038	
Mortar bar made with 50% natural aggregate plus 50% EAF slag aggregate.	MB	MB-1	0.042	0.043
		MB-2	0.044	
Mortar bar made with 100% EAF slag aggregate.	MC	MC-1	0.057	0.057
		MC-2	0.056	

Additionally, all specimens were not broken (Figure 40) when the entire hydration reactions took place under autoclave condition [36], so it can be said that EAF slag used in this study is volume stability. Consequently, EAF slag is eligible for replacing natural aggregate in RCCP after leaving several months in environmental condition.

1-Portlandite: $Ca(OH)_2$
2-Calcite: $CaCO_3$
3-Larnite: Ca_2SiO_4
4-Wustite: FeO
5-Quartz: SiO_2
6-Albite: $Na(AlSi_3O_8)$
7-Microcline $K(AlSi_3O_8)$
8-Clinochlore: $(Mg,Fe)_6(Si,Al)_4O_{10}(OH)_8$
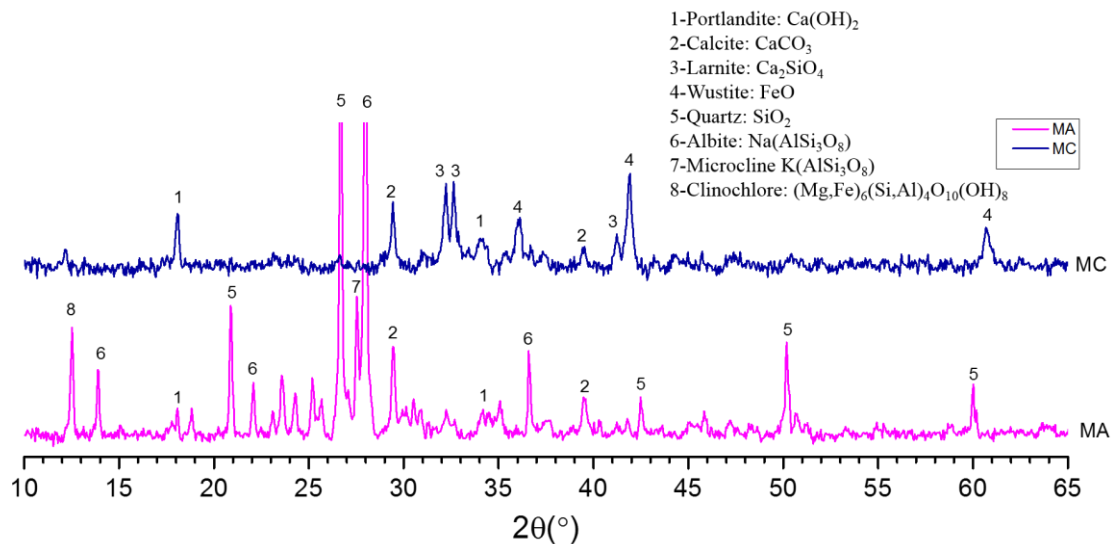
Figure 39. X-ray diffraction analysis of MA's and MC's pattern after autoclave testing
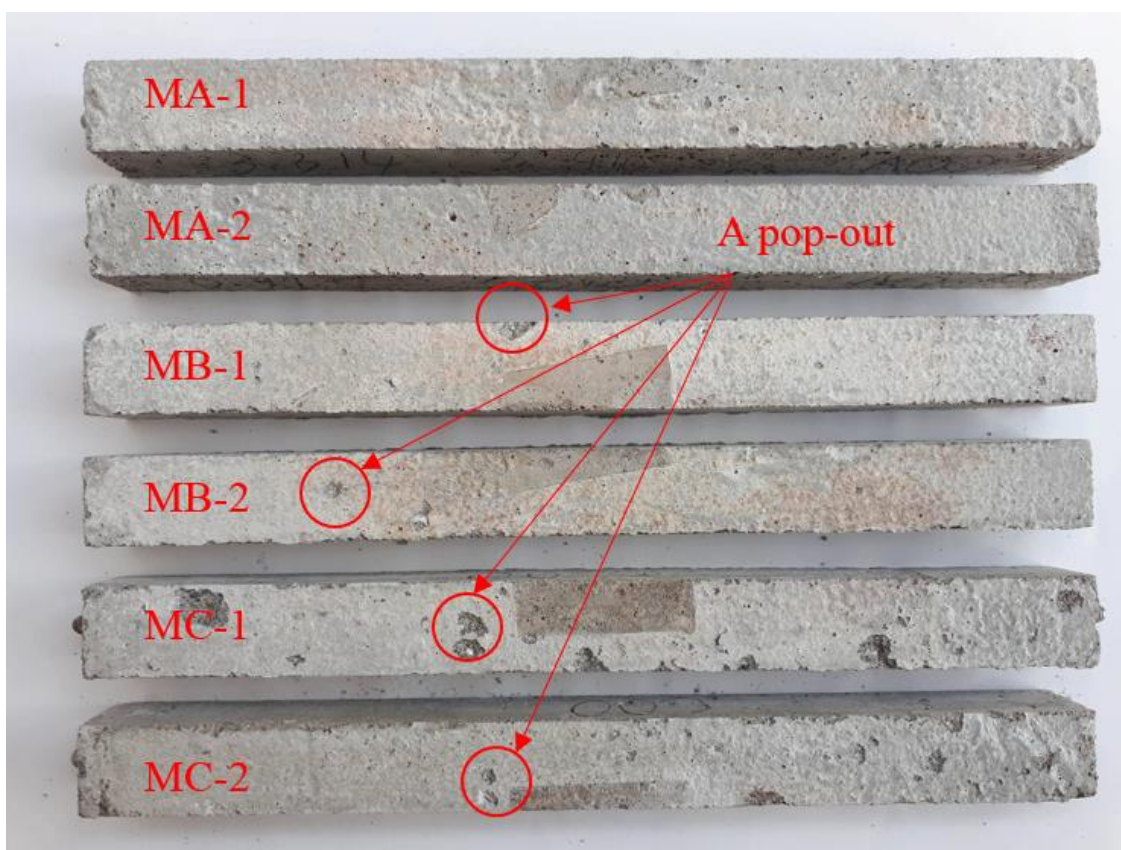
Figure 40. The mortar bars after autoclave testing

4.3.2. Expansion by alkali-silica reactivity (ASR)

Figure 41 shows the expansion values in terms of length change of mortar bars caused by ASR. It can be seen that 14-day expansion value of MC00 is 0.036% below the limit value (0.1%) according to ASTM C1260, so EAF slag aggregate is non-reactive aggregate. When the immersing time was extended until 28 days, the expansion of MA00, MB00, and MC00 was 0.32%, 0.21%, and 0.05%, respectively. In this case, a combination of 50% EAF slag and 50% natural aggregate is considered a non-reactive aggregate.

In addition, the cement replacement by 20% fly ash decreased the expansion due to alkali-silica reaction, especially in MA20 and MB20 mixture. The 14-day expansion values of MA20, MB20, and MC20 were 0.058%, 0.044%, and 0.034%, respectively. A decrease of 66% in MA20 in comparison to MA00; a decrease of 61% in MB20 in comparison to MB00. The pozzolanic properties of fly ash contribute to ASR reduction [78].
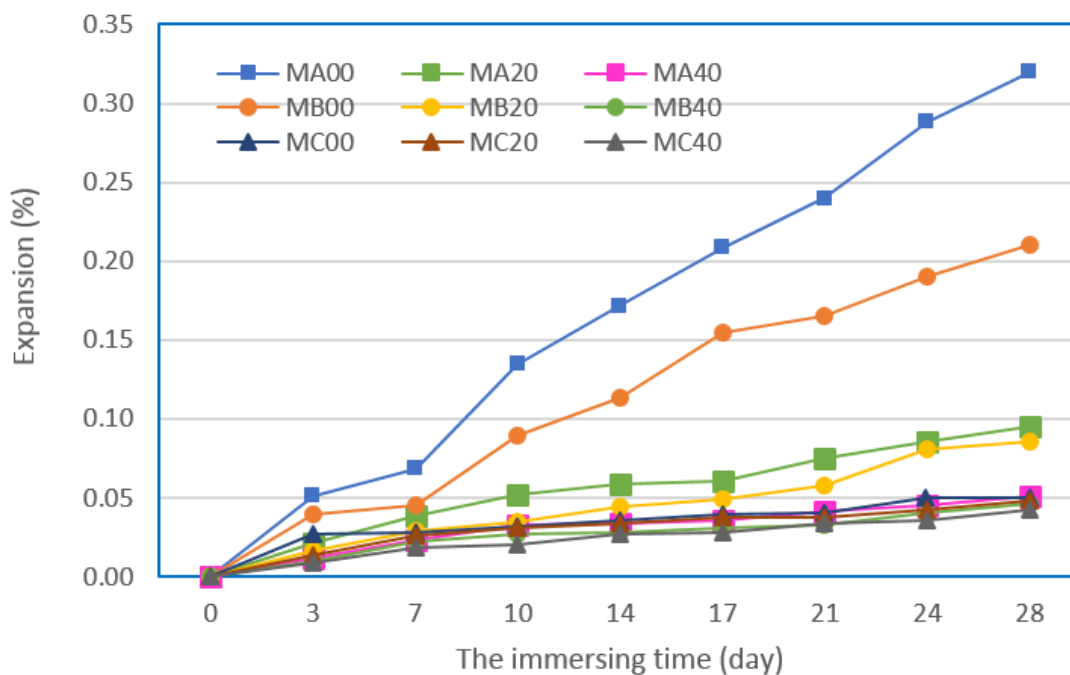
Figure 41. Expansion values of mortar bars immersing in 1N NaOH solution

On the other hand, the results of XRD analysis (Figure 42) of dried powder samples extracted from mortar bars after 28-day testing revealed that the crystalline phases of MA00 were portlandite, calcite, albite, microcline, quartz, and clinochlore, whereas MC00 pattern displayed the presence of portlandite, larnite, and wustite.
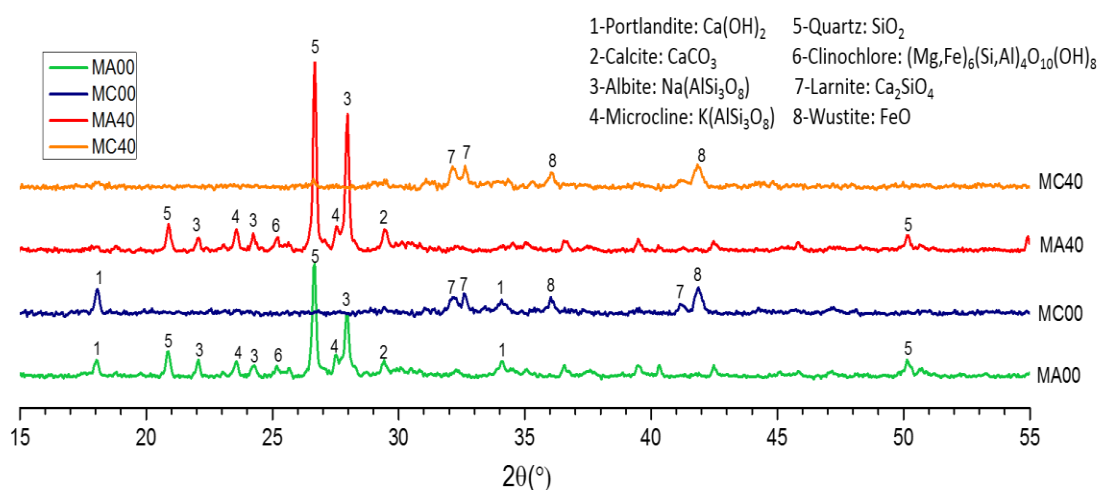
Figure 42. XRD analysis of patterns after immersing 28 days in NaOH solution

Table 23. Comprehensive results of this study

Stage I	Experiments on EAF slag aggregate		
	Content	**Conclusion**	
	The treatment of EAF slag aggregate by the weathering process at least 3 months	EAF slag aggregate exhibited the volume stability and can be replaced coarse natural aggregates in RCCP	
	The study on the physical properties of EAF slag aggregate		
	The study on the chemical composition of EAF slag aggregate		
	The study on the expansive potential of EAF slag aggregate from hydration reactions		

Stage II	Experiments on RCCP made of EAF slag aggregate			
	Content		**Conclusion**	
	The mixing proportions	The optimum moisture content of mixture	7% - 9%	
	The mechanical properties	The compressive strength	Decrease as compared to conventional RCCP	RCCP made of EAF slag aggregate fulfill the strength requirements for pavements
		The splitting tensile strength	Decrease as compared to conventional RCCP	
		The modulus of elasticity	Decrease as compared to conventional RCCP	
	The durability properties	The water absorption	Increase as compared to conventional RCCP	
		The abrasion resistance	Increase as compared to conventional RCCP	
		The sulfate resistance	Similar to conventional RCCP	
	The delay in compaction	The compressive strength	The highest value attained when compaction immediately after mixing	90 min of delay in compaction produced RCCP fulfilling the strength requirements for pavements
		The splitting tensile strength	The highest value attained when compaction at 60 min of the delay	
		The modulus of elasticity	Almost no influence by the delay	

Table 23: Comprehensive results of this study (cont.)

	Experiments on RCCP made of EAF slag aggregate and fly ash		
	Content		**Conclusion**
Stage III	The mixing proportions	The optimum moisture content of mixture	7% - 9%
	The mechanical properties	The compressive strength	• RCCP made of EAF slag aggregate and 20% fly ash can be used for pavements • RCCP made of EAF slag aggregate and 40% fly ash can be considered to apply for subbase constructions
		The splitting tensile strength	
		The modulus of elasticity	
	The durability properties	The water absorption	• The replacement cement by 20% fly ash was improved the durability properties of RCCP made of EAF slag aggregate • 40% fly ash as cement substitution resulted in the decrease of the durability properties of RCCP made of EAF slag aggregate
		The abrasion resistance	
		The sulfate resistance	
Stage IV	Experiments on mortar bars		
	Content		**Conclusion**
	Expansion by autoclave testing		EAF slag aggregate exhibited the volume stability
	Expansion by alkali-silica reactions		EAF slag aggregate is non-active aggregate by alkali-silica reactions

CHAPTER 5: CONCLUSIONS AND SUGGESTIONS

5.1. Conclusions

Based on the experimental results of this research, some of highlighted conclusions could be drawn:

1) The physical properties and chemical composition of EAF slag, EAF slag aggregate is eligible to replace natural aggregates.

2) After the weathering process, the expansion values caused by hydration reactions have demonstrated that EAF slag aggregate showed the volume stability.

3) The optimum moisture content of RCCP mixture containing EAF slag aggregate and fly ash was found in the range 7% to 9%. It depended on the material replacement ratios.

4) The fresh and hardened unit weight of RCCP with EAF slag as an aggregate replacement increased in all mixtures due to the higher unit weight of EAF slag aggregate as compared to that of crushed stone aggregate. However, there was a unit weight reduction when EAF slag aggregate and fly ash were used as substitute materials in RCCP mixtures.

5) When EAF slag was used to replace crushed stone aggregate, there was a slight decrease in compressive strength, splitting tensile strength and elastic modulus. This is because the limited improvement of the rough-textured EAF slag in low water-cement ratio concretes resulted in bad interfacial transition zone between EAF slag aggregate and cementitious matrix. However, EAF slag can be replaced 100% coarse aggregate in RCCP to produce pavements which met the requirements of the exposed surface.

6) There was a strength decrease when cement was partially replaced by fly ash. Nevertheless, the RCCP containing EAF slag aggregate and 20% fly ash also produces the good concrete which can be used for pavements. Therefore, it was recommended that the mixture containing EAF slag aggregate and 20% fly ash is the best for recycling a large amount of waste

materials. Moreover, the substitution of cement by 40% fly ash in RCCP using EAF slag aggregate can be considered to apply for sub-base construction.

7) A predicting model for compressive strength of RCCP has been successfully established. It was observed that the mean absolute percentage error of measured strength and calculated strength by the predicting model is less than 10%.

8) A natural coarse aggregate alternative by EAF slag leads to increase water absorption and abrasion resistance of RCCP. With proper fly ash dosage (20%) as cement substitution, slag-RCCP was improved significantly water absorption and abrasion resistance properties.

9) The sulfate resistance of RCCP made with EAF slag aggregate is similar to that of conventional RCCP. There was a continuous increase of compressive strength and mass in early period of exposure. After that, the loss of adhesion and stiffness caused by expansion force of ettringite resulted in the strength reduction.

10) EAF slag aggregate is non-active aggregate by alkali-silica reactions.

11) The new mixing method has mitigated a negative effect of the high water absorption feature of the EAF slag on the water of RCCP containing EAF slag aggregate.

12) The water content of the slag-RCCP mixed by the new method may maintain its workability for 90 min.

13) There was an improvement of slag-RCCP compressive strength when the mixture was mixed by the new method.

14) 90 min of delay in compaction also produced slag-RCCP fulfilling the strength requirement for pavements.

5.2. Suggestions

Some possible ideas are considered for further works:

1) The study on the cost of RCCP made of EAF slag coarse aggregate. And the comparision of the cost of slag-RCCP to that of conventional concrete pavement and asphalt concrete pavement in Southern Vietnam.

2) The environmental benefit analysis of RCCP made of EAF slag coarse aggregate in Vietnam.

3) The field study on the mechanical and durability properties of RCCP made of EAF slag coarse aggregate.

4) The research on the mechanical and durability properties of RCCP containing both of coarse and fine EAF slag aggregate.

REFERENCES

[1]   ACI Committe 325, "ACI 325.10R-95 Report on Roller-Compacted Concrete Pavements," vol. 95, no. Reapproved, pp. 1–32, 2001.

[2]   D. Harrington, F. Abdo, W. Adaska, and C. Hazaree, "Guide for Roller-Compacted Concrete Pavements," *Inst. Transp. Iowa state univerisity*, no. August, p. 104, 2010.

[3]   Y. Ketema, P. E. T. Quezon, and G. Kebede, "Cost and Benefit Analysis of Rigid and Flexible Pavement: A Case Study at Chancho –Derba-Becho Road Project," *Int. J. Sci. Eng. Res.*, vol. 7, no. 10, pp. 181–188, 2016.

[4]   T. D. Nguyen and L. X. Le, "Research of Asphalt Pavement Rutting on National Roads in Vietnam," *ResearchGate*, no. August, 2016.

[5]   World Steel Association, "World Steel in Figures 2016," *World Steel Assoc.*, pp. 3–30, 2016.

[6]   I. Arribas, I. Vegas, J. T. San-José, and J. M. Manso, "Durability studies on steelmaking slag concretes," *Mater. Des.*, vol. 63, pp. 168–176, 2014.

[7]   F. Faleschini, M. Alejandro Fernandez-Ruiz, M. A. Zanini, K. Brunelli, C. Pellegrino, and E. Hernandez-Montes, "High performance concrete with electric arc furnace slag as aggregate: Mechanical and durability properties," *Constr. Build. Mater.*, vol. 101, pp. 113–121, 2015.

[8]   N. Palankar, A. U. Ravi Shankar, and B. M. Mithun, "Durability studies on eco-friendly concrete mixes incorporating steel slag as coarse aggregates," *J. Clean. Prod.*, vol. 129, pp. 437–448, 2016.

[9]   American Concrete Pavement Association, "Roller-Compacted Concrete Pavements as Exposed Wearing Surface," pp. 1–29, 2014.

[10]   ASA-Australasian Slag Association, "A guide to the use of iron and steel slag in roads," 2002.

[11]   M. Prezzi and I. Z. Yildirim, "Use of steel slag in subgrade applications," *Final Rep. INDOT Off. Res. Dev.*, no. October, 2009.

[12]   M. Ameri, S. Hesami, and H. Goli, "Laboratory evaluation of warm mix

asphalt mixtures containing electric arc furnace (EAF) steel slag," *Constr. Build. Mater.*, vol. 49, pp. 611–617, 2013.

[13] M. Pasetto and N. Baldo, "Mix design and performance analysis of asphalt concretes with electric arc furnace slag," *Constr. Build. Mater.*, vol. 25, no. 8, pp. 3458–3468, 2011.

[14] D. F. Lin, L. H. Chou, Y. K. Wang, and H. L. Luo, "Performance evaluation of asphalt concrete test road partially paved with industrial waste - Basic oxygen furnace slag," *Constr. Build. Mater.*, vol. 78, pp. 315–323, 2015.

[15] J. A. . Rohde, L., Nunez, W.P and Ceratti, "Electric arc furnace steel slag - base material for low - volume roads," *Transp. Res. Rec. 1819, Transp. Res. Board, Natl. Res. Counc. Washington, D.C.,* vol. 1, pp. 201–207, 2003.

[16] S. Mathur, S. Soni, and A. Murty, "Utilization of Industrial Wastes in Low-Volume Roads," *Transp. Res. Rec. J. Transp. Res. Board*, vol. 1652, pp. 246–256, 1999.

[17] S. Pamukcu and A. Tuncan, "Laboratory characterization of cement-stabilized iron-rich slag for reuse in transportation facilities," *Transp. Res. Rec.*, no. 1424, 1993.

[18] J. M. Manso, J. A. Polanco, M. Losañez, and J. J. González, "Durability of concrete made with EAF slag as aggregate," *Cem. Concr. Compos.*, vol. 28, no. 6, pp. 528–534, 2006.

[19] G. Adegoloye, A. L. Beaucour, S. Ortola, and A. Noumowé, "Concretes made of EAF slag and AOD slag aggregates from stainless steel process: Mechanical properties and durability," *Constr. Build. Mater.*, vol. 76, pp. 313–321, 2015.

[20] G. Singh and R. Siddique, "Effect of iron slag as partial replacement of fine aggregates on the durability characteristics of self-compacting concrete," *Constr. Build. Mater.*, vol. 128, pp. 88–95, 2016.

[21] Y. N. Sheen, D. H. Le, and T. H. Sun, "Innovative usages of stainless steel slags in developing self-compacting concrete," *Constr. Build. Mater.*, vol. 101, pp. 268–276, 2015.

[22] M. S. H. Khan, A. Castel, A. Akbarnezhad, S. J. Foster, and M. Smith, "Utilisation of steel furnace slag coarse aggregate in a low calcium fly ash geopolymer concrete," *Cem. Concr. Res.*, vol. 89, pp. 220–229, 2016.

[23] Q. Wang, P. Yan, J. Yang, and B. Zhang, "Influence of steel slag on mechanical properties and durability of concrete," *Constr. Build. Mater.*, vol. 47, pp. 1414–1420, 2013.

[24] Y. N. Sheen, D. H. Le, and T. H. Sun, "Greener self-compacting concrete using stainless steel reducing slag," *Constr. Build. Mater.*, vol. 82, pp. 341–350, 2015.

[25] H. Motz and J. Geiseler, "Products of steel slags an opportunity to save natural resources," *Waste Manag.*, vol. 21, no. 3, pp. 285–293, 2001.

[26] A. Sekaran, M. Palaniswamy, and S. Balaraju, "A Study on Suitability of EAF Oxidizing Slag in Concrete: An Eco-Friendly and Sustainable Replacement for Natural Coarse Aggregate," *Sci. World J.*, vol. 2015, 2015.

[27] W. Yeih, T. C. Fu, J. J. Chang, and R. Huang, "Properties of pervious concrete made with air-cooling electric arc furnace slag as aggregates," *Constr. Build. Mater.*, vol. 93, pp. 737–745, 2015.

[28] I. Arribas, A. Santamaría, E. Ruiz, V. Ortega-López, and J. M. Manso, "Electric arc furnace slag and its use in hydraulic concrete," *Constr. Build. Mater.*, vol. 90, pp. 68–79, 2015.

[29] F. Faleschini, K. Brunelli, M. A. Zanini, M. Dabalà, and C. Pellegrino, "Electric Arc Furnace Slag as Coarse Recycled Aggregate for Concrete Production," *J. Sustain. Metall.*, no. November, pp. 44–50, 2015.

[30] S. Monosi, M. L. Ruello, and D. Sani, "Electric arc furnace slag as natural aggregate replacement in concrete production," *Cem. Concr. Compos.*, vol. 66, pp. 66–72, 2016.

[31] H. Yi, G. Xu, H. Cheng, J. Wang, Y. Wan, and H. Chen, "An Overview of Utilization of Steel Slag," *Procedia Environ. Sci.*, vol. 16, pp. 791–801, 2012.

[32] W. Ten Kuo, C. Y. Shu, and Y. W. Han, "Electric arc furnace oxidizing slag

mortar with volume stability for rapid detection," *Constr. Build. Mater.*, vol. 53, pp. 635–641, 2014.

[33] V.S.Ramachandran, P. J. Sereda, and R. F. Feldman, "Mechanism of hydration of calcium oxide," *Nature*, vol. 201, pp. 288–289, 1964.

[34] D. Le, Y. Sheen, and Q. Bui, "An assessment on volume stabilization of mortar with stainless steel slag sand," *Constr. Build. Mater.*, vol. 155, pp. 200–208, 2017.

[35] G. Wang, Y. Wang, and Z. Gao, "Use of steel slag as a granular material: Volume expansion prediction and usability criteria," *J. Hazard. Mater.*, vol. 184, no. 1–3, pp. 555–560, 2010.

[36] Y. Lun, M. Zhou, X. Cai, and F. Xu, "Methods for improving volume stability of steel slag as fine aggregate," *J. Wuhan Univ. Technol. Mater. Sci. Ed.*, vol. 23, no. 5, pp. 737–742, 2008.

[37] W. C. Wang, "Feasibility of stabilizing expanding property of furnace slag by autoclave method," *Constr. Build. Mater.*, vol. 68, pp. 552–557, 2014.

[38] V. Ramakrishnan, "Optimized Aggregate Gradation for Structural Concrete," *Rep. SD2002-02 South Dakota Dep. Transp.*, no. April, 2004.

[39] F. Debieb, L. Courard, S. Kenai, and R. Degeimbre, "Roller compacted concrete with contaminated recycled aggregates," *Constr. Build. Mater.*, vol. 23, no. 11, pp. 3382–3387, 2009.

[40] C. Settari, F. Debieb, E. H. Kadri, and O. Boukendakdji, "Assessing the effects of recycled asphalt pavement materials on the performance of roller compacted concrete," *Constr. Build. Mater.*, vol. 101, pp. 617–621, 2015.

[41] A. Meddah, M. Beddar, and A. Bali, "Use of shredded rubber tire aggregates for roller compacted concrete pavement," *J. Clean. Prod.*, vol. 72, pp. 187–192, 2014.

[42] A. Mardani-Aghabaglou and K. Ramyar, "Mechanical properties of high-volume fly ash roller compacted concrete designed by maximum density method," *Constr. Build. Mater.*, vol. 38, no. 1, pp. 356–364, 2013.

[43] A. Yerramala and K. Ganesh Babu, "Transport properties of high volume

fly ash roller compacted concrete," *Cem. Concr. Compos.*, vol. 33, no. 10, pp. 1057–1062, 2011.

[44] S. K. Rao, P. Sravana, and T. C. Rao, "Investigating the effect of M-sand on abrasion resistance of Fly Ash Roller Compacted Concrete (FRCC)," *Constr. Build. Mater.*, vol. 118, pp. 352–363, 2016.

[45] L. Coppola, A. Buoso, D. Coffetti, P. Kara, and S. Lorenzi, "Electric arc furnace granulated slag for sustainable concrete," *Constr. Build. Mater.*, vol. 123, pp. 115–119, 2016.

[46] G. Singh and R. Siddique, "Strength properties and micro-structural analysis of self-compacting concrete made with iron slag as partial replacement of fine aggregates," *Constr. Build. Mater.*, vol. 127, pp. 144–152, 2016.

[47] S. K. Rao, P. Sravana, and T. C. Rao, "Experimental studies in Ultrasonic Pulse Velocity of roller compacted concrete pavement containing fly ash and M-sand," *Int. J. Pavement Res. Technol.*, 2016.

[48] ASTM C127-07, "Standard Test Method for Density, Relative Density (Specific Gravity) and Absorption of Coarse Aggregate." .

[49] ASTM C128-07a, "Standard Test Method for Density , Relative Density (Specific Gravity), and Absorption of Fine Aggregate." .

[50] ASTM C131-06, "Standard Test Method for Resistance to Degradation of Small-Size Coarse Aggregate by Abrasion and Impact in the Los Angeles Machine."

[51] ASTM C25, "Standard Test Methods for Chemical Analysis of Limestone , Quicklime , and Hydrated."

[52] "Method of Test for Determination of Free Lime Content," Test method of Ministry of Transportation of Ontario, no. 16, pp. 3–5.

[53] ASTM D4792-06, "Standard Test Method for Potential Expansion of Aggregates from Hydration Reactions."

[54] ASTM D1557-12, "Standard Test Methods for Laboratory Compaction Characteristics of Soil Using Modified Effort (56 , 000 ft-lbf / ft 3 (2 , 700

kN-m / m 3)) 1."

[55] ASTM D 1883-99, "Standard Test Method for CBR (California Bearing Ratio) of Laboratory-Compacted Soils."

[56] ASTM C150-07, "Standard Specification for Portland Cement."

[57] ASTM C 618-05, "Standard Specification for Coal Fly Ash and Raw or Calcined Natural Pozzolan for Use in Concrete," *Annu. B. ASTM Stand.*, pp. 3–6, 2010.

[58] ASTM C33/C33M-08, "Standard Specification for Concrete aggregates." .

[59] ASTM C1435/C1435M-08, "Standard Practice for Molding Roller-Compacted Concrete in Cylinder Molds Using a Vibrating Hammer."

[60] ASTM C617/C617M − 12, "Standard Practice for Capping Cylindrical Concrete Specimens."

[61] ASTM C39/C39M-14, "Standard Test Method for Compressive Strength of Cylindrical Concrete Specimens."

[62] ASTM C496/C496M, "Standard Test Method for Splitting Tensile Strength of Cylindrical Concrete Specimens."

[63] ASTM C 469-02, "Standard Test Method for Static Modulus of Elasticity and Poisson's Ratio of Concrete in Compression."

[64] ASTM C 597-02, "Standard Test Method for Pulse Velocity Through Concrete."

[65] BS EN 1338:2003, "Concrete paving blocks-Requirements and test methods." .

[66] ASTM C1260-07, "Standard Test Method for Potential Alkali Reactivity of Aggregates (Mortar-Bar Method)."

[67] ASTM C151-05, "Standard Test Method for Autoclave Expansion of Hydraulic Cement."

[68] M. P. Luxán, R. Sotolongo, F. Dorrego, and E. Herrero, "Characteristics of the slags produced in the fusion of scrap steel by electric arc furnace," *Cem. Concr. Res.*, vol. 30, no. 4, pp. 517–519, 2000.

[69] D. Mombelli, C. Mapelli, S. Barella, C. Di Cecca, G. Le Saout, and E.

Garcia-Diaz, "The effect of chemical composition on the leaching behaviour of electric arc furnace (EAF) carbon steel slag during a standard leaching test," *J. Environ. Chem. Eng.*, vol. 4, no. 1, pp. 1050–1060, 2016.

[70] J. M. Manso, D. Hernández, M. M. Losáñez, and J. J. González, "Design and elaboration of concrete mixtures using steelmaking slags," *ACI Mater. J.*, vol. 108, no. 6, pp. 673–681, 2011.

[71] C. Cao, W. Sun, and H. Qin, "The analysis on strength and fly ash effect of roller-compacted concrete with high volume fly ash," *Cem. Concr. Res.*, vol. 30, no. 1, pp. 71–75, 2000.

[72] C. D. Atiş, "Strength properties of high-volume fly ash roller compacted and workable concrete, and influence of curing condition," *Cem. Concr. Res.*, vol. 35, no. 6, pp. 1112–1121, 2005.

[73] A. Mardani-Aghabaglou, Ö. Andiç-Çakir, and K. Ramyar, "Freeze-thaw resistance and transport properties of high-volume fly ash roller compacted concrete designed by maximum density method," *Cem. Concr. Compos.*, vol. 37, no. 1, pp. 259–266, 2013.

[74] ACI-Committee:209, *Guide for Modeling and Calculating Shrinkage and Creep in Hardened Concrete*, vol. 4, no. Reapproved. 1995.

[75] E. A. Whitehurst, "Soniscope tests concrete structures, Int. Concr. Abstr. Portal.," no. 47(2), pp. 433–444, 1951.

[76] CEB-FIP, "Diagnosis and assessment of concrete structures-state of art report.," *CEB Bull*, no. 192, pp. 83–5, 1989.

[77] M. N. T. Lam, S. Jaritngam, and D. H. Le, "Roller-compacted concrete pavement made of Electric Arc Furnace slag aggregate: Mix design and mechanical properties," *Constr. Build. Mater.*, vol. 154, pp. 482–495, 2017.

[78] M. H. Shehata and M. D. A. Thomas, "The effect of fly ash composition on the expansion of concrete due to alkali-silica reaction," *Cem. Concr. Res.*, vol. 30, no. 7, pp. 1063–1072, 2000.

Paper 1
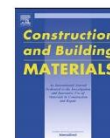
Roller-compacted concrete pavement made of Electric Arc Furnace slag aggregate: Mix design and mechanical properties

My Ngoc-Tra Lam [a,*], Saravut Jaritngam [a], Duc-Hien Le [b]

[a] Department of Civil Engineering, Faculty of Engineering, Prince of Songkla University, Hat Yai, Songkhla, Thailand
[b] Sustainable Developments in Civil Engineering Research Group, Faculty of Civil Engineering, Ton Duc Thang University, Ho Chi Minh City, Viet Nam

HIGHLIGHTS

- EAF slag aggregate and fly ash were employed to develop Roller-compacted concrete pavement (RCCP).
- EAF slag aggregate is stable the volume after treatment process.
- The optimum moisture content of RCCP were determined by the soil compaction method.
- The unit weight and mechanical properties of RCCP were studied.
- A predicting model for compressive strength was proposed.

ARTICLE INFO

ABSTRACT

This research investigates the feasibility of using Electric Arc Furnace (EAF) slag aggregate and fly ash in Roller-compacted concrete pavement (RCCP). After treatment process, EAF slag aggregate was examined the potential expansion caused by hydration reactions and alkali-silica reactions. The test results showed that EAF slag aggregate is stable the volume and can be used in concrete. In the RCCP mixtures, EAF slag was used as a subsititute for natural coarse aggregates with three percentages (i.e. 0%, 50% and 100%) and cement was partially replaced by fly ash at three content levels (i.e. 0%, 20% and 40%). The optimum moisture content of RCCP mixtures containing EAF slag aggregate and fly ash were determined by the soil compaction method. The unit weight and mechanical properties (i.e. compressive strength, splitting tensile strength and elastic modulus) of RCCP were examined through testing program. As a result, the fresh and hardened unit weight are similar to those of conventional RCCP. Moreover, the compressive strength, splitting tensile strength and elastic modulus of RCCP decreased with increasing EAF slag aggregate ratio at all ages. Nevertheless, the conjunction of EAF slag aggregate and 20% fly ash in the RCCP mixtures improved the mechanical properties in the long-term ages. This study has proved that the RCCP containing EAF slag aggregate and fly ash can be employed to develop pavements as an exposed wearing surface. In addition, a predicting model was proposed to calculate compressive strength of RCCP.

© 2017 Elsevier Ltd. All rights reserved.

1. Introduction

Nowadays, sustainable infrastructure development has become increasingly important to all countries around the world. One approach to achieve infrastructure sustainability is the use of waste or by-product materials which reduces environmental impacts and limits natural aggregates consumption. Electric Arc Furnace (EAF) slag is a by-product of steel production, which is generated during the manufacture of crude steel by the Electric Arc Furnace process. World crude steel production reached 1621

million tons for the year 2015 [1]. Based on the production levels of crude steel, world output of steel slag was estimated in the range of 170 million to 250 million tons [2]. A huge quantity of steel slag has been produced every year. In 2015, Vietnam produced 6 million tons of crude steel, up by 5% compared to 2014 [1]. This resulted in about 1 million tons of steel slag produced. The traditional stockpile method has created challenging environmental issues such as a lack of waste storage areas and pollution of soil and underground water. In recent years, many scholars have been interested in studying the recycling of steel slag in concrete industry and have demonstrated that EAF slag can be appropriate to use in concrete (e.g. conventional concrete, high performance concrete, alkali activated concrete) [3–5]. For Roller-compacted

* Corresponding author.
E-mail address: ngoctramys@gmail.com (M.N.-T. Lam).

Table 1
Chemical composition and physical properties of OPC and fly ash used in this study.

	OPC, Type 1	Fly ash
Chemical composition (%)		
Silica (SiO₂)	20.7	52.3
Alumina (Al₂O₃)	4.5	24.9
Ferric oxide (Fe₂O₃)	3.3	14.1
Calcium oxide (CaO)	63.0	–
Magnesium oxide (MgO)	1.8	–
Sodium oxide (Na₂O)	0.10	0.67
Potassium oxide (K₂O)	0.74	–
Sulphuric anhydride (SO₃)	2.3	0.47
Loss on ignition (LOI)	2.8	0.15
Physical characteristics		
Fineness (Blaine) (m²/kg)	347	289
Specific gravity	3.14	2.40
Initial setting time (min)	110	NA
Final setting time (min)	170	NA
Particle composition		
Retaining on 45 μm sieve (%)	NA	7.92
Compressive strength (N/mm²)		
1 day	14.6	–
3 days	26.2	–
7 days	33.0	–
28 days	43.0	–

Note: NA means not available.

concrete pavement (RCCP), many studies have investigated the use of various recycled aggregates from concrete slabs, asphalt pavement and shredded rubber tires as substitute for natural aggregates [6–8]. Nevertheless, there were no specific studies that reported the utilization of EAF slag aggregate in RCCP.

Roller-Compacted concrete pavement is a special type of concrete, which is stiff and no-slump. The difference between RCCP and traditional concrete is mixing proportions. RCCP mixture has a higher volume of fine aggregate and a lower volume of cementitious materials, coarse aggregate and water. It is placed with a standard or high-density asphalt-type paver equipment and compacted by vibratory rollers to attain a target density and homogeneous surface pavement. RCCP mixture should be dry enough to maintain the stability of vibratory roller and wet enough to distribute the paste. Therefore, the mixing proportion has to be calculated carefully. Two main approaches to determine RCCP mixing proportion are soil compaction and consistency. Soil compaction method establishes the compaction curve to obtain maximum dry density in conjunction with optimum moisture content. The mixture with optimum water and low water-cement ratio can reduce the cement content. Hazaree et al. [9] reported that the optimum cement content was 250–300 kg/m³. After this optimum cement point, density, compressive strength, permeable void content and water absorption of RCCP declined with increasing cement content. The cement content is selected based on strength, durability of RCCP and characteristics of available aggregates. American Concrete Pavement Association recommends a minimum compressive strength of 28 MPa or 31 MPa, if RCCP is to be used in areas without freeze-thaw conditions or freeze-thaw conditions, respectively [10].

Besides, many scholars have studied the replacement of cement by waste or by-product materials in RCCP. Fly ash is usually used to replace cement. For example, Mardani-Aghabaglou et al. studied the mechanical [11] and transport properties [12] of high-volume fly ash of RCCP designed by maximum density method. In this study, total binder content was kept constant at 250 kg/m³, cement

Table 2
Physical properties of the crushed stone aggregate and EAF slag aggregate used in this study.

Properties	Crushed stone		EAF slag
	Fine aggregate (4.75–0 mm)	Coarse aggregate (19–4.75 mm)	Coarse aggregate (19–4.75 mm)
Apparent specific gravity	2.71	2.72	3.40
Density (OD) (kg/m³)	2609	2680	3085
Density (SSD) (kg/m³)	2644	2691	3176
Bulk density (kg/m³)	1493	1466	1686
Water absorption (%)	1.36	0.44	2.93
Los Angeles abrasion value (%)	NA	13.98	19.37

Note: NA means not available.

Fig. 1. The suggested limits of RCCP aggregate gradation, the 0.45-power curve for 19 mm maximum size and the designing gradation used in this study.

Fig. 2. Three particle sizes (i.e. 4.75–9.5 mm, 9.5–12.5 mm and 12.5–19 mm) of EAF slag aggregate used in this study.

Fig. 3. The testing specimens were stored in water at 70 ± 3 °C.

Fig. 4. Record the comparator reading of the specimen.

Fig. 5. The 150 × 300 mm cylinder mold and vibrating hammer.

was replaced with 20, 40 and 60% fly ash. It is reported that there was a slight decrease in the strength and durability values as fly ash content increased at early ages. However, at later ages, the development of strength and durability attained satisfactory level for pavement application. In a similar study, Yerramala and Babu [13] examined the transport properties of RCCP that contains fly ash in high volume ranging from 40% to 85% by mass of the total

cementitious materials. It was observed that their mixtures with moderate amount of cement ranging from 150 to 190 kg/m^3 and fly ash percentage ranging from 60% to 70% performed low values of the permeability, absorption, sorption and chloride diffusivity. Rao et al. [14] conducted abrasion resistance tests on RCCP containing fly ash and manufactured sand. Experimental results showed that incorporating fly ash and manufactured sand in RCCP improved the Cantabro abrasion resistance and surface abrasion resistance in comparison with its referenced concrete.

From the advantages of using EAF slag aggregate in concrete and fly ash in RCCP, in this study, the recycling of EAF slag in conjunction with fly ash sourced from Southern Vietnam in RCCP has been proposed as a solution to save cost and reduce waste storage areas and environmental pollution. For application of EAF slag in concrete, the volume stability must be controlled before using, so EAF slag aggregate was examined the potential expansion caused

by hydration reactions and alkali-silica reactions. Then, the optimum moisture content of RCCP mixtures using EAF slag aggregate and fly ash were determined by the soil compaction method. Finally, the unit weight (i.e. fresh and hardened) and mechanical properties (i.e. compressive strength, splitting tensile strength and elastic modulus) of RCCP were investigated.

2. Testing program

2.1. Materials used

In this study, Ordinary Portland Cement (OPC) type I with the specifications in accordance with ASTM C150 was used [15]. Fly ash sourced in Southern Vietnam was used to replace cement. The chemical composition and physical characteristics of OPC and fly ash are shown in Table 1. Since the total of SAF($SiO_2 + Al_2O_3 + Fe_2O_3$) = 91.3% > 70%, fly ash is classified as low-calcium Class F fly ash according to ASTM C618 [16].

Coarse and fine aggregate were used in this study are the crushed stone. Their physical properties were listed in Table 2 fulfilling the quality requirements of ASTM C33 [17]. The maximum aggregate size is 19 mm to reduce the potential segregation and improve smooth pavement surface. Mixture should contain 50–65% of fine aggregate passing No.4 (4.75 mm) [18], which consists of 2–8% of aggregate finer than No.200 (75 μm) [19]. The 0.45-power curve is the best gradation that is used to reach the maximum density of RCCP at any maximum size [20]. Fig. 1 shows the suggested aggregate gradation was recommended by American Concrete Pavement Association [10], the 0.45-power curve for 19 mm maximum size and the designing gradation in this study. The designing gradation was obtained by mixing 42% wt. of the coarse aggregate (19–4.75 mm) and 58% wt. of the fine aggregate (4.75–0 mm).

EAF slag aggregate from Southern Vietnam (Fig. 2) was used to substitute for coarse aggregate. In order to limit the risk of expansion, EAF slag was subjected to weathering in outdoor conditions and sprayed with water every day for at least 90 days. After the treatment process, the physical and chemical properties of EAF slag aggregate were examined. The volume stability of EAF slag aggregate was measured through the expansion tests. The potential expansion from hydration reactions and the potential alkali reactivity of EAF slag aggregate were examined following ASTM D4792 [21] and ASTM C1260 [22].

Table 3
The testing approaches and the quantity of samples used in this study.

No.	Testing items	Sample dimension (mm)	Quantity of sample	ASTM standard
1	Expansion of EAF slag aggregate	6-in (152.4 mm) diameter mold	6	ASTM D4792
2	Expansion of mortar bars	$25 \times 25 \times 250$	9	ASTM C1260
3	Optimum moisture content	6-in (152.4 mm) diameter mold	45	ASTM D1557
4	Fresh unit weight	–	–	ASTM C138
5	Hardened unit weight	150×300, cylinder	–	ASTM C642
6	Compressive strength	150×300, cylinder	108	ASTM C39
7	Splitting tensile strength	150×300, cylinder	108	ASTM C496
8	Modulus of elasticity	150×300, cylinder	27	ASTM C469

Table 4
Chemical composition of the weathered EAF slag aggregate.

Oxide composition (wt.%)	In this study	Manso et al. [36]	Arribas et al. [37]	Faleschini et al. [38]	Monosi et al. [39]
CaO	25.94	23.9	25.72	30.30	26
$\sum$ Iron oxides	34.73	42.5	27.54	33.28	35
SiO_2	16.32	15.3	17.88	14.56	14
MgO	6.86	5.1	3.82	2.97	5
Al_2O_3	8.31	7.4	11.62	10.20	12
MnO	5.18	4.5	4.15	4.34	6
TiO_2	1.98	–	0.71	–	0.41
Na_2O	0.30	–	0.1	–	0.2
K_2O	0.10	–	–	–	0.1
P_2O_5	0.25	–	0.46	–	–
Free CaO	<0.1%	0.45	–	–	–
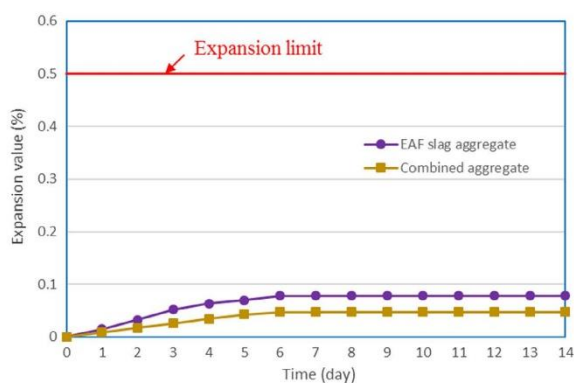
Fig. 6. Volume expansion curves of the EAF slag and combined aggregate.

Table 5
Expansion values of aggregates.

Day	Expansion values (%)	
	EAF slag aggregate	Combined aggregate (50% crushed stone plus 50% EAF slag)
0	0	0
1	0.015	0.009
2	0.033	0.017
3	0.052	0.026
4	0.064	0.034
5	0.070	0.043
6	0.078	0.047
7	0.078	0.047
8	0.078	0.047
9	0.078	0.047
10	0.078	0.047
11	0.078	0.047
12	0.078	0.047
13	0.078	0.047
14	0.078	0.047

2.2. Testing approaches and sample preparation

2.2.1. EAF slag aggregate

After the treatment process, EAF slag aggregate had the physical properties and chemical composition examined following the ASTM standards [23–26]. EAF slag may be contain free CaO. When the free CaO forms strained $Ca(OH)_2$, its volume becoming about twice its original size. This characteristic is a serious concern because it leads to cracking and deterioration. Therefore, it is very important to estimate total free CaO content in EAF slag aggregate after treatment process. In this study, free CaO content was determined following a test method of Ministry of Transportation of Ontario [27] through ethylene glycol and complexometric titration. According to this method, the finely ground EAF slag was mixed with ethylene glycol and methyl alcohol and heated to dissolve the free CaO. After filtering, the filtrate was added bromothymol blue as an indicator. Then, the filtrate was titrated with hydrochloric acid (HCl) to determine free CaO content.

Besides, the ASTM D4792 standard was used to test the potential expansion of EAF slag aggregate from hydration reactions. Besides, this test method can also be used to evaluate the effectiveness of treatment process for reducing the expansive potential of EAF slag. Two types of aggregate (i.e. 100% EAF slag and 50% EAF slag plus 50% crushed stone) were prepared following ASTM D1883 [28]. For each aggregate type, three test specimens were compacted at their optimum moisture content to reach the maximum density in a 6-in cylinder mold in accordance with ASTM D1557 [29]. To accelerate the hydration reaction, the testing molds were stored in water at 70 ± 3 °C (Fig. 3). After 30 min, the initial dial gage readings were recorded. The volume expansion was calculated daily for 14 days by dividing the difference between the daily dial gage reading and the base reading by the initial specimen height (116.43 mm).

Additionally, in order to detect the potential for deleterious alkali-silica reaction of EAF slag aggregate in mortar bars, three mortar mixtures were prepared in accordance with ASTM C1260 [22]. Rhyolite rocks were crushed to fine aggregate sizes which were used in the first mixture. Reactive siliceous minerals are often present in Rhyolite rocks. The second mixture was 50% crushed Rhyolite rock in conjunction with 50% EAF slag (combined mixture). Finally, the third mixture used 100% EAF slag. In the mortar mixture, the aggregate-cement ratio is 2.25 and the water-cement ratio is 0.47 by mass. Three test specimens (25 × 25 × 250 mm) were produced for each mortar mixture. The specimens shall remain in the molds for 24 ± 2 h in the moist cabinet. After the specimens were removed from the mold, make and record the initial comparator reading. Place each sample group in a storage container with sufficient tap water to totally immerse them. Then seal and place the containers in an oven at 80.0 ± 2.0 °C for a period of 24 h. After 24 h, remove the containers from the oven one at a time. Remove the bars one at a time from the water and dry their surface and take the zero reading of each bar immediately. Place all specimens made with each sample group in a container with sufficient 1 N NaOH at 80.0 ± 2.0 °C for the samples to be totally immersed. Seal the container and return it to the oven. Make subsequent comparator readings of the specimens periodically (Fig. 4).

2.2.2. Mixing proportion of RCCP

Three combinations of coarse aggregates were prepared to produce RCCP, i.e. 100% crushed stone (group A), 50% crushed stone plus 50% EAF slag (group B) and 100% EAF slag (group C). According to Guide for Roller-Compacted Concrete Pavements [19], the cement content in RCCP has usually been recommended between 11% and 13% by weight of cement and oven-dried aggregates. Therefore, in this study the weight of cement was fixed at 12% of total weight of cement and oven-dried aggregates in the mix. In each aggregate group, fly ash (Class F) substituted for cement at three percentages (i.e. 0%, 20% and 40%) as shown in Table 8.

2.2.3. RCCP testing program

In the RCCP testing program, nine RCCP mixtures were prepared to conduct the modified Proctor test [29]. According to ASTM D1557 [29], the RCCP mixture is placed in five layers into the 6-in (152.4 mm) mold. Each layer will be compacted by 56 blows of a rammer. The resulting dry density is determined. The results establish a relationship between the dry density and the moisture content of RCCP mixture to obtain the optimum moisture content and maximum dry density.

After identifying the RCCP mixing proportions, the unit weight (i.e. fresh and hardened) and the mechanical properties (i.e. compressive strength, splitting tensile strength and modulus of elasticity) were studied. Hence, standard cylindrical specimens were prepared. Their dimensions are 150 mm diameter and 300 mm height. The RCCP mixture was compacted in molds by vibrating hammer in four layers (Fig. 5), and the compaction time is 20 s per layer conforming to ASTM C1435 [30]. Fresh unit weight was measured after molding. All specimens were molded for 24 h at the temperature of 23 ± 2 °C after casting. After 24 h, samples were removed from the mold and their hardened unit weight were measured. Then, specimens were cured in tap water at the temperature of 23 ± 2 °C until testing ages were reached. At least 16 h before testing, the cylinder specimens underwent capping procedure in accordance with ASTM C617 [31], in which sulfur mortar was used to give them a plane surface. The compressive and splitting tensile strength were tested at 3, 7, 28 and 91-day ages in accordance with ASTM C39 [32] and ASTM C496 [33]. The modulus of elasticity was obtained at the age of 91 days in accordance with ASTM C469 [34]. Table 3 shows the testing approaches and the quantity of samples in this study.

3. Results and discussions

3.1. Properties of EAF slag used

Physical properties of EAF slag aggregate are eligible to replace crushed stone aggregate as shown in Table 2. The chemical composition of weathered EAF slag was listed in Table 4. It was found that free CaO content (<0.1%) was too low to create cracking or instability problems.

Luxan et al. [35] called EAF black basic slag which is generated from the cold loading of scrap and contains lower than 40% of Calcium Oxide (CaO). EAF slag used in this study contains 25.94% of CaO. Hence, it can be classified as EAF black basic slag. Several other researchers reported similar common oxide compositions of EAF slag in Table 4 [36–39]. EAF black basic slag has high density, low water absorption and low porosity. Mombelli et al. [40] demonstrated that EAF slag can be reused if MgO and Al_2O_3 contents are in the range of 5–7% and 7–10% by weight, respectively. Furthermore, CaO content should not exceed 30% by weight. According to chemical composition results, EAF slag in Southern Vietnam has stable and non-leachable characteristics which can be appropriate for recycling.

3.2. Expansion of EAF slag aggregate

The volume expansion of aggregate is caused by unstable compound (e.g. free CaO, free MgO) that can hydrate and results in vol-

Table 6
Expansion values of mortar bars (%).

Mix ID.	The immersing time of mortar bars in NaOH solution (day)								
	0	3	7	10	14	17	21	24	28
A00	0	0.05	0.07	0.13	0.17	0.21	0.24	0.29	0.32
B00	0	0.04	0.05	0.09	0.11	0.15	0.17	0.19	0.21
C00	0	0.03	0.03	0.03	0.04	0.04	0.04	0.05	0.05

ume increase. Free CaO can react with water to produce Ca(OH)$_2$ in a few days. It is clear from the Fig. 6 that the volume expansion both of combined (50% crushed stone plus 50% EAF slag) and EAF slag aggregates were occurred for 5 days. The Table 5 showed the expansion value of combined aggregate was 0.009% and that of EAF slag aggregate was 0.015% at day 1. After that, the volume expansion rose rapidly within 5 days and reached the peak at day 6. EAF slag aggregate showed a higher volume expansion than the combined aggregate. According to the ASTM D4972 standard, the limit value of expansion is 0.5%. The highest expansion value of the used slag (0.078%) is lower than the limit value (0.5%) given by the ASTM D4792. Therefore, the expansive potential of EAF slag aggregate is very low. Unlike free CaO, free MgO (periclase) usually forms solid solution mainly with FeO and MnO leading to expansive phenomena in the long term. Luo [41] proposed that if the percentage ratio by weight of MgO to FeO plus MnO less than 1, MgO is stable. According to the chemical composition (Table 4), it can be said that MgO content in the used slag is stable compound. As a result, EAF slag aggregate in this study is stable the volume with hydration reactions.

3.3. Expansion of mortar bar made with EAF slag aggregate

Alkali-silica reactions result from siliceous minerals in aggregates can react with alkali hydroxides in concrete. Reaction products swell as it draws water from surrounding cement paste leading to expansion of concrete [42].

As can be seen from the Table 6, the expansion values of crushed stone sample, combined sample and EAF slag sample were 0.17%, 0.11% and 0.04% at 14 days after immersing in NaOH solution, respectively. According to the ASTM C1260 standard, at 14 days, expansion of less than 0.1% is indicative of innocuous behavior in most case, so the EAF slag sample in this study is indicative of innocuous behavior. Whereas, the crushed stone sample and combined sample are indicative both of innocuous and deleterious behavior because expansion values of mortar bars are between 0.1% and 0.2%. In such a situation, it can be useful to observe the expansion until 28 days. As shown in the Fig. 7, when the immersing time was expanded until 28 days, the expansion of EAF slag sample was 0.05% which was below the limit (0.1%). Thomas et al. [43] have demonstrated that the accelerated mortar bar tests produce an outcome which agrees well with the performance of concrete in the laboratory or under field condition. Aggregates

are indicative of harmless behavior when tested in the mortar bar have a very low risk of resulting in damage when used in concrete. It can be said that the using of 100% of EAF slag aggregate in this study in RCCP is acceptable. At 28 days, the expansion value of crushed stone and combined sample were 0.32% and 0.21%. Therefore, the crushed stone sample is indicative of deleterious behavior, whereas the combine EAF slag with crushed stone aggregate in mortar bar mitigated the deleterious alkali-silica reaction.

3.4. Study on the RCCP mixing proportion

The optimum moisture content of RCCP for most aggregates is found to be within the range of 5–8% [19]. The moisture content was calculated according to the following Eq. (1):

$$w = \frac{m_w}{m_c + m_a} \times 100 \tag{1}$$

where m_w is the weight of water, m_c is the weight of cement, m_a is the weight of oven-dried aggregates, w (%) is the moisture content;

In each RCCP mixture, the modified Proctor test was conducted at five points of moisture content with increment by 1% to establish the compaction curve. It began with 5% of moisture content in group A mixtures and 6% of moisture content in group B/C mixtures. From the test results, the compaction curve was plotted in Fig. 8. From this figure, the optimum moisture content and maximum dry density of each mixture were obtained in Table 7.

It can be observed in Fig. 9, the optimum moisture content and maximum dry density increased with a higher amount of EAF slag aggregate. This observation can be explained by higher water absorption and bulk density of EAF slag as compared to crushed stone aggregate. Test results revealed that the optimum moisture content of group B and C grew by 15% and 22% when compared to group A. The maximum dry density in group B and C increased slightly by 1% and 4% when compared to group A. On the other hand, there was a slight decrease in the optimum moisture content and maximum dry density when increasing amount of fly ash used in the mixture. This may be because the spherical-shaped particles of fly ash provide water-reducing characteristics that is similar to a water-reducing admixture and fly ash has lower unit weight as compared to cement. When 20% and 40% of cement was substituted with fly ash, the optimum moisture content of these mixtures decreased by 4% and 7% and the maximum dry density

Fig. 7. Expansion curves of the mortar bars.
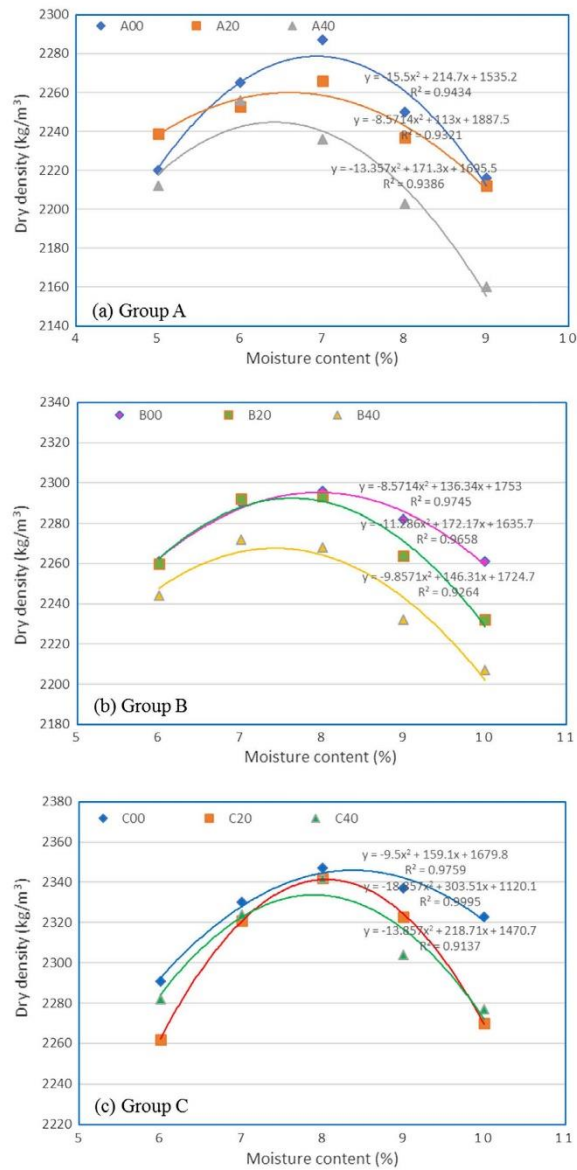
Fig. 8. The compaction curve of the RCCP mixtures.

decreased by 0.5% and 1% as compared to the mixtures without fly ash.

As a result, nine mixture proportions with optimum moisture content were prepared to investigate the unit weight and mechanical properties of RCCP as shown in Table 8.

3.5. Fresh and hardened unit weight

Fig. 10 presents the fresh and hardened unit weight of RCCP mixtures. Group A achieved the average fresh unit weight of 2458 kg/m³, whereas group B and C achieved the average fresh

unit weight of 2511 kg/m³ and 2570 kg/m³, respectively; an increase of 2% and 4% in comparison with group A. The unit weight increased because EAF slag aggregate has unit weight higher than crushed stone aggregate. Moreover, the hardened unit weight had the same trend of the fresh unit weight. The average hardened unit weight of group C (i.e. 2565 kg/m³) was highest and group A was lowest (i.e. 2453 kg/m³). On the other hand, it can be seen that the replacement of cement by fly ash in group C caused a sharp decrease in the fresh and hardened unit weight, leading to an improvement of their unit weight.

3.6. Compressive strength

The compressive strength, splitting tensile strength and elastic modulus results of RCCP mixtures were obtained at various ages as presented in Table 9. Fig. 11 presents the compressive and splitting tensile strength of the RCCP mixtures at 3, 7, 28 and 91-day ages.

From Fig. 11a, the A00 mixture has the highest values in comparison with B00 and C00 mixtures in all ages. This may be because of the following reasons. Firstly, the A00 mixture has lower water-cement ratio than that in the B00 and C00 mixtures. The water

Table 7
The optimum moisture content and maximum dry density of RCCP mixtures.

Group	Mixture	Dry density (γ) = moisture content relationship (W)	R^2	Optimum moisture content (%)	Maximum dry density (kg/m³)
A	A00	$\gamma = -15.5W^2 + 214.7W + 1535.2$	0.94	6.93	2279
	A20	$\gamma = -8.57W^2 + 113W + 1887.5$	0.93	6.59	2260
	A40	$\gamma = -13.36W^2 + 171.3W + 1695.5$	0.94	6.41	2245
B	B00	$\gamma = -8.57W^2 + 136.34W + 1753$	0.97	7.95	2295
	B20	$\gamma = -11.29W^2 + 172.17W + 1635.7$	0.97	7.63	2292
	B40	$\gamma = -9.86W^2 + 146.31W + 1724.7$	0.93	7.42	2268
C	C00	$\gamma = -9.5W^2 + 159.1W + 1679.8$	0.98	8.37	2346
	C20	$\gamma = -18.86W^2 + 303.51W + 1120.1$	1.00	8.04	2341
	C40	$\gamma = -13.86W^2 + 218.71W + 1470.7$	0.91	7.89	2334
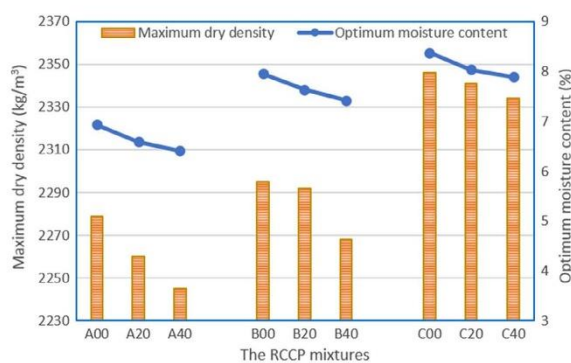
Fig. 9. The optimum moisture content and maximum dry density of RCCP mixtures.

Table 8
Mixing proportions of RCCP with optimum water content.

Group	Mixture	Cementitious materials			Coarse aggregate			Fine aggregate	Optimum water content (kg/m³)
		Fly ash (%)	Fly ash (kg/m³)	OPC (kg/m³)	EAF slag (%)	EAF slag (kg/m³)	Crushed stone (kg/m³)	Crushed stone (kg/m³)	
A	A00	0	0	274	0	0	842	1163	158
	A20	20	54	217	0	0	835	1154	149
	A40	40	108	161	0	0	830	1146	144
B	B00	0	0	275	50	424	424	1172	182
	B20	20	55	220	50	423	423	1171	175
	B40	40	109	163	50	419	419	1158	168
C	C00	0	0	282	100	867	0	1197	196
	C20	20	56	225	100	865	0	1195	188
	C40	40	112	168	100	863	0	1191	184

Note: Cementitious materials are fixed at 12% of total weight of cementitious materials and oven-dried aggregates.

absorption of crushed stone and EAF slag aggregate are 0.44% and 2.93%. Hence, the amount of effective water can be calculated as 154, 168 and 171 L/m^3 from the total water added to the mixtures. As a result, the effective water-cement ratio in the A00, B00, C00 mixtures are 0.56, 0.61 and 0.61, respectively [44]. Secondly, from Fig. 12, the width of Interfacial Transition Zone (ITZ) of the RCCP mixture is about 30 µm, which results in the weak bond between EAF slag aggregate and matrix. Moreover, Adegoloye et al. [3] reported that the ITZ in high water-cement ratio concretes are better than in low water-cement ratio concretes. Finally, Palankar et al. [5] showed that the reduction in strength of concrete made with EAF slag aggregate may be the weak bond strength between the cement paste and aggregates. This problem happened due to the formation of calcite coating during the weathering treatment process of EAF slag aggregate. It is all of reasons to explain the strength declined.

At 3-day age, the compressive strength of A00 and B00 mixture reached 25.87 and 22.08 MPa. The strength of these mixtures rose sharply by 54% at 7-day age and 85% at 28-day age when compared to the strength at 3-day age. On the other hand, there was a significant effect on compressive strength in C00 mixture due to the water absorption of EAF slag aggregate. At 7-day and 28-day ages, its strength (i.e. 27.43 MPa, 35.56 MPa) was lower than B00's strength (i.e. 34.02 MPa, 41.46 MPa). However, at 91-day age, its strength (i.e. 43.29 MPa) was similar to B00's strength (i.e. 43.01 MPa). It can be said that EAF slag aggregate retains water and leads to restrain the development of strength at early-age. Nevertheless, the strength was improved in the long run. Fig. 13

shows the 28-day compressive strength of A00, B00 and C00 mixtures which have remarkably exceeded the compressive strength requirement for Roller-Compacted concrete pavements [10].

From Fig. 11b and c, all mixtures with fly ash had low strength at early ages due to the pozzolanic characteristic of fly ash. At 7-day age, the compressive strength of B20 and C20 mixtures (i.e. 23.85, 21.02 MPa) reached approximately 70% of compressive strength of B00 and C00 mixtures (i.e. 34.02, 27.43 MPa). Because of the pozzolanic reactions, their strength increased dramatically and reached 42.84 and 43.35 MPa at 91-day age, which were similar to the strength of B00 and C00 mixtures. In addition, fly ash was also used as a filler that improved strength in the mixture. This result proves that RCCP containing EAF slag aggregate and 20% fly ash produces good concrete, which can be used for pavements [10]. However, if fly ash is used more than the optimum content, this leads the strength will be decreased. This observation was presented in the B40 and C40 mixtures. Their compressive strength was 15.98 and 15.16 MPa at 7-day age and 26.99 and 23.20 MPa at 28-day age. It is because fly ash is not as good as cement in terms of strength contribution. These results are in agreement with some previous studies on Roller-compacted concrete [11], [45], [46]. It was observed that the compressive strength of B40 and C40 mixture are not suitable for Roller-Compacted concrete pavements as an exposed wearing surface [10]. Nevertheless, the long-term strength was improved by pozzolanic reaction of fly ash. The compressive strength of B40 and C40 mixtures reached 37.69 and 35.37 MPa at 91-day age. These mixtures could be used in application for sub-base construction.
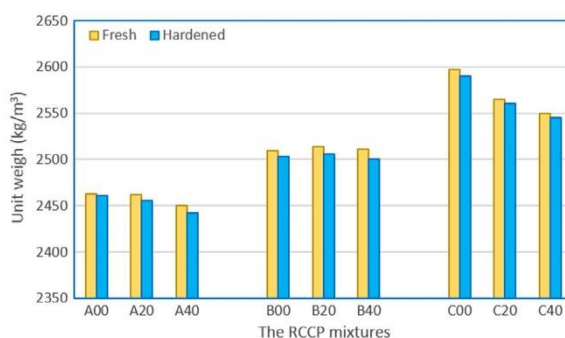
Fig. 10. Fresh and hardened unit weight of RCCP mixtures.

Table 9
Compressive strength, splitting tensile strength and elastic modulus results of RCCP.

Group	Mix	Compressive strength (MPa)				Splitting tensile strength (MPa)				Modulus of elasticity (GPa)
		3-day	7-day	28-day	91-day	3-day	7-day	28-day	91-day	91-day
A	A00	25.87	39.63	47.04	56.45	3.68	4.07	4.51	5.28	34.80
	A20	22.52	29.39	42.44	58.40	3.01	3.46	4.53	5.54	37.29
	A40	17.88	23.77	38.03	50.42	2.07	2.60	4.47	5.14	34.53
B	B00	22.08	34.02	41.46	43.01	2.86	3.25	4.12	4.74	33.64
	B20	17.45	23.85	37.82	42.84	2.29	2.59	3.99	5.09	35.71
	B40	11.89	15.98	26.99	37.69	1.56	2.01	3.76	4.19	33.49
C	C00	21.58	27.43	35.56	43.29	2.77	3.09	4.07	4.68	33.23
	C20	15.73	21.02	30.07	43.35	2.01	2.43	3.72	4.26	35.56
	C40	11.05	15.16	23.20	35.37	1.49	1.97	2.79	4.14	33.04

Note: Each value is the average of three measurements on three different samples.
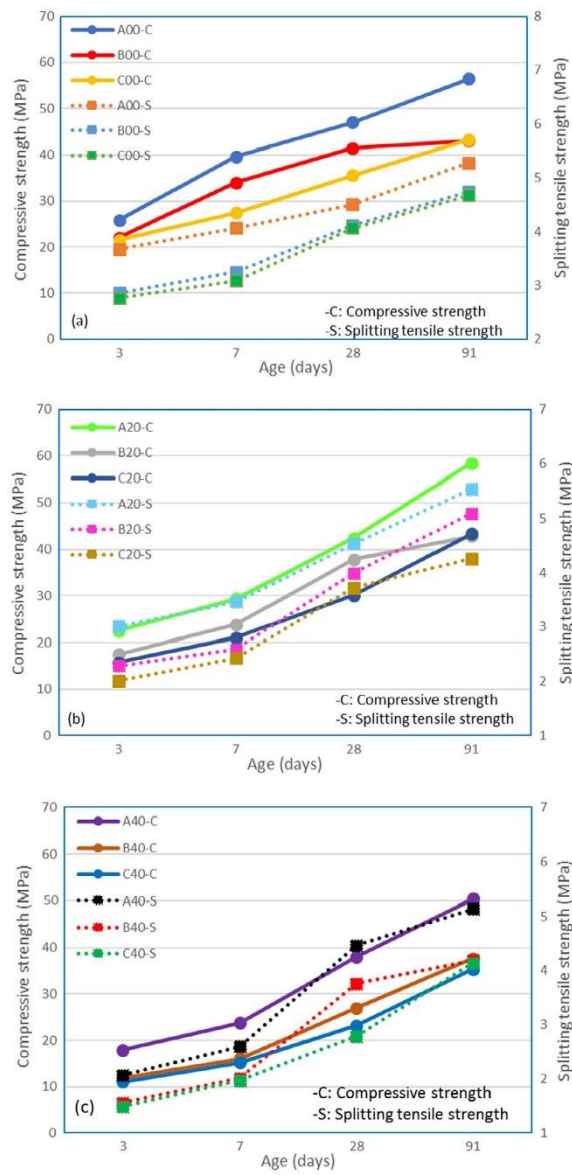
Fig. 11. Compressive and splitting tensile strength of RCCP mixtures at various ages.

3.7. Splitting tensile strength

From Fig.11a, for the series mixtures without fly ash, the A00 mixture had the highest splitting tensile strength in all ages. When EAF slag was used to replace crushed stone aggregate, there was a dramatic decrease in splitting tensile strength. However, the strength of B00 and C00 mixtures were similar in all ages. That
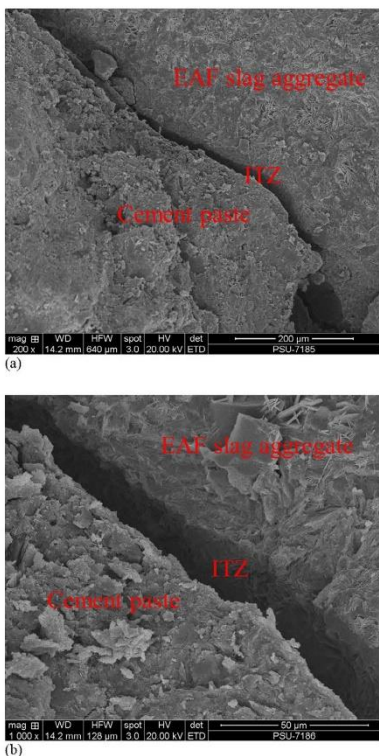
Fig. 12. SEM images of ITZ: (a) 200 magnification and (b) 1000 magnification.

means EAF slag replacement ratio had a minor effect on the splitting tensile strength.

For the series mixtures with 20% fly ash used to replace cement, it can be seen that this series mixture had lower strength than the series mixtures without fly ash at early ages. However, there was an improvement on strength at long-term ages. For example, the splitting tensile strength of A20, B20 and C20 mixtures were 5.54, 5.09 and 4.26 MPa at 91-day age (Fig. 11b). In addition, the effect of fly ash on the splitting tensile strength was different from the compressive strength. At 91-day age, the splitting tensile strength of C20 mixture was lower than that of B20 mixture, whereas the compressive strength was similar. That means the contribution of 20% fly ash to the splitting tensile strength is lower than the compressive strength.

Similar to the compressive strength trend, the series mixtures with 40% fly ash had the lowest splitting tensile strength at all ages. These were 2.07, 1.56 and 1.49 MPa at 3-day age and 5.14, 4.19 and 4.14 MPa at 91-day age for A40, B40 and C40 mixtures, respectively (Fig. 11c). These results are in agreement with previous studies conducted on RCCP with fly ash [37]–[39]. These mixtures can be used as sub-base for road pavements.

3.8. Modulus of elasticity

Fig. 14 presents the elastic modulus of RCCP mixtures at 91-day age. In each group, the elastic modulus value was highest in the mixture which replaced 20% cement with fly ash (i.e. A20, B20, C20 mixture). The values were 37.29, 35.71 and 35.56 GPa for A20, B20 and C20, respectively. It was observed that their values were impacted when replaced crushed stone aggregate with EAF slag aggregate. Their values decreased with increasing replaced ratio. Like the strength variation, the lowest elastic modulus values belong to RCCP mixtures that substituted 40% cement with fly ash. There were 34.53, 33.49 and 33.04 GPa for A40, B40 and C00 mixtures, respectively.

3.9. Analysis of SEM

The ITZ is a zone surrounding the aggregate particles. The ITZ plays an important role in the strength and porosity of concrete because it is the weakest phase in three phases of concrete (i.e. aggregate, ITZ and matrix). The better the quality of the ITZ, the
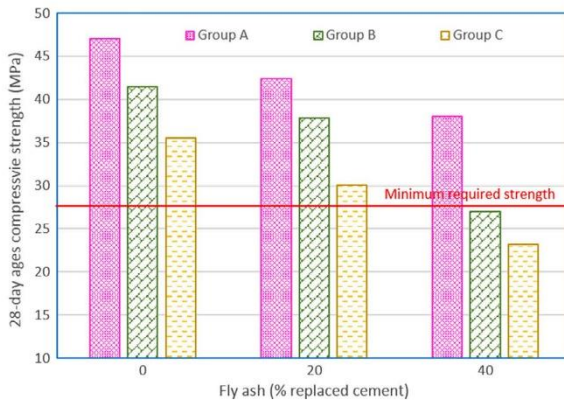
Fig. 13. The 28-day compressive strength with various fly ash replacement ratio.

89
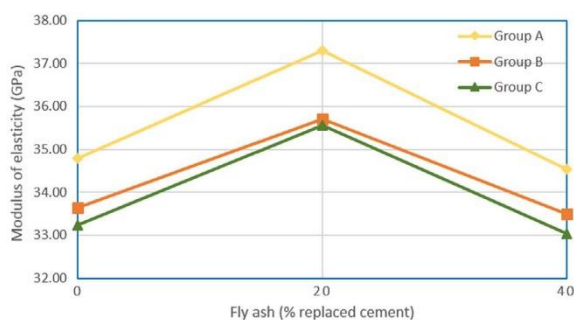
Fig. 14. Modulus of elasticity of RCCP mixtures at 91 days.

Table 10
The *a*-coefficient and *b*-coefficient values.

Group	Mixture	*a*-Coefficient	*b*-Coefficient	R²
0% fly ash	A00	2.9124	0.8289	0.9839
	B00	2.8624	0.8909	0.9825
	C00	2.4199	0.9624	0.9624
20% fly ash	A20	3.3662	0.8238	0.9429
	B20	3.9908	0.8873	0.9788
	C20	3.5100	0.8001	0.9446
40% fly ash	A40	4.1052	0.8336	0.9528
	B40	4.6415	0.8120	0.9483
	C40	4.1885	0.7739	0.9475

Fig. 15. *a*-Coefficient versus various EAF slag ratio.

better the strength. Arribas et al. [37] have demonstrated that EAF oxidizing slag aggregate is very good in terms of strength contribution in conventional concrete because the width of ITZ was 2–4 μm. Based on SEM images (Fig. 12), the width of ITZ in the RCCP mixture is about 30 μm, which results in the weak bond between EAF slag aggregate and matrix. Furthermore, SEM images showed that EAF slag aggregate has a rough surface and low porosity.

3.10. Predicting model for compressive strength

Based on ACI model, a mathematical model was proposed to calculate compressive strength of RCCP. Some previous scholars have used the ACI model for normal concrete to predict compressive strength [47], [48]. According to ACI-Committee 209 [49], compressive strength at $t-$ and 28 days are correlated by the following Eq. (2)

$$f_c(t) = \frac{t}{a + b.t} f_c(28) \qquad (2)$$

where $f_c(t)$ and $f_c(28)$ are the cylindrical compressive strength at $t-$ and 28 days (MPa), respectively; t is testing age (days); a and b are model coefficients and their values are 4 and 0.85 for normal concrete, respectively.
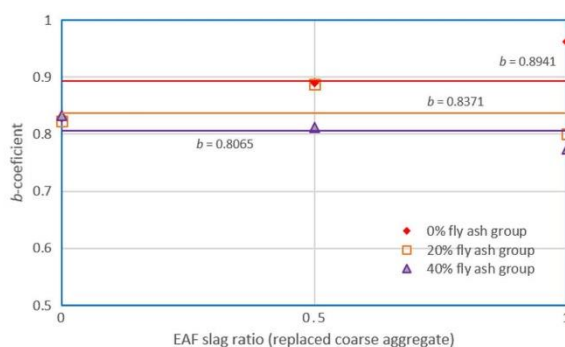
Fig. 16. *b*-Coefficient versus various EAF replacement ratio.

Table 11
The a_1, a_2, a_3, b values.

Group	a_1	a_2	a_3	b
0% fly ash	−0.7850	0.2925	2.9124	0.8941
20% fly ash	−2.2108	2.3546	3.3662	0.8371
40% fly ash	−1.9786	2.0619	4.1052	0.8065
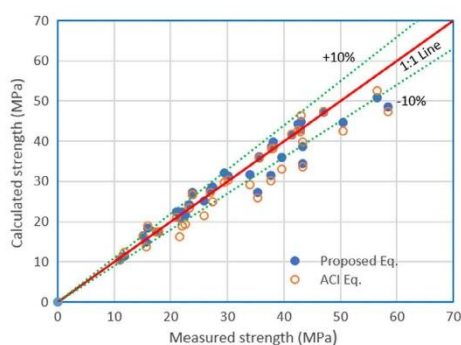
Fig. 17. Measured strength and calculated strength values of proposed and ACI model.

As discussed in Section 3.6, the EAF slag aggregate and fly ash replacement level have an impact on compressive strength of RCCP. Moreover, the compressive strength of RCCP with the same fly ash replacement level has the same developing rule. Therefore, this study proposed a predicting model for three groups with three levels of fly ash replacement (i.e. 0%, 20% and 40%).

Based on Eq. (2) and analyzing the compressive strength results, the *a*-coefficient and *b*-coefficient of three groups were shown in Table 10. It can be said that the *a*-coefficient and *b*-coefficient in each group depend on EAF slag coarse aggregate replacement level (i.e. 0%, 50% and 100%).

The *a*-coefficient and *b*-coefficient values were plotted in Figs. 15 and 16. From Fig. 15, the relationship between *a*-coefficient and EAF slag coarse aggregate replacement level can be described with a hyperbolic function, which is presented by Eq. (3). The *b*-coefficient values were the average of three values

in each group. The *b*-coefficient is constant because the testing values were close (Fig. 16).

$$a = a_1 \times S^2 + a_2 \times S + a_3 \qquad (3)$$

where S is the EAF slag coarse aggregate replacement level; a_1, a_2, a_3 are model coefficients.

Consequently, the a_1, a_2, a_3, b values are summarized in Table 11. Fig. 17 shows the relationship between the measured strength and the calculated strength by ACI equation and the proposed equation with the model coefficients were taken from Table 11. It was observed that most of the calculated values by the proposed model had error in the range within ±10%.

The mean absolute percentage error (MAPE) is expressed by Eq. (4), which describes the error between the measured values and the model analysis values.

$$MAPE(\%) = \frac{1}{p} \sum_{j}^{p} \left(\left| \frac{o_j - t_j}{o_j} \right| \right) \qquad (4)$$

where t_j and o_j are measured values and model analysis values; p is the number of data points.

According to Eq. (4), the MAPE value was 7.51% calculated from measured data and calculated data by the proposed model; and the MAPE value was 10.15% calculated from measured data and calculated data by ACI model. It demonstrated that the proposed model performed good predictive ability because the MAPE value is less than 10%.

4. Conclusion

(1) Based on the physical and chemical properties of EAF slag, EAF slag aggregate is eligible to replace natural aggregates. After treatment process, the expansion values have demonstrated that EAF slag aggregate showed the volume stability with hydration reactions and alkali-silica reactions. Therefore, EAF slag in this study can be appropriate to use in RCCP.
(2) The optimum moisture content of RCCP mixture containing EAF slag aggregate and fly ash was found in the range 7–9%. It depended on the material replacement ratios.
(3) The fresh and hardened unit weight of RCCP with EAF slag as an aggregate replacement increased in all mixtures due to the higher unit weight of EAF slag aggregate as compared to that of crushed stone aggregate. However, there was a unit weight reduction when EAF slag aggregate and fly ash were used as substitute materials in RCCP mixtures.

(4) When EAF slag was used to replace crushed stone aggregate, there was a slight decrease in compressive strength, splitting tensile strength and elastic modulus. This is because the limited improvement of the rough-textured EAF slag in low water-cement ratio concretes resulted in bad interfacial transition zone between EAF slag aggregate and cementitious matrix. However, EAF slag can be replaced 100% coarse aggregate in RCCP to produce pavements which met the exposed wearing surface requirements.

(5) Besides, there was a strength decrease when cement was partially replaced by fly ash. Nevertheless, the RCCP containing EAF slag aggregate and 20% fly ash also produces the good concrete which can be used for pavements. Therefore, it was recommended that the mixture containing EAF slag aggregate and 20% fly ash is the best for recycling a large amount of waste materials.

(6) A predicting model for compressive strength of RCCP has been successfully established. It was observed that the mean absolute percentage error of measured strength and calculated strength by the predicting model is less than 10%.

Acknowledgements

References

[1] World Steel Association, "World Steel in Figures 2016," World Steel Assoc., 2016, pp. 3–30.
[2] U.S. Geological Survey, "Mineral Commodity Summaries 2016: Iron and Steel Slag," no. 703, 2016, pp. 88–89.
[3] G. Adegoloye, A.L. Beaucour, S. Ortola, A. Noumowé, Concretes made of EAF slag and AOD slag aggregates from stainless steel process: mechanical properties and durability, Constr. Build. Mater. 76 (2015) 313–321.
[4] F. Faleschini, M. Alejandro Fernandez-Ruiz, M.A. Zanini, K. Brunelli, C. Pellegrino, E. Hernandez-Montes, High performance concrete with electric arc furnace slag as aggregate: Mechanical and durability properties, Constr. Build. Mater. 101 (2015) 113–121.
[5] N. Palankar, A.U. Ravi Shankar, B.M. Mithun, Durability studies on eco-friendly concrete mixes incorporating steel slag as coarse aggregates, J. Clean. Prod. 129 (2016) 437–448.
[6] F. Debieb, L. Courard, S. Kenai, R. Degeimbre, Roller compacted concrete with contaminated recycled aggregates, Constr. Build. Mater. 23 (11) (2009) 3382–3387.
[7] C. Settari, F. Debieb, E.H. Kadri, O. Boukendakdji, Assessing the effects of recycled asphalt pavement materials on the performance of roller compacted concrete, Constr. Build. Mater. 101 (2015) 617–621.
[8] A. Meddah, M. Beddar, A. Bali, Use of shredded rubber tire aggregates for roller compacted concrete pavement, J. Clean. Prod. 72 (2014) 187–192.
[9] C. Hazaree, H. Ceylan, K. Wang, Influences of mixture composition on properties and freeze-thaw resistance of RCC, Constr. Build. Mater. 25 (1) (2011) 313–319.
[10] American Concrete Pavement Association, "Roller-Compacted Concrete Pavements as Exposed Wearing Surface," 2014, pp. 1–29.
[11] A. Mardani-Aghabaglou, K. Ramyar, Mechanical properties of high-volume fly ash roller compacted concrete designed by maximum density method, Constr. Build. Mater. 38 (1) (2013) 356–364.
[12] A. Mardani-Aghabaglou, Ö. Andiç-Çakir, K. Ramyar, Freeze-thaw resistance and transport properties of high-volume fly ash roller compacted concrete designed by maximum density method, Cem. Concr. Compos. 37 (1) (2013) 259–266.
[13] A. Yerramala, K. Ganesh, Babu, "Transport properties of high volume fly ash roller compacted concrete", Cem. Concr. Compos. 33 (10) (2011) 1057–1062.
[14] S.K. Rao, P. Sravana, T.C. Rao, Investigating the effect of M-sand on abrasion resistance of Fly Ash Roller Compacted Concrete (FRCC), Constr. Build. Mater. 118 (2016) 352–363.
[15] ASTM C150-07, "Standard Specification for Portland Cement".
[16] ASTM C 618-05, "Standard Specification for Coal Fly Ash and Raw or Calcined Natural Pozzolan for Use in Concrete".
[17] ASTM C33/C33M-08, "Standard Specification for Concrete aggregates".
[18] K.H. Khayat, N.A. Libre, "Roller Compacted Concrete - Field Evaluation and Mixture Optimization," A Natl. Univ. Transp. Cent. Missouri Univ. Sci. Technol., vol. August, no. NUTC R363, p. 118, 2014.
[19] D. Harrington, F. Abdo, W. Adaska, C. Hazaree, "Guide for Roller-Compacted Concrete Pavements," Inst. Transp. Iowa State University, no. August, 2010, p. 104.
[20] V. Ramakrishnan, "Optimized Aggregate Gradation for Structural Concrete," Rep. SD2002-02 South Dakota Dep. Transp., no. April, 2004.
[21] ASTM D4792-06, "Standard Test Method for Potential Expansion of Aggregates from Hydration Reactions".
[22] ASTM C1260-07, "Standard Test Method for Potential Alkali Reactivity of Aggregates (Mortar-Bar Method)".
[23] ASTM C127-07, "Standard Test Method for Density, Relative Density (Specific Gravity) and Absorption of Coarse Aggregate".
[24] ASTM C128-07a, "Standard Test Method for Density, Relative Density (Specific Gravity), and Absorption of Fine Aggregate".
[25] ASTM C131-06, "Standard Test Method for Resistance to Degradation of Small-Size Coarse Aggregate by Abrasion and Impact in the Los Angeles Machine".
[26] ASTM C25, "Standard Test Methods for Chemical Analysis of Limestone, Quicklime, and Hydrated".
[27] Ministry of Transportation of Ontario, Method of Test for Determination of Free Lime Content.
[28] ASTM D 1883-99, "Standard Test Method for CBR (California Bearing Ratio) of Laboratory-Compacted Soils" .
[29] ASTM D1557-12, "Standard Test Methods for Laboratory Compaction Characteristics of Soil Using Modified Effort (56,000ft-lbf /ft3 (2,700 kN-m/m3)".
[30] ASTM C1435/C1435M-08, "Standard Practice for Molding Roller-Compacted Concrete in Cylinder Molds Using a Vibrating Hammer" .
[31] ASTM C617/C617M – 12, "Standard Practice for Capping Cylindrical Concrete Specimens".
[32] ASTM C39/C39M-14, "Standard Test Method for Compressive Strength of Cylindrical Concrete Specimens".
[33] ASTM C496/C496M, "Standard Test Method for Splitting Tensile Strength of Cylindrical Concrete Specimens".
[34] ASTM C 469-02, "Standard Test Method for Static Modulus of Elasticity and Poisson's Ratio of Concrete in Compression".
[35] M.P. Luxán, R. Sotolongo, F. Dorrego, E. Herrero, Characteristics of the slags produced in the fusion of scrap steel by electric arc furnace, Cem. Concr. Res. 30 (4) (2000) 517–519.
[36] J.M. Manso, J.A. Polanco, M. Losañez, J.J. González, Durability of concrete made with EAF slag as aggregate, Cem. Concr. Compos. 28 (6) (2006) 528–534.
[37] I. Arribas, A. Santamaría, E. Ruiz, V. Ortega-López, J.M. Manso, Electric arc furnace slag and its use in hydraulic concrete, Constr. Build. Mater. 90 (2015) 68–79.
[38] F. Faleschini, K. Brunelli, M. A. Zanini, M. Dabalà, and C. Pellegrino, "Electric Arc Furnace Slag as Coarse Recycled Aggregate for Concrete Production," J. Sustain. Metall., no. November, 2015, pp. 44–50.
[39] S. Monosi, M.L. Ruello, D. Sani, Electric arc furnace slag as natural aggregate replacement in concrete production, Cem. Concr. Compos. 66 (2016) 66–72.
[40] D. Mombelli, C. Mapelli, S. Barella, C. Di Cecca, G. Le Saout, E. Garcia-Diaz, The effect of chemical composition on the leaching behaviour of electric arc furnace (EAF) carbon steel slag during a standard leaching test, J. Environ. Chem. Eng. 4 (1) (2016) 1050–1060.
[41] L. Coppola, A. Buoso, D. Coffetti, P. Kara, S. Lorenzi, Electric arc furnace granulated slag for sustainable concrete, Constr. Build. Mater. 123 (2016) 115–119.
[42] J. A. Farny and B. Kerkhoff, "Diagnosis and Control of Alkali-Aggregate Reactions in Concrete," 1975.
[43] M. Thomas, B. Fournier, K. Folliard, M. Shehata, J. Ideker, and C. Rogers, "Performance Limits for Evaluating Supplementary Cementing Materials Using the Accelerated Mortar Bar Test," no. 2892, 2005.
[44] J.M. Manso, D. Hernández, M.M. Losáñez, J.J. González, Design and elaboration of concrete mixtures using steelmaking slags, ACI Mater. J. 108 (6) (2011) 673–681.
[45] C. Cao, W. Sun, H. Qin, The analysis on strength and fly ash effect of roller-compacted concrete with high volume fly ash, Cem. Concr. Res. 30 (1) (2000) 71–75.
[46] C.D. Atiş, Strength properties of high-volume fly ash roller compacted and workable concrete, and influence of curing condition, Cem. Concr. Res. 35 (6) (2005) 1112–1121.
[47] Y.N. Sheen, D.H. Le, T.H. Sun, Innovative usages of stainless steel slags in developing self-compacting concrete, Constr. Build. Mater. 101 (2015) 268–276.
[48] Y.N. Sheen, D.H. Le, T.H. Sun, Greener self-compacting concrete using stainless steel reducing slag, Constr. Build. Mater. 82 (2015) 341–350.
[49] ACI-Committee:209, Guide for Modeling and Calculating Shrinkage and Creep in Hardened Concrete, vol. 4, no. Reapproved, 1995.

Paper 2

Article

EAF Slag Aggregate in Roller-Compacted Concrete Pavement: Effects of Delay in Compaction

My Ngoc-Tra Lam [1,2,*], Saravut Jaritngam [1] and Duc-Hien Le [3]

1   Department of Civil Engineering, Faculty of Engineering, Prince of Songkla University, Hat Yai,
     Songkhla 90112, Thailand; jaritngam@gmail.com
2   Faculty of Civil Engineering, Ho Chi Minh City Open University, 97 Vo Van Tan, District 3,
     Ho Chi Minh City 700000, Vietnam
3   Sustainable Developments in Civil Engineering Research Group, Faculty of Civil Engineering,
     Ton Duc Thang University, Ho Chi Minh City 700000, Vietnam; leduchien@tdt.edu.vn
*   Correspondence: ngoctramys@gmail.com

check for updates

Abstract: This study investigates the effect of delay in compaction on the optimum moisture content and the mechanical propertie s (i.e., compressive strength, ultrasonic pulse velocity, splitting tensile strength, and modulus of elasticity) of roller-compacted concrete pavement (RCCP) made of electric arc furnace (EAF) slag aggregate. EAF slag with size in the range of 4.75–19 mm was used to replace natural coarse aggregate in RCCP mixtures. A new mixing method was proposed for RCCP using EAF slag aggregate. The optimum moisture content of RCCP mixtures in this study was determined by a soil compaction method. The Proctor test assessed the optimum moisture content of mixtures at various time after mixing completion (i.e., 0, 15, 30, 60, and 90 min). Then, the effect of delay in compaction on the mechanical properties of RCCP mixtures at 28 days of age containing EAF slag aggregate was studied. The results presented that the negative effect on water content in the mixture caused by the higher water absorption characteristic of EAF slag was mitigated by the new mixing method. The optimum water content and maximum dry density of RCCP experience almost no effect from the delay in compaction. The compressive strength and splitting tensile strength of RCCP using EAF slag aggregate fulfilled the strength requirements for pavement with 90 min of delay in compaction.

Keywords: delay in compaction; optimum moisture; mechanical properties; roller-compacted concrete pavement; EAF slag aggregate

1. Introduction

Electric arc furnace (EAF) slag is a by-product of steel production, which is generated during the manufacture of crude steel by the electric arc furnace process. The output of EAF slag was estimated at about 15–20% of crude steel production. Total world production of crude steel reached approximately 1560, 1650, and 1670 million tons in 2012, 2013, and 2014, respectively [1], leading to a huge quantity of EAF slag being produced every year. The use of EAF slag as a natural aggregate replacement in concrete has attracted much research over the last years [2–5], because the recycling of EAF slag has reduced the consumption of natural aggregates and the environmental impacts such as those due to a lack of waste storage areas and the pollution of soil. Many research works have demonstrated that natural aggregates in many types of concrete can be replaced by EAF slag. For example, Manso et al. [2] indicated that EAF slag aggregate created good concrete in terms of mechanical properties. Adegologe et al. [3] presented the findings that concrete made using EAF slag aggregate slightly improved the mechanical properties. The compressive strength and tensile strength of slag concrete increased by 9% and 3%,

respectively, in comparison to those of control concrete. Similarly, the improvement of mechanical properties was observed in Sekaran et al. research [4]. Besides, EAF slag also performed as a good aggregate in high-performance concrete. Faleschini et al. [5] showed that high-performance concrete containing 100% EAF slag as the coarse aggregate had mechanical properties better than the reference concrete, including compressive strength, tensile strength, and elastic modulus. Review of the literature shows that EAF slag aggregate is eligible for use in concrete, but very few reports have studied roller-compacted concrete made with EAF slag aggregate. Roller-compacted concrete is a special concrete that is stiff and "no-slump". The application of roller-compacted concrete for pavements has rapidly increased in several decades because of its strength, durability, and cost efficiency. Because aggregate in a roller-compacted concrete pavement (RCCP) mixture comprises 75% of its volume, the substitution of traditional natural aggregate by EAF slag aggregate has become important for the development of sustainable infrastructure.

RCCP using EAF slag as coarse aggregate has produced pavement fulfilling strength requirements, as has been discussed previously [6]. Unlike natural aggregate replacement by EAF slag in conventional concrete and high-performance concrete, EAF slag as coarse aggregate substitute caused the decrease of RCCP strength (i.e., compressive strength and splitting tensile strength). The higher water absorption feature of EAF slag aggregate had a significant effect on the amount of water needed for the mixture, especially in low-water concrete such as RCCP. Therefore, the complement of water absorbed by EAF slag aggregate in RCCP is an effective solution for improving the strength.

Similar to asphalt pavement, RCCP is compacted with vibratory rollers to achieve a target density and homogeneous surface pavement. The timing of compaction is very important because of its effect on the density and strength of RCCP. Normally, RCCP should be compacted as soon as possible after its spreading. Furthermore, the time span between mixing (the timing of the addition of water in the mixture) and compaction of RCCP is usually within 45 to 90 min [7]. Moreover, some scholars have reported that there is an optimized compaction time. Karimpour [8] found that compacting the mixture at the optimized time resulted in the maximum compressive strength. In addition, the improvement of mechanical properties was observed in the RCCP mixture compacted at the optimized time [9]. The optimum time of compaction depended on materials, mixing design, and water-to-cement ratio in mixture.

In order to enhance RCCP strength, the aim of this study is to investigate the water absorption process of EAF slag aggregate. The water absorption function of EAF slag aggregate was used to propose a new mixing method for RCCP made with EAF slag aggregate. Futhermore, the effect of delay in compaction on the optimum moisture content and the mechanical properties of RCCP using EAF slag aggregate was assessed (i.e., compressive strength, ultrasonic pulse velocity, splitting tensile strength, and modulus of elasticity). In this work, the time span between mixing and compaction was 0, 15, 30, 60, and 90 min.

2. Testing Program

2.1. Materials

2.1.1. Cement

Table 1 shows the chemical composition and physical characteristics of ordinary Portland cement (OPC) type I conforming to ASTM C150 used in this study [10].

Table 1. The chemical composition and physical characteristics of ordinary Portland cement (OPC).

Chemical Composition (%)	OPC, Type I
Silica (SiO_2)	20.7
Alumina (Al_2O_3)	4.5
Ferric oxide (Fe_2O_3)	3.3
Calcium oxide (CaO)	63.0
Magnesium oxide (MgO)	1.8
Sodium oxide (Na_2O)	0.10
Potassium oxide (K_2O)	0.74
Sulphuric anhydride (SO_3)	2.3
Loss on ignition (LOI)	2.8
Physical Characteristics	
Fineness (Blaine) (m^2/kg)	347
Specific gravity	3.14
Initial setting time (min)	110
Final setting time (min)	170
Particle composition	NA
Retaining on 45 μm sieve (%)	
Compressive Strength (N/mm^2)	
1 day	14.6
3 days	26.2
7 days	33.0
28 days	43.0

Note: NA: not available.

2.1.2. Aggregates

Natural aggregate used in this study with the designed gradation as shown in Table 2 is crushed stone. EAF slag aggregate from Southern Vietnam with size in the range of 4.75–19 mm (Figure 1) reaching the requirements of ASTM C33 standard (Table 3) was used to replace natural aggregate in RCCP [11–14]. After leaving in an environmental condition for several months as a treatment process to reduce the volume expansion [15], the free CaO content of the EAF slag aggregate is less than 0.1% [6]. On the other hand, the expansion value of the EAF slag aggregate was 0.078%, which is lower than the limit value (0.5%) following ASTM D4792 [6,16]. Consequently, the EAF slag aggregate in this study exhibited the required volume stability.

Table 2. The suggested limits and the gradation of designed aggregate for the roller-compacted concrete pavement (RCCP) used in this study.

Sieve Size	Passing Mass (%)		
	The Lower Limit	The Upper Limit	The Designed Gradation
19 mm	95	100	100
12.5 mm	70	95	83
9.5 mm	60	85	73
4.75 mm (No. 4)	40	60	54
2.36 mm (No. 8)	30	50	41
1.18 mm (No. 16)	20	40	30
600 μm (No. 30)	15	30	22
300 μm (No. 50)	10	25	15
150 μm (No. 100)	2	16	10
<75 μm (No. 200)	0	8	7

Figure 1. Electric arc furnace (EAF) slag aggregate used in this study.

Table 3. Physical properties of the crushed stone aggregate and EAF slag aggregate.

Properties	Crushed Stone		EAF Slag
	Fine Aggregate (0–4.75 mm)	Coarse Aggregate (4.75–19 mm)	Coarse Aggregate (4.75–19 mm)
Apparent specific gravity	2.71	2.72	3.40
Density (OD) (kg/m^3)	2609	2680	3085
Density (SSD) (kg/m^3)	2644	2691	3176
Bulk density (kg/m^3)	1493	1466	1686
Water absorption (%)	1.36	0.44	2.93
Los Angeles abrasion value (%)	NA	13.98	19.37

Note: NA: not available.

2.2. Testing Approaches and Sample Preparation

This study is composed of three parts. In the first part, the water absorption process of the EAF slag aggregate was investigated. In the second part, the Proctor test determined the optimum moisture content of mixtures compacted at various time after mixing completion (i.e., 0, 15, 30, 60, and 90 min). In the third part, the effect of delay in compaction on the mechanical properties of RCCP using EAF slag aggregate at 28 days of age was examined.

2.2.1. The Water Absorption of EAF Slag Aggregate

Because of the higher water absorption characteristic, the relationship between water absorption of the EAF slag aggregate and immersion time was investigated to mitigate the effect of this feature on the water content of the RCCP mixture. Ten samples of the EAF slag aggregate were prepared in accordance with ASTM C127 standard [11]. All samples were dried in the oven to constant mass at a temperature of $110 \pm 5\ °C$ and cooled in air at room temperature for 2 h. Then, ten samples were immersed in water at room temperature for 5 min, 10 min, 15 min, 30 min, 60 min, 90 min, 2 h, 4 h, 8 h, and 24 h to determine the water absorption. Experiments were repeated five times to calculate the average value and the sample immersion times were changed after each test.

2.2.2. Mixing Proportion of RCCP

RCCP made of 100% EAF slag coarse aggregate (s-RCCP) and a reference RCCP made of 100% natural aggregate (r-RCCP) with 12% cement (Table 4) were subjected to the modified Proctor test

(ASTM D1557) [17] after mixing completion at five levels of moisture content to determine the optimum moisture content of the mixture. According to ASTM D1557, the mixture is placed in five layers into the 6-in (152.4 mm) mold and compacted by 56 blows of a rammer per layer. After conducting the Proctor test, the density of mixture is determined to establish a relationship between the dry density and moisture content (the compaction curve). From the compaction curve, the optimum moisture content of the mixture was observed. Besides, four mixtures of r-RCCP and four mixtures of s-RCCP were subjected to delay in compaction of 15 min, 30 min, 60 min, and 90 min to evaluate the optimum moisture content of mixtures at various times of compaction.

Table 4. Mixture proportions of RCCPs. r-RCCP: reference RCCP with 100% natural aggregate; s-RCCP: 100% EAF slag coarse aggregate.

Mixture	Cement (kg/m^3)	Coarse Aggregate (kg/m^3)		Fine Aggregate (kg/m^3)
		EAF Slag	Crushed Stone	Crushed Stone
r-RCCP	274	0	842	1163
s-RCCP	282	867	0	1197

Note: Cement is fixed at 12% of total weight of cement and oven-dried aggregates.

2.2.3. Mechanical Properties of RCCP

Ten mixtures containing the optimum moisture content were prepared to make the specimens. The standard cylinder specimens with diameter of 150 mm and height of 300 mm were molded by using a vibrating hammer conforming to ASTM C1435 [18]. After 24 h of casting, all specimens were removed from the mold and cured in tap water at the temperature of 23 ± 2 °C until 28 days of age, to determine the mechanical properties of RCCP.

At 28 days of age, the measurement of ultrasonic pulse velocity transmitted from surface to surface of the cylinder specimen was conducted in accordance with ASTM C597 [19]. The pulse velocity is calculated by the transit time of the longitudinal stress wave through the sample received from the ultrasonic apparatus. Then, before the compressive strength testing conforming to ASTM C39 [20], the cylinder specimens underwent a capping procedure to make a plane surface for sampling. For splitting tensile strength testing (ASTM C496), the load is applied along the length of a cylindrical specimen at a constant rate in the range of 100 to 200 psi/min (0.7 to 1.4 MPa/min) until failure occurs [21]. Finally, the modulus of elasticity of r-RCCP and s-RCCP samples was measured following ASTM 469 [22]. All experiments were conducted on groups of three specimens to obtain the average value.

Table 5 shows the testing approaches and the quantity of samples in this study.

Table 5. The testing approaches and the quantity of RCCP samples used in this study.

No.	Testing Items	Sample Dimension (mm)	Quantity of Sample	ASTM Standard
1	Optimum moisture content	6-in (152.4 mm) diameter mold	50	ASTM D1557
2	Compressive strength	150 × 300, cylinder	30	ASTM C39
3	Ultrasonic pulse velocity	150 × 300, cylinder	-	ASTM C597
4	Splitting tensile strength	150 × 300, cylinder	30	ASTM C496
5	Modulus of elasticity	150 × 300, cylinder	30	ASTM C469

3. Results and Discussion

3.1. The Relationship between Water Absorption of EAF Slag Aggregate and Immersion Time

The relationship between the water absorption ratio of the EAF slag aggregate and immersion time is shown in Figure 2. It was observed that the water absorption of the EAF slag aggregate occurred quickly within the first 5 min, reaching 77.66% of the total water absorption. This behavior resulted

from the water absorption of large pores in the EAF slag aggregate. After 5 min, the water absorption took place at small pores, leading to water absorption rate reduction. The water absorption ratio was 81.16%, 83.06%, and 86.86% after 10 min, 15 min, and 30 min, respectively (Table 6). After that, the water absorption happened very slowly and reached 88.94% after 60 min. It can be seen that the water absorption of the EAF slag aggregate after 10 min of immersion comprised over 80% of the total water absorption.
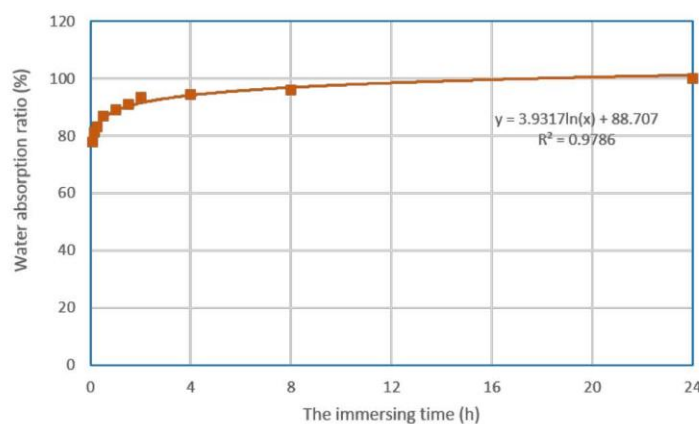
Figure 2. The relationship between the water absorption ratio of EAF slag aggregate and immersion time.

Table 6. The water absorption ratio of EAF slag aggregate and immersion time.

Immersion Time	% of Total Water Absorption
5 min	77.66
10 min	81.16
15 min	83.06
30 min	86.86
60 min	88.94
90 min	91.10
2 h	93.46
4 h	94.25
8 h	96.03
24 h	100.00

3.2. Mixing Proportion of RCCP

As discussion in Section 3.1, the EAF slag aggregate rapidly absorbed the water during the first 10 min of immersion. Therefore, a new mixing method of RCCP was designed in this study to mitigate the negative effect of the higher water absorption of the EAF slag aggregate on the mixing water dosage of the mixture. The new mixing method consists of two stages (Figure 3). In the first stage, 50% of the water dosage is mixed with aggregates within 10 min, in order to allow most of the large pores of the EAF slag aggregate to absorb water. The second mixing stage is 5 min, to create a homogeneous consistency of mixture.
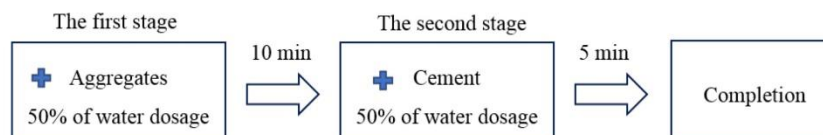
Figure 3. The new mixing method of RCCP in this study.

In this study, all RCCP mixtures were mixed following the new mixing method. After mixing completion, two mixtures (i.e., r-RCCP and s-RCCP) were compacted immediately, while eight mixtures were delayed in compaction for 15, 30, 60, and 90 min. The relationship between the dry density and moisture content of the RCCP mixtures was determined by Proctor testing results as listed in Table 7.

Table 7. The relationship between the dry density and moisture content of RCCP mixtures at various time of compaction.

Mixture	Delay Time (min)	Dry Density (γ) = Moisture Content Relationship (W)	R^2
r-RCCP	0	$\gamma = -12.95W^2 + 179.55W + 1662.10$	0.94
	15	$\gamma = -10.10W^2 + 141.99W + 1776.10$	0.92
	30	$\gamma = -12.09W^2 + 171.85W + 1684.50$	0.96
	60	$\gamma = -10.07W^2 + 145.97W + 1747.80$	0.95
	90	$\gamma = -17.56W^2 + 282.18W + 1147.40$	0.97
s-RCCP	0	$\gamma = -10.10W^2 + 161.34W + 1734.90$	0.99
	15	$\gamma = -21.46W^2 + 344.76W + 1013.70$	0.99
	30	$\gamma = -16.32W^2 + 262.93W + 1314.00$	0.96
	60	$\gamma = -16.41W^2 + 265.31W + 1299.20$	0.93
	90	$\gamma = -19.80W^2 + 322.23W + 1071.20$	0.96

According to Table 7, the optimum moisture content and maximum dry density of mixtures at various time of compaction were calculated, as listed in Table 8. It can be seen that the optimum moisture of s-RCCP (7.99%) compacted immediately after mixing is higher than that of r-RCCP (6.93%). This behavior resulted from the higher water absorption feature of the EAF slag aggregate. Most of the large pores of the EAF slag aggregate quickly absorbed the water when the EAF slag aggregate contacted the water in the first stage of the mixing process (Figure 3). From the optimum moisture content values, the total water needed for r-RCCP and s-RCCP were determined as 158 L/m^3 and 187 L/m^3, respectively. Hence, the effective water can be estimated as 138 L/m^3 for r-RCCP and 146 L/m^3 for s-RCCP. Similar values for the effective water in RCCP have been found in a number of published works [23–25]. These values demonstrate that the new mixing method in this study helps complement the amount of water absorbed by the EAF slag aggregate. Furthermore, the increase of delay in compaction leads to the workability reduction of the mixture. Thus, the optimum moisture content of r-RCCP increases from 6.93% at 0 min to 8.04% at 90 min. Besides, the optimum moisture of s-RCCP increases slightly from 7.99% at 0 min to 8.14% at 90 min. The results stated that the workability reduction of the s-RCCP mixture is lower than that of r-RCCP, especially with 90 min of delay. This phenomenon may result from the water in the pore structure of the EAF slag aggregate being pushed out through compaction. As a result, the delay in compaction hardly affected the total water content of s-RCCP mixed by the new mixing method.

Table 8. The optimum moisture and maximum dry density of RCCP mixtures at various time of compaction.

Mixture	Delay Time (min)	Optimum Moisture (%)	Total Water (L/m³)	Maximum Dry Density (kg/m³)
r-RCCP	0	6.93	158	2284
	15	7.03	160	2275
	30	7.11	162	2295
	60	7.24	165	2276
	90	8.04	183	2281
s-RCCP	0	7.99	187	2379
	15	8.03	188	2398
	30	8.06	189	2373
	60	8.08	190	2371
	90	8.14	191	2382

On the other hand, the natural aggregate replacement by EAF slag leads to the increase of maximum dry density of s-RCCP because of the higher density of slag. The average maximum dry density of s-RCCP is 2381 kg/m³, an increase of 4% in comparison with that of r-RCCP (2282 kg/m³). Similar to the optimum water content, the delay in compaction has almost no effect on the maximum dry density of RCCP mixtures.

3.3. Compressive Strength of RCCP

Figure 4 shows the 28-day-age compressive strength of r-RCCP and s-RCCP at various times of compaction. The compressive strength of r-RCCP is higher than that of s-RCCP at all compaction times. This may be a result of the bad quality of the interfacial transition zone between the EAF slag aggregate and cementitious matrix in low water concretes such as RCCP [6]. Moreover, the new mixing method in this study has enhanced the compressive strength of s-RCCP. For instance, s-RCCP compacted immediately after mixing by the new method obtained 43.54 MPa of compressive strength, whereas the compressive strength of s-RCCP reached 35.56 MPa in a previous research work [6].
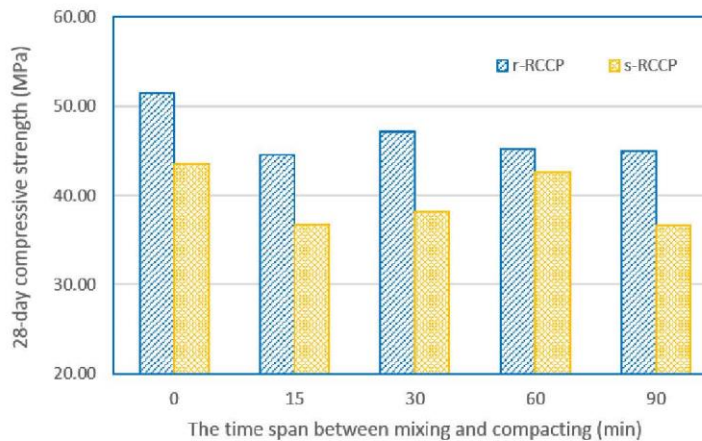
Figure 4. Compressive strength of r-RCCP and s-RCCP at various times of compaction.

As shown in Figure 4, the compressive strengths of r-RCCP and s-RCCP attained the highest value (i.e., 51.46 and 43.54 MPa, respectively) with compaction immediately after mixing completion.

Good workability of mixtures resulted in the effective compaction process. Increasing the delay led to a compressive strength reduction. The compressive strength of r-RCCP at 15 min decreased by 13%, and that of s-RCCP decreased by 16% in comparison to its compressive strength at 0 min. However, both of r-RCCP and s-RCCP showed slightly improved compressive strength after 15 min of delay. For instance, the compressive strength of r-RCCP reached 47.18 MPa at 30 min, while that of s-RCCP reached 42.64 MPa at 60 min. This behavior may result from the formation of ettringite of the hydrated cement process. The formation of ettringite filled up the pores in structure concrete [26]. Consequently, the compressive strength increased with the compaction process in this period. Nevertheless, when the mixture was compacted in the period of the formation of the Calcium-Silicate-Hydrate (C-S-H) phase, it resulted in the crystallized product being destroyed. As a result, for r-RCCP and s-RCCP mixtures compacted at 90 min, a decrease in compressive strength was observed.

Based on the results of this part, it is revealed that s-RCCP compacted at various times achieved compressive strengths in the range of 35 MPa to 45 MPa. This range of values is popularly found in many research works on RCCP [23,24,27,28]. This result proved that s-RCCP can be delayed in compaction until 90 min while producing pavements fulfilling the strength requirement both in areas without freeze–thaw conditions (28 MPa) and in areas exposed to freeze–thaw conditions (31 MPa) [29].

3.4. Ultrasonic Pulse Velocity (UPV) of RCCP

Similarly to conventional paving concrete, the pulse velocities for r-RCCP and s-RCCP in this study were in the range of 4500 m/s to 4900 m/s (Figure 5) [30]. According to UPV values, both the r-RCCP and s-RCCP specimens with various times of compaction are classified as "excellent" quality (UPV > 4500 m/s) [31]. r-RCCP provided higher UPV values than s-RCCP due to the higher compressive strength of r-RCCP. Moreover, there was a good relationship between UPV and compressive strength values, as presented by a best-fit exponential formula (Figure 6). Increasing UPV values accompanied the increase in compressive strength. In addition, the replacement of natural coarse aggregate in mixtures by EAF slag aggregate resulted in s-RCCP specimens with less uniformity than r-RCCP specimens.
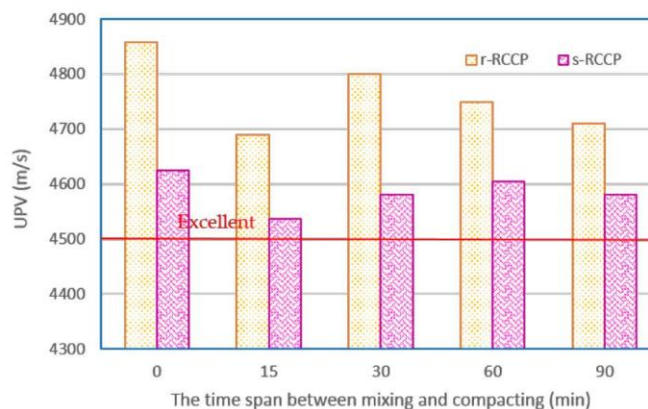
Figure 5. Measurement of ultrasonic pulse velocity (UPV) transmitted in compressive strength specimens of r-RCCP and s-RCCP at 28 days of age.
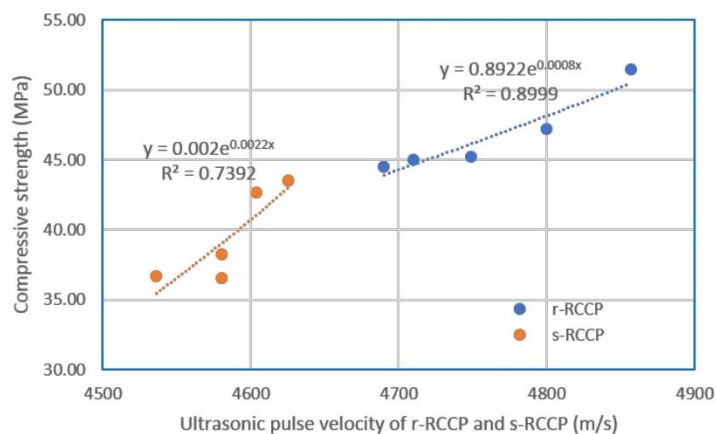
Figure 6. The relationship between compressive strength and ultrasonic pulse velocity of r-RCCP and s-RCCP.

3.5. Splitting Tensile Strength of RCCP

The splitting tensile strength of RCCP samples compacted at various times at 28 days of age are shown in Figure 7. r-RCCP attained the highest splitting tensile strength (4.81 MPa) with compaction immediately after mixing completion. Then, the delay in compaction led to the reduction of splitting tensile strength.
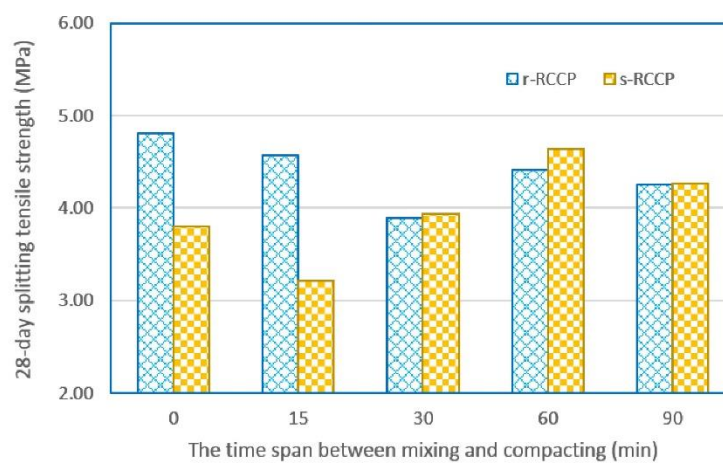
Figure 7. Splitting tensile strength of r-RCCP and s-RCCP at various times of compaction.

Splitting tensile strength values of s-RCCP at 28 days of age at various times of compaction were in the range of 3.2 MPa to 4.6 MPa. This result is similar to that of conventional RCCP, which is generally between 3.1 MPa to 4.2 MPa [30]. In addition, it has been found that the splitting

tensile strength of s-RCCP reached a peak (4.64 MPa) with compaction at 60 min. The rough texture characteristic of the EAF slag aggregate improved the splitting tensile strength of s-RCCP. Besides, the filling of the pores by ettringite may be the cause of the strength increase when there was a delay in compaction [32]. Furthermore, the splitting tensile strength and compressive strength ratio of s-RCCP that was compacted after 30 min of delay is about 10 percent. This result is higher than a typical 8 to 9 percent of splitting tensile strength and compressive strength ratio of ordinary concrete [26]. The improvement of the splitting tensile strength of the EAF aggregate is appreciated in RCCP due to the load distribution characteristics of a rigid pavement.

3.6. Elastic Modulus of RCCP

As can be seen from Figure 8, the elastic modulus at 28 days of age of all RCCP mixtures in this study was in the range of 30 GPa to 36 GPa. This range of values is found to be similar to that of conventional RCCP provided by a number of former scholars [28,33,34]. Therefore, the delay in compaction slightly affected the elastic modulus of RCCP. Both r-RCCP and s-RCCP achieved the highest values of elastic modulus (36 GPa) with compaction at 15 min after mixing. The lowest elastic modulus of r-RCCP (31 GPa) was obtained in the sample compacted at 30 min, whereas that of s-RCCP (30 GPa) was obtained in the sample compacted immediately after mixing.
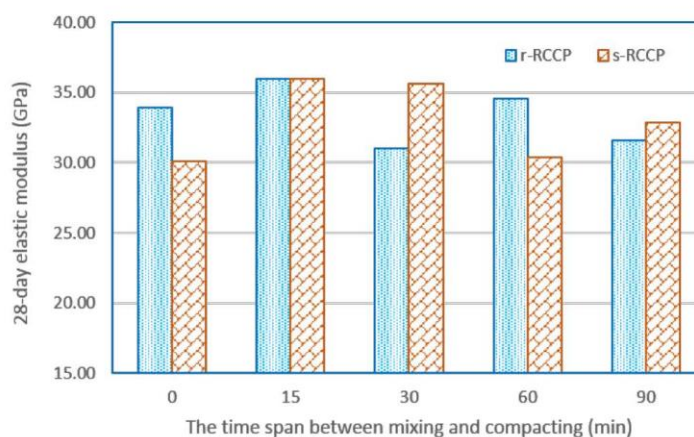
Figure 8. The elastic modulus of r-RCCP and s-RCCP at various times of compaction.

According to the CEB-FIP Model Code (1990) [26], the modulus of elasticity of concrete can be estimated from Equation (1):

$$E = b(f_c/10)^{1/3} \tag{1}$$

where f_c is the cylindrical compressive strength at 28 days of age (MPa) and the b coefficient is 2.15×10^4 for normal concrete.

Based on the results and Equation (1), the b coefficient of r-RCCP is 2.00×10^4 and the b coefficient of s-RCCP is 2.09×10^4 (see Figure 9). Hence, the elastic modulus of r-RCCP and s-RCCP can be predicted by the compressive strength of samples at 28 days of age.

103
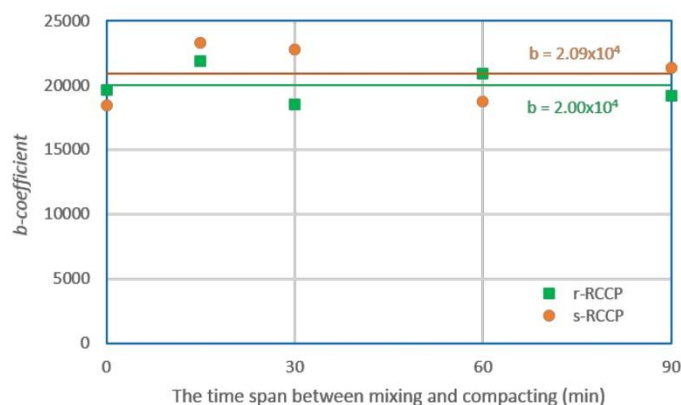
Figure 9. *b* coefficient of r-RCCP and s-RCCP.

4. Conclusions

(1) The water absorption ratio of the EAF slag aggregate obtained over 80% of the total water absorption after 10 min of immersion in water.

(2) The new mixing method has mitigated a negative effect of the high water absorption feature of the EAF slag on the water of s-RCCP.

(3) The optimum water content of the s-RCCP mixture is higher than that of the r-RCCP mixture because of the higher water absorption of the EAF slag aggregate. Moreover, the optimum water content and maximum dry density of s-RCCP experiences almost no effect from the delay in compaction. The water content of the s-RCCP mixture mixed by the new method may maintain its workability for 90 min.

(4) There was an improvement of s-RCCP compressive strength when the mixture was mixed by the new method. In addition, the compressive strength reached the highest value with compaction immediately after mixing. Increasing the delay in compaction led to a decline in the compressive strength of s-RCCP. However, 90 min of delay in compaction also produced s-RCCP fulfilling the strength requirement for pavements.

(5) The rough texture of the EAF slag aggregate caused the improvement of s-RCCP splitting tensile strength. Besides, the occurrence of the highest splitting tensile strength value of s-RCCP when delay in compaction was 60 min may be a result of the filling of the pores with ettringite.

(6) With UPV values > 4500 m/s, both the r-RCCP and s-RCCP specimens compacted at various times reached uniformity and "excellent" quality.

(7) The elastic modulus of r-RCCP and s-RCCP at 28 days of age was hardly affected by the delay in compaction. The range of values (30–36 GPa) is similar to that of conventional paving concrete. Furthermore, the elastic modulus of r-RCCP and s-RCCP can be predicted by the compressive strength of samples at 28 days of age.

Author Contributions: My Ngoc-Tra Lam and Duc-Hien Le designed the experiments. My Ngoc-Tra Lam conducted the experiments and wrote the paper. Saravut Jaritngam and Duc-Hien Le contributed discussion.

Conflicts of Interest: The authors declare no conflict of interest.

References

1. Worldsteel Association. World Steel in Figures 2016. In *Worldsteel Association*; Worldsteel Association: Brussels, Belgium, 2016; pp. 3–30.
2. Manso, J.M.; Polanco, J.A.; Losañez, M.; González, J.J. Durability of concrete made with EAF slag as aggregate. *Cem. Concr. Compos.* **2006**, *28*, 528–534. [CrossRef]
3. Adegoloye, G.; Beaucour, A.L.; Ortola, S.; Noumowé, A. Concretes made of EAF slag and AOD slag aggregates from stainless steel process: Mechanical properties and durability. *Constr. Build. Mater.* **2015**, *76*, 313–321. [CrossRef]
4. Sekaran, A.; Palaniswamy, M.; Balaraju, S. A Study on Suitability of EAF Oxidizing Slag in Concrete: An Eco-Friendly and Sustainable Replacement for Natural Coarse Aggregate. *Sci. World J.* **2015**, *2015*. [CrossRef] [PubMed]
5. Faleschini, F.; Fernández-Ruíz, M.A.; Zanini, M.A.; Brunelli, K.; Pellegrino, C.; Hernández-Montes, E. High performance concrete with electric arc furnace slag as aggregate: Mechanical and durability properties. *Constr. Build. Mater.* **2015**, *101*, 113–121. [CrossRef]
6. Lam, M.N.T.; Jaritngam, S.; Le, D.H. Roller-compacted concrete pavement made of Electric Arc Furnace slag aggregate: Mix design and mechanical properties. *Constr. Build. Mater.* **2017**, *154*. [CrossRef]
7. ACI Committe 325. *ACI 325.10R-95 Report on Roller-Compacted Concrete Pavements*; Federal Highway Administration: Washington, DC, USA, 2001; pp. 1–32. reapproved.
8. Karimpour, A. Effect of time span between mixing and compacting on roller compacted concrete (RCC) containing ground granulated blast furnace slag (GGBFS). *Constr. Build. Mater.* **2010**, *24*, 2079–2083. [CrossRef]
9. Dasmeh, A.; Fakher, A.; Shekarchi, M.; Gharavy, M. The influence of compaction time on the mechanical properties of RCC. *Int. J. Hydropower Dams* **2000**, *7*, 60–63.
10. ASTM. *C150-07 Standard Specification for Portland Cement*; ASTM International: West Conshohocken, PA, USA, 2009.
11. ASTM. *C127-07 Standard Test Method for Density, Relative Density (Specific Gravity) and Absorption of Coarse Aggregate*; ASTM International: West Conshohocken, PA, USA, 2012.
12. ASTM. C128-07a Standard Test Method for Density , Relative Density (Specific Gravity), and Absorption of Fine Aggregate. In *Annual Book of ASTM (American Society of Testing Material) Standards, 04.02*; ASTM International: West Conshohocken, PA, USA, 2012.
13. ASTM. C131-06 Standard Test Method for Resistance to Degradation of Small-Size Coarse Aggregate by Abrasion and Impact in the Los Angeles Machine. In *Annual Book of ASTM Standards, 4*; ASTM International: West Conshohocken, PA, USA, 2000.
14. ASTM. *C33/C33M-08 Standard Specification for Concrete Aggregates*; American Society for Testing and Materials: Philadelphia, PA, USA, 2003.
15. Le, D.H.; Sheen, Y.N.; Bui, Q.B. An assessment on volume stabilization of mortar with stainless steel slag sand. *Constr. Build. Mater.* **2017**, *155*, 200–208. [CrossRef]
16. ASTM. *D4792-06 Standard Test Method for Potential Expansion of Aggregates from Hydration Reactions*; ASTM International: West Conshohocken, PA, USA, 2006.
17. ASTM. D1557-12 Standard Test Methods for Laboratory Compaction Characteristics of Soil Using Modified Effort (56,000 ft-lbf/ft3 (2,700 kN-m/m3)). In *Annual Book of ASTM Standards, 4*; ASTM International: West Conshohocken, PA, USA, 2000.
18. ASTM. C1435/C1435M-08 Standard Practice for Molding Roller-Compacted Concrete in Cylinder Molds Using a Vibrating Hammer. In *Annual Book of ASTM Standards, 4*; ASTM International: West Conshohocken, PA, USA, 1999.
19. ASTM. C597-02 Standard Test Method for Pulse Velocity through Concrete. In *American Society for Testing and Materials*; 100 Barr Harbor Drive: West Conshohocken, PA, USA, 2002.
20. ASTM. *C39/C39M-14 Standard Test Method for Compressive Strength of Cylindrical Concrete Specimens*; ASTM International: West Conshohocken, PA, USA, 1997.
21. ASTM. C496/C496M Standard Test Method for Splitting Tensile Strength of Cylindrical Concrete Specimens. In *Annual Book of ASTM Standards 04.02*; American Society for Testing and Materials Philadelphia: West Conshohocken, PA, USA, 1984.

22. ASTM. C469-02 Standard Test Method for Static Modulus of Elasticity and Poisson's Ratio of Concrete in Compression. In *Annual Book of ASTM (American Society of Testing Material) Standards, 04.02*; ASTM International: West Conshohocken, PA, USA, 2002.
23. Rao, S.K.; Sravana, P.; Rao, T.C. Investigating the effect of M-sand on abrasion resistance of Fly Ash Roller Compacted Concrete (FRCC). *Constr. Build. Mater.* **2016**, *118*, 352–363. [CrossRef]
24. Modarres, A.; Hosseini, Z. Mechanical properties of roller compacted concrete containing rice husk ash with original and recycled asphalt pavement material. *Mater. Des.* **2014**, *64*, 227–236. [CrossRef]
25. Courard, L.; Michel, F.; Delhez, P. Use of concrete road recycled aggregates for Roller Compacted Concrete. *Constr. Build. Mater.* **2010**, *24*, 390–395. [CrossRef]
26. Mehta, P.K.; Monterio, P.J.M. *Concrete-Microstucture, Properties and Materials*, 3rd ed.; McGraw-Hill Companies, Inc.: New York, NY, USA, 2006.
27. Mardani-Aghabaglou, A.; Ramyar, K. Mechanical properties of high-volume fly ash roller compacted concrete designed by maximum density method. *Constr. Build. Mater.* **2013**, *38*, 356–364. [CrossRef]
28. Hesami, S.; Modarres, A.; Soltaninejad, M.; Madani, H. Mechanical properties of roller compacted concrete pavement containing coal waste and limestone powder as partial replacements of cement. *Constr. Build. Mater.* **2016**, *111*, 625–636. [CrossRef]
29. American Concrete Pavement Association. *Roller-Compacted Concrete Pavements as Exposed Wearing Surface*; American Concrete Pavement Association: Washington, DC, USA, 2014.
30. Tayabji, S.D.; Okamoto, P.A. Engineering properties of Roller-compacted concrete. *Transp. Res. Rec.* **1987**, *1136*, 33–45.
31. Whitehurst, E.A. Soniscope tests concrete structures. *Int. Concr. Abstr. Portal.* **1951**, *47*, 433–444.
32. Abu-Eishah, S.I.; El-Dieb, A.S.; Bedir, M.S. Performance of concrete mixtures made with electric arc furnace (EAF) steel slag aggregate produced in the Arabian Gulf region. *Constr. Build. Mater.* **2012**, *34*, 249–256. [CrossRef]
33. Rao, S.K.; Sravana, P.; Rao, T.C. Experimental studies in Ultrasonic Pulse Velocity of roller compacted concrete pavement containing fly ash and M-sand. *Int. J. Pavement Res. Technol.* **2016**, *9*, 289–301. [CrossRef]
34. Settari, C.; Debieb, F.; Kadri, E.H.; Boukendakdji, O. Assessing the effects of recycled asphalt pavement materials on the performance of roller compacted concrete. *Constr. Build. Mater.* **2015**, *101*, 617–621. [CrossRef]

APPENDIX A

2018 2nd The International Conference on Civil Engineering (ICOCE 2018)

May 5-7, Da Nang, Vietnam

Certificate of Presentation

This certificate is awarded to

My Ngoc-Tra Lam

Prince of Songkla University, Thailand

Paper Title: A Study on Mixing Proportion of Roller-Compacted Concrete Pavement Made of EAF Slag Aggregate and Fly Ash by Using Taguchi Method

for giving your oral presentation at the 2018 2nd International Conference on Civil Engineering (ICOCE 2018) during May 5-7, 2018 in Da Nang, Vietnam.

For and on behalf of
Engineering and Technology Publishing

Conference Chair/Session Chair

ICOCE 2018

A Study on Mixing Proportion of Roller-Compacted Concrete Pavement Made of EAF Slag Aggregate and Fly Ash by Using Taguchi Method

My Ngoc-Tra Lam *(Correspondence Author)*
Department of Civil Engineering, Faculty of Engineering, Prince of Songkla University,
Hat Yai, Songkhla, Thailand.
e-mail: ngoctramsy@gmail.com
Faculty of Civil & Electrical Engineering, Ho Chi Minh City Open University,
Ho Chi Minh City, Vietnam.
e-mail: my.lnt@ou.edu.vn

Saravut Jaritngam *(Author)*
Department of Civil Engineering, Faculty of Engineering, Prince of Songkla University,
Hat Yai, Songkhla, Thailand.
e-mail: jaritngam@gmail.com

Duc-Hien Le *(Author)*
Sustainable Developments in Civil Engineering Research Group, Faculty of Civil Engineering,
Ton Duc Thang University, Ho Chi Minh City, Vietnam.
e-mail: leduchien@tdt.edu.vn

Abstract— **The aim of this study is to investigate the effect of factors in mixing proportion on the dry density of Roller-compacted concrete pavement made of EAF slag aggregate and fly ash by using Taguchi method. In this study, EAF slag with size in range of 4.75 – 19 mm was used as a substitute for natural coarse aggregate with three percentages (i.e. 0%, 50% and 100%). Cement was partially replaced by fly ash at three content levels (i.e. 0%, 20% and 40%). Four factors are considered to study including the percentage of EAF slag aggregate, the percentage of binder (cement + fly ash), the fly ash ratio, and the moisture content. And, three levels of four factors were proposed to study the influence of them on the dry density of RCCP. Thus, nine mixtures conforming the orthogonal array L₉ of Taguchi method were prepared to determine the dry density of RCCP by Proctor test. The results were assessed by the analysis of variance (ANOVA). The results of this research indicated that increasing of the percentage of EAF slag as aggregate replacement led to rise the dry density, whereas increasing of the fly ash ratio as cement substitution resulted in the decrease of dry density. The percentage of binder is range of 10-14% and moisture content in range of 6-8% affected slightly on the dry density. When the moisture content exceeded 8% leading to the reduction of the dry density.**

I.   Introduction

Electric Arc Furnace (EAF) slag is a by-product of steel production, which is generated during the manufacture of crude steel by the Electric Arc Furnace process. World crude steel production reached 1,621 million tons for the year 2015 leading to the world output of EAF slag was estimated in the range of 170 -250 million tons [1], [2]. The traditional stockpile method of EAF slag has created challenging environmental issues such as a lack of waste storage areas and pollution of soil and underground water. Nowadays, many research on EAF slag as aggregate replacement in conventional concrete, high-performance concrete, and alkali-activated concrete are found in literature. And, scholars have demonstrated that EAF slag can replace natural aggregates in many kinds of concrete [3]–[8]. For example, the replacement of natural aggregates by EAF slag in conventional concrete led to increase compressive strength and splitting tensile strength [3], [4], [6], [7]. Similarly, the increase of mechanical properties in high-performance concrete made of EAF slag aggregate was also observed [5]. Furthermore, alkali-activated concrete containing steel slag as coarse aggregate attained sufficient strength for structure, whereas the values of durability reduced slightly [8]. But very few reports conducted on the using of EAF slag as aggregate in Roller-compacted concrete. Roller-compacted concrete is a stiff and no-slump concrete, which is usually used for pavement (called Roller-compacted concrete pavement) due to its fast construction and cost efficiency. Because aggregate in Roller-compacted concrete pavement (RCCP) mixture consists of 75% volume, the substitution aggregate in RCCP by EAF slag is very important to limit the natural aggregates consumption. In addition, fly ash as cement alternative in RCCP has created several benefits in concrete industry [9]–[11]. Mardani-Aghabaglou et al. studied the mechanical and durability properties of RCCP using 20%, 40%, and 60% of fly ash as a partial cement substitution. It is reported that there was a slight decrease in the strength and durability values as fly ash content increased at early ages. However, at later ages, the development of strength and durability attained satisfactory level for pavement application [9]. The similar

results are found in Yerramala and Babu research [10]. It was observed that RCCP mixtures with moderate amount of cement ranging from 150 to 190 kg/m^3 and fly ash percentage ranging from 60% to 70% performed low values of the permeability, absorption, sorption and chloride diffusivity.

Based on the previous research, the incorporation of EAF slag aggregate and fly ash in Roller-compacted concrete pavement (RCCP) is proposed an effective solution to reduce the environmental impacts and develop a sustainable infrastructure. In this study, EAF slag was used as a substitute for natural coarse aggregate with three percentages (i.e. 0%, 50% and 100%). And, cement was partially replaced by fly ash at three content levels (i.e. 0%, 20% and 40%). RCCP is compacted by vibratory rollers to attain a target density and homogeneous surface pavement [12]. RCCP mixture should be dry enough to maintain the stability of vibratory roller and wet enough to distribute the paste. Hence, RCCP mixing proportion has to be calculated carefully. Soil compaction method is the popular approach to determine the optimum moisture content and maximum dry density of RCCP mixture. Typically, mixtures compacted with maximum dry density would provide the highest performance, especially strength. Therefore, an assessment the influence of materials (i.e. aggregate, binder, and water content) on dry density of mixture is important to enhance strength of RCCP.

Taguchi method developed by Genichi Taguchi is an approach provides an efficient way to optimize designs and keep the experimental cost at the minimum level. A set of orthogonal arrays (OA) to design experiments was designed in Taguchi method [13]. The using of OA provides the optimum working conditions of the affected factors. In addition, Taguchi method allows finding out the effective parameters of target value. Taguchi method is suitable for a wide range of applications. In recent years, Taguchi method has been interested by some scholars in civil engineering. For instance, Joshaghani et al. [14] was used Taguchi method to optimize the performance of density, strength, porosity, and permeability on pervious concrete pavement. Furthermore, Ozbay et al. [15] determined the optimum levels of parameters in mix proportion of high strength

self- compacting concrete by Taguchi method. Additionally, Tanyildizi et al. [16] conducted the thirty-two experiments conforming the orthogonal array L_{32} of Taguchi method to analyze the effects of the polymerization type, the percentage of silica fume, and heating degree on the concrete strengthened with polymer after exposure to high temperature.

The aim of this study is investigation the effect of factors of mixing proportion (i.e. EAF slag aggregate, cement, fly ash, and water content) on dry density of RCCP by Taguchi method.

II. Method

A. Materials

Ordinary Portland Cement (OPC) type I conforming to ASTM C150 was used in this study [17]. Class F fly ash conforming to ASTM C618 [18] replaced cement. Table I shows the chemical composition and physical characteristics of OPC and fly ash.

Natural aggregates used in this study with gradation as shown in Table II is crushed stone. EAF slag aggregate with size in range of 4.75-19 mm (Figure I) was used to replace natural coarse aggregate in mixture. The properties of natural aggregates and EAF slag aggregate conform to ASTM C33 [19] for concrete making (Table III).

Figure I. EAF slag aggregate used in this study.

Table I. Chemical composition and physical properties of OPC and fly ash

	OPC, Type I	Fly ash, Class F
Chemical composition (%)		
Silica (SiO_2)	20.7	52.3
Alumina (Al_2O_3)	4.5	24.9
Ferric oxide (Fe_2O_3)	3.3	14.1
Calcium oxide (CaO)	63.0	-
Magnesium oxide (MgO)	1.8	-
Sodium oxide (Na_2O)	0.10	0.67
Potassium oxide (K_2O)	0.74	-
Sulphuric anhydride (SO_3)	2.3	0.47
Loss on ignition (LOI)	2.8	0.15
Physical characteristics		
Fineness (Blaine) (m^2/kg)	347	289
Specific gravity	3.14	2.40
Initial setting time (min)	110	NA
Final setting time (min)	170	NA
Particle composition		
Retaining on 45 µm sieve (%)	NA	7.92
Compressive strength (N/mm^2)		
1 day	14.6	-
3 days	26.2	-
7 days	33.0	-
28 days	43.0	-

Note: NA means not available

Table II. The suggested limits and the designing gradation of RCCP used in this study

Sieve size	Passing mass (%)		
	The lower limit	The upper limit	The designing gradation
19 mm	95	100	100
12.5 mm	70	95	83
9.5 mm	60	85	73
4.75 mm (No. 4)	40	60	54
2.36 mm (No. 8)	30	50	41
1.18 mm (No. 16)	20	40	30
600 µm (No. 30)	15	30	22
300 µm (No. 50)	10	25	15
150 µm (No. 100)	2	16	10
< 75 µm (No. 200)	0	8	7

Table III. Physical properties of the crushed stone and EAF slag aggregate

Properties	Crushed stone		EAF slag
	Fine aggregate (4.75 - 0 mm)	Coarse aggregate (19 - 4.75 mm)	Coarse aggregate (19 - 4.75 mm)
Apparent specific gravity	2.71	2.72	3.40
Density (OD) (kg/m^3)	2609	2680	3085
Density (SSD) (kg/m^3)	2644	2691	3176
Bulk density (kg/m^3)	1493	1466	1686
Water absorption (%)	1.36	0.44	2.93
Los Angeles abrasion (%)	NA	13.98	19.37

Note: NA means not available

B. Testing approach

Four factors of mixture affected on dry density of RCCP in this study day are considered:

- The percentage of EAF slag aggregate replaced natural coarse aggregate in the mixture.

- The percentage of binder (cement + fly ash) is a ratio of the weight of binder and total the weight of binder plus the weight of aggregates in the mixture.

- The moisture content of mixture is a ratio of the weight of water and total the weight of binder plus the weight of aggregates in the mixture.

- The fly ash ratio replaced cement in the mixture.

Typically, the weight of binder was in range of 10-14% of total weight of binder and oven-dried aggregates in the mixture. And, the moisture content of the mixture was in range of 6-10% [12]. Therefore, three levels of four factors were proposed to investigate the effect of them on mix proportions as shown in Table IV.

Table IV. Design factors and their levels

No.	Factors	ID.	Level 1	Level 2	Level 3
1	EAF slag aggregate	E	0%	50%	100%
2	Binder	B	10%	12%	14%
3	Moisture content	M	6%	8%	10%
4	Fly ash	F	0%	20%	40%

For four factors and three levels, the proper orthogonal array L_9 of Taguchi method was used to design experiments of this study with the standard L_9 table [13] as listed in Table V.

Table V. The standard orthogonal array L_9 (4 factors, 3 levels)

Experiment no.	E	B	M	F
1	Level 1	Level 1	Level 1	Level 1
2	Level 1	Level 2	Level 2	Level 2
3	Level 1	Level 3	Level 3	Level 3
4	Level 2	Level 1	Level 2	Level 3
5	Level 2	Level 2	Level 3	Level 1
6	Level 2	Level 3	Level 1	Level 2
7	Level 3	Level 1	Level 3	Level 2
8	Level 3	Level 2	Level 1	Level 3
9	Level 3	Level 3	Level 2	Level 1

Table VI shows nine experiments were proposed conforming to the standard L_9 table. From Table VI, the mixing proportion of each mixture presented in Table VII was calculated to conduct Proctor test in accordance with ASTM D1557 [20].

Table VI. Nine experiments used in this study

Experiment no.	ID. mixture	E	B	M	F
1	C1	0%	10%	6%	0%
2	C2	0%	12%	8%	20%
3	C3	0%	14%	10%	40%
4	C4	50%	10%	8%	40%
5	C5	50%	12%	10%	0%
6	C6	50%	14%	6%	20%
7	C7	100%	10%	10%	20%
8	C8	100%	12%	6%	40%
9	C9	100%	14%	8%	0%

Table VII. RCCP mixing proportions

ID. mixture	Coarse aggregate (kg/m^3)		Fine aggregate (kg/m^3)	Binder (kg/m^3)		Water content (kg/m^3)
	EAF slag	Crushed stone		Cement	Fly ash	
C1	0	842	1163	222.8	0.0	133.7
C2	0	842	1163	219.2	54.8	182.3
C3	0	842	1163	195.8	130.6	233.1
C4	424	424	1172	134.7	89.8	179.6
C5	424	424	1172	275.4	0.0	229.5
C6	424	424	1172	263.1	65.8	140.9
C7	867	0	1197	183.5	45.9	229.3
C8	867	0	1197	169.2	112.8	140.8
C9	867	0	1197	336.0	0.0	192.0

According to ASTM D1557, the mixture is placed five layers into the 6-in (152.4 mm) mold and compacted 56 blows of a rammer per layer (Figure II). Each mixture is conducted with three trials to determine the average of dry density. Then, the analysis of variance (ANOVA) was applied to assess the contribution of each factor in the mixture.

Figure II. Proctor test, (a) compacting the mixture in the mold, (b) determining the density of mixture after compacting.

III.   Results and discussion

Table VIII shows the dry density of nine mix proportions determined by Proctor test. This result was analyzed by Minatab software to assess the effect of four factors on the dry density of mixture. Figure III presents the result of the analysis of variance (ANOVA).

Table VIII. The dry density results of RCCP (kg/m^3)

ID. mixture	Trial 1	Trial 2	Trail 3	Average
C1	2235	2292	2277	2268
C2	2220	2241	2250	2237
C3	2107	2113	2149	2123
C4	2233	2258	2262	2251
C5	2255	2234	2294	2261
C6	2301	2297	2308	2302
C7	2244	2255	2272	2257
C8	2280	2290	2276	2282
C9	2381	2359	2349	2363
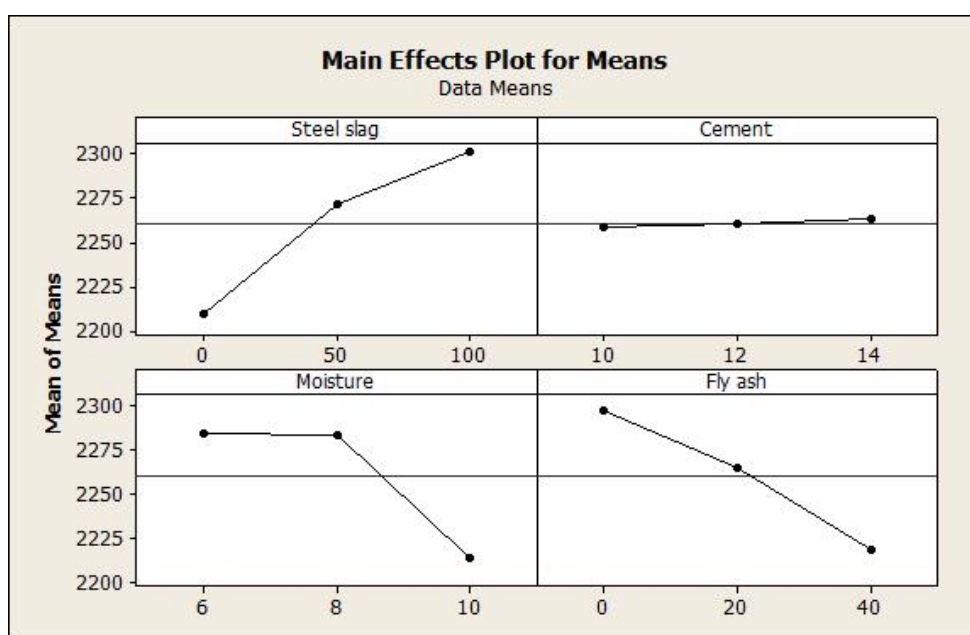
Figure III. Analysis of Variance of the results

As can be seen in Figure III, increasing the EAF slag as aggregate replacement in mixture led to rise the dry density. This behavior resulted from the high-density feature of EAF slag aggregate. Whereas increasing the fly ash as cement substitution in mixture resulted in declining the dry density, because specific gravity of fly ash is lower than that of cement.

Besides, the percentage of binder in mixture hardly affected on the dry density of RCCP. Therefore, when design the mixing proportion, the mass of binder was determined by the strength requirement of RCCP.

On the other hand, the moisture content in range of 6-8% affected slightly on the dry density. And, the moisture content exceeded 8% leading the reduction of the dry density.

IV.   Concluding remarks

Based on the experimental work, some of highlighted remarks could be drawn:

(1) The higher percentage of EAF slag coarse aggregate led to the higher dry density of the mixture.

(2) Increasing the fly ash content as cement substitution in the mixture led to decrease the dry density of the mixture.

(3) The moisture content in range of 6-8% affected slightly on the dry density of the mixture. And, there was a dramatic reduction of the dry density when the moisture content exceeded 8%.

(4) The percentage of binder in range of 10-14% hardly affected on the dry density of the RCCP mixture.

Refrences

[1]   World Steel Association, "World Steel in Figures 2016," *World Steel Assoc.*, pp. 3–30, 2016.

[2]   U.S. Geological Survey, "Mineral Commodity Summaries 2016: Iron and Steel Slag," no. 703, pp. 88–89, 2016.

[3]   J. M. Manso, J. A. Polanco, M. Losañez, and J. J. González, "Durability of concrete made with EAF slag as aggregate," *Cem. Concr. Compos.*, vol. 28, no. 6, pp. 528–534, 2006.

[4]   G. Adegoloye, A. L. Beaucour, S. Ortola, and A. Noumowé, "Concretes made of EAF slag and AOD slag aggregates from stainless steel process: Mechanical properties and durability," *Constr. Build. Mater.*, vol. 76, pp. 313–321, 2015.

[5]   F. Faleschini, M. Alejandro Fernandez-Ruiz, M. A. Zanini, K. Brunelli, C. Pellegrino, and E. Hernandez-Montes, "High performance concrete with electric arc furnace slag as aggregate: Mechanical and durability properties," *Constr. Build. Mater.*, vol. 101, pp. 113–121, 2015.

[6]   S. I. Abu-Eishah, A. S. El-Dieb, and M. S. Bedir, "Performance of concrete mixtures made with electric arc furnace (EAF) steel slag aggregate produced in the Arabian Gulf region," *Constr. Build. Mater.*, vol. 34, pp. 249–256, 2012.

[7]   S. Monosi, M. L. Ruello, and D. Sani, "Electric arc furnace slag as natural aggregate replacement in concrete production," *Cem. Concr. Compos.*, vol. 66, pp. 66–72, 2016.

[8]   N. Palankar, A. U. Ravi Shankar, and B. M. Mithun, "Durability studies on eco-friendly concrete mixes incorporating steel slag as coarse aggregates," *J. Clean. Prod.*, vol. 129, pp. 437–448, 2016.

[9]   A. Mardani-Aghabaglou and K. Ramyar, "Mechanical properties of high-volume fly ash roller compacted concrete designed by maximum density method," *Constr. Build. Mater.*, vol. 38, no. 1, pp. 356–364, 2013.

[10]   A. Yerramala and K. Ganesh Babu, "Transport properties of high volume

fly ash roller compacted concrete," *Cem. Concr. Compos.*, vol. 33, no. 10, pp. 1057–1062, 2011.

[11] S. K. Rao, P. Sravana, and T. C. Rao, "Investigating the effect of M-sand on abrasion resistance of Fly Ash Roller Compacted Concrete (FRCC)," *Constr. Build. Mater.*, vol. 118, pp. 352–363, 2016.

[12] D. Harrington, F. Abdo, W. Adaska, and C. Hazaree, "Guide for Roller-Compacted Concrete Pavements," *Inst. Transp. Iowa state univerisity*, no. August, p. 104, 2010.

[13] R. Roy, "A-Primer-on-the-Taguchi-Method.pdf." Society of Manufacturing Engineers, 1990.

[14] A. Joshaghani, A. A. Ramezanianpour, O. Ataei, and A. Golroo, "Optimizing pervious concrete pavement mixture design by using the Taguchi method," *Constr. Build. Mater.*, vol. 101, pp. 317–325, 2015.

[15] E. Ozbay, A. Oztas, A. Baykasoglu, and H. Ozbebek, "Investigating mix proportions of high strength self compacting concrete by using Taguchi method," *Constr. Build. Mater.*, vol. 23, no. 2, pp. 694–702, 2009.

[16] H. Tanyildizi and M. Şahin, "Application of Taguchi method for optimization of concrete strengthened with polymer after high temperature," *Constr. Build. Mater.*, vol. 79, pp. 97–103, 2015.

[17] ASTM C150-07, "Standard Specification for Portland Cement."

[18] ASTM C 618-05, "Standard Specification for Coal Fly Ash and Raw or Calcined Natural Pozzolan for Use in Concrete," *Annu. B. ASTM Stand.*, pp. 3–6, 2010.

[19] ASTM C33/C33M-08, "Standard Specification for Concrete aggregates." .

[20] ASTM D1557-12, "Standard Test Methods for Laboratory Compaction Characteristics of Soil Using Modified Effort (56 , 000 ft-lbf / ft 3 (2 , 700 kN-m / m 3)) 1."

APPENDIX B

Eight International Conference on Maintenance and Rehabilitation of Pavements (MAIRE PAV8, 2016)

27-29 July 2016, Singapore

Home

Copyright

Welcome Messages

Committees

Keynote Speakers

Technical Papers

Author Index

Search

Help

The Possibility of Using Steel Slag for Pavement Structure Application in Vietnam

My Lam[a], Saravut Jaritngam[b], Kiattisak Wongsopanakul[c], Pichai Taneerananon[d]

Faculty of Engineering, Prince of Songkla University
[a]*my.lnt@ou.edu.vn*
[b]*jaritngam@gmail.com*
[c]*kiattis@hotmail.com*
[d]*2007tao@gmail.com*

ABSTRACT

Sustainability has become an important aspect of developed countries throughout the world. Therefore, the utilization of industrial by-products and wastes is becoming more important. In the last 30 years, steel slag was used in civil engineering projects such as road construction, asphalt mixtures, Portland cement manufacture, Portland cement concrete, geotechnical engineering projects. This paper presents the properties and utilization of steel slag in Vietnam, for pavement structure application.

Keywords: Steel slag, Properties, Utilization, Pavement.

VITAE

Name   Mrs. Lam Ngoc Tra My

Student ID   5810130005

Educational Attainment

Degree	Name of Institution	Year of Graduation
Bachelor of Engineering (Civil Engineering)	University of Transport and Communication, Vietnam	2005
Master of Engineering (Civil Engineering)	Ho Chi Minh University of Technology, Vietnam	2010

Scholarship Awards during Enrollment

1. Thailand's Education Hub for Southern Region of ASEAN Countries, Prince of Songkla University, 2015 – 2018 (Grant No. TEH-AC 032/2015).

2. PSU.GS. Financial Support for Thesis, Prince of Songkla University, 2017.

Work – Position and Address

1. Lecturer, Faculty of Civil Engineering, Ho Chi Minh Open University, Ho Chi Minh city, Vietnam, from 2007 to now.

List of Publication and Proceeding

1. M.N. Lam, S. Jaritngam, D. Le, Roller-Compacted Concrete Pavement Made of Electric Arc Furnace Slag Aggregate : Mix Design and Mechanical Properties, Constr. Build. Mater. 154 (2017) 482–495. doi:10.1016/j.conbuildmat.2017.07.240.

2. M.N. Lam, S. Jaritngam, D. Le, EAF Slag Aggregate in Roller-Compacted Concrete Pavement: Effects of Delay in Compaction, Sustainability (Switzerland), 10(4), 1122.

doi:10.3390/su10041122.

3. M.N. Lam, S. Jaritngam, D. Le, A Study on Mixing Proportion of Roller-Compacted Concrete Pavement Made of EAF Slag Aggregate and Fly Ash by Using Taguchi Method, The oral presentation to be delivered at 2018 2nd International Conference on Civil Engineering, Vietnam 2018 (Abstract).

4. M. Lam, S. Jaritngam, K. Wongsopanakul, P. Taneerananon, The possibility of using steel slag for pavement structure application in Vietnam, Proceeding of MAIREPAV8, Singapore 2016. doi:10.3850/978-981-11-0449-7-159-cd (Abstract).